

POLYMERIC PRINT HYDROGEL NANOPARTICLES AS A DELIVERY PLATFORM FOR
SUBUNIT VACCINE ANTIGENS AND ADJUVANTS

Sarah Nicole Mueller

A dissertation submitted to the faculty of the University of North Carolina at Chapel Hill
in partial fulfillment of the requirements for the degree of Doctor of Philosophy
in the Department of Chemistry.

Chapel Hill
2014

Approved by:

Joseph M. DeSimone

Alexander V. Kabanov

Sergei S. Sheiko

Jenny P.Y. Ting

Wei You

© 2014
Sarah Nicole Mueller
ALL RIGHTS RESERVED

ABSTRACT

Sarah Nicole Mueller: POLYMERIC PRINT HYDROGEL NANOPARTICLES AS A DELIVERY PLATFORM FOR SUBUNIT VACCINE ANTIGENS AND ADJUVANTS
(Under the direction of Joseph M. DeSimone)

Vaccines consisting of purified soluble antigens rather than killed or attenuated whole pathogens have shown great promise in increasing vaccine safety. However, these subunit vaccines (proteins, DNA, polysaccharides, lipids) are susceptible to degradation and are usually less immunogenic than whole pathogen vaccines. Subunit vaccines have shown increased efficacy when delivered in particulate form compared to soluble form. Previous research, however, has been limited by particle fabrication methods that are often incapable of yielding homogeneous particles and are incompatible with industrial scale-up. The use of Particle Replication in Non-wetting Templates (PRINT[®]) technology avoids these issues, allowing for precise control over particle size, shape, composition, and surface characteristics. In addition, PRINT is a highly scalable, GMP compliant process. Herein, PRINT is employed to fabricate polymeric hydrogel nanoparticles for the delivery of novel pro-adjuvants and protein antigens *in vitro* and *in vivo*. The model protein antigen, ovalbumin (OVA), was directly conjugated to the surface of nanoparticles through a poly(ethylene glycol) (PEG) linker. Surface presentation of OVA led to antigen processing and presentation by antigen presenting cells and elicited robust immune responses. The linker chemistries utilized for this model antigen are applicable to a range of clinically relevant vaccine antigens, with studies toward a dengue virus vaccine and an influenza vaccine in preliminary phases. Resiquimod, a toll-like receptor 7/8 agonist and vaccine adjuvant, was used to synthesize a polymerizable, acid-labile pro-adjuvant. The pro-adjuvant

loaded nanoparticles were capable of steadily releasing the original, active adjuvant when exposed to endosomal pH (pH 5), while protecting the adjuvant from premature release at physiological pH (pH 7.4). This allowed for intracellular delivery of resiquimod and limited systemic exposure. Therefore, PRINT nanoparticles can be formulated into potent particulate vaccines for controlled and efficiently co-delivery of adjuvants and antigens. Overall, these efforts may lead to new and efficacious vaccines to a wide variety of infectious diseases.

ACKNOWLEDGEMENTS

I would sincerely like to thank my friends and family who made all of this possible. I would especially like to thank Dr. Joseph DeSimone who has served as my mentor for the last four and a half years. We're probably the first Hokie and Wahoo who have learned to successfully work together. To all of the wonderful core facilities staff and scientists at UNC, I would have been lost without your assistance and guidance. To the DeSimone lab members and alums, you all have made the late nights and long weekends so much more pleasant. I would have pulled out all of my hair after year one without your support in the lab and in activities outside of the lab as well. Special thank you to the soon to be Drs. Dominica H.C. Wong and Tessa Carducci – it's not often you find women in science who can show you how to run an NMR in the morning and watch *The Bachelor* with you at night. I appreciate all of the science and non-science conversations we've had, especially ones about the science of girly things like gel manicures. To another soon to be Dr. Kevin Reuter – my partner in crime for all of this. You've pushed me to be a better scientist, and I hope I have encouraged and inspired you as much as you have done for me. To my parents – thank you for only mentioning once or twice a year how I should have gotten a job instead of going to graduate school and for not kicking me off of the family cellphone plan. Hopefully this will all be worth it in the end and I'll be making the big bucks, so I can support you when you're old with an unlimited supply of Zaxby's. To my sisters and brother – how did I get two degrees in the time it took the three of you to get one??? Just kidding though, I love you all and hope none of you ever have to go to graduate school. Thank you all again; wish me luck! Wahoowa!

TABLE OF CONTENTS

LIST OF FIGURES.....	x
LIST OF TABLES.....	xii
LIST OF SCHEMES.....	xiii
LIST OF ABBREVIATIONS AND SYMBOLS.....	xiv
CHAPTER 1 VACCINATION AND THE POTENTIAL OF PARTICLE MEDIATED IMMUNITY	1
1.1 Modern Vaccination Strategies and Subunit Vaccines.....	1
1.2 Activating Toll-Like Receptors as Vaccine Adjuvants	3
1.3 Current Strategies for Particle-Based Delivery Vehicles for Subunit Vaccines.....	5
1.4 Fabrication of Nanoparticles Via PRINT Technology – Controlling Size, Shape, Composition, and Surface Properties.....	8
1.5 References.....	12
CHAPTER 2 MANIPULATING PHYSICOCHEMICAL PROPERTIES OF POLYMERIC HYDROGEL PARTICLES TO ENHANCE LYMPHATIC TRAFFICKING AND IMMUNOGENICITY OF A MODEL SUBUNIT VACCINE.....	15
2.1 Introduction.....	15
2.2 Results and Discussion	19
2.2.1 Lymphatic Trafficking of Bare Particles	19
2.2.2 Conjugation of Model Antigen and Surface Characteristics	23
2.2.3 Influence of Particle Drainage on Immune Response.....	35
2.3 Conclusions.....	39
2.4 Materials and Methods.....	40

2.4.1	Materials	40
2.4.2	Animals	41
2.4.3	Fabrication of Hydrogel NPs via the PRINT Process.....	41
2.4.4	Nanoparticle Characterization	43
2.4.5	Lymphatic Drainage Studies.....	43
2.4.6	<i>Ex Vivo</i> Imaging.....	43
2.4.7	Flow Cytometry	44
2.4.8	<i>In Vivo</i> CD4 ⁺ T Cell Proliferation.	44
2.4.9	Complement Activation.....	44
2.4.10	Confocal Microscopy.....	45
2.4.11	Immunizations and Antibody ELISA.	45
2.5	References.....	47
CHAPTER 3 A PRO-ADJUVANT APPROACH TO ACHIEVE CONTROLLED DELIVERY OF VACCINE COMPONENTS VIA PRINT NANOPARTICLES		51
3.1	Introduction.....	51
3.2	Results and Discussion	54
3.2.1	Synthesis and Characterization of R848 Pro-Adjuvant Monomer	54
3.2.2	Release of R848 from R848-NPs.....	55
3.2.3	<i>In Vitro</i> Analysis of R848.....	60
3.2.4	R848-NPs as a Vaccine Adjuvant <i>In Vivo</i>	64
3.3	Conclusions.....	69
3.4	Materials and Methods.....	70
3.4.1	Materials	70
3.4.2	Animals.....	70

3.4.3	Synthesis of Pro-Adjuvant	70
3.4.4	Fabrication of Hydrogel NPs via PRINT Process.....	72
3.4.5	Characterization of R848-NPs	73
3.4.6	<i>In Vitro</i> Studies.	73
3.4.7	Serum Cytokine Study	74
3.4.8	Immunizations and Antibody ELISA.	75
3.5	References.....	76
CHAPTER 4 PRINT BASED VACCINES FOR CLINICALLY RELEVANT DISEASE MODELS.....		79
4.1	Introduction.....	79
4.1.1	Dengue Virus as a Global Threat and Current Vaccine Strategies.....	79
4.1.2	Influenza Virus: Overcoming Barriers Towards Total Immunization.....	82
4.2	Results and Discussion	86
4.2.1	Conjugation of Dengue Virus Envelope Protein to PRINT NPs	86
4.2.2	Vaccination with Soluble Versus Particulate Dengue Recombinant E Protein Antigen.....	88
4.2.3	PRINT-Based Vaccine Against Hemagglutinin Protein for Influenza Virus	91
4.3	Conclusion	91
4.4	Materials and Methods.....	92
4.4.1	Materials	92
4.4.2	Dengue E Protein Characterization.....	92
4.4.3	Animals.....	93
4.4.4	Fabrication of Hydrogel NPs via the PRINT Process and Protein Conjugation.....	93
4.4.5	Nanoparticle Characterization	95
4.4.6	Immunization and Antibody ELISA.....	95

4.5	References.....	97
CHAPTER 5 FUTURE DIRECTIONS AND SUMMARY		102
5.1	Future Directions	102
5.1.1	Combining Vaccine Antigens and Adjuvants into a Single Particle Formulation..	102
5.1.2	Exploring the Synergy Between Multiple Adjuvants in Augmenting Vaccine Efficacy	105
5.2	Summary	109
5.2.1	Manipulating Physicochemical Properties of Polymeric Hydrogel PRINT Nanoparticles to Enhance Lymphatic Trafficking and Immunogenicity of a Model Subunit Vaccine	109
5.2.2	A Pro-Adjuvant Approach to Achieve Controlled Delivery of Vaccine Components via PRINT Nanoparticles.....	110
5.2.3	PRINT Based Vaccines for Clinically Relevant Disease Models	110
5.3	References.....	112
APPENDIX.....		115

LIST OF FIGURES

Figure 1.1 Particle Replication in Non-wetting Templates..	10
Figure 2.1 Lymphatic drainage and cell uptake of blank hydrogel particles.....	21
Figure 2.2 Localization of NPs in the PLNs was confirmed by confocal microscopy.....	21
Figure 2.3 Flow cytometry of cells from lymph nodes resected 48 hours after injection..	23
Figure 2.4 Total drainage OVA-loaded hydrogel of NPs in lymph nodes.	26
Figure 2.5 80×180 nm PEG(500)OVA NPs drained rapidly to the lymph nodes accumulated over 48 h.	27
Figure 2.6 Persistent delivery of antigen to B cells in soluble form or by hydrogel NPs.	28
Figure 2.7 80×180 nm NPs are efficiently taken up by key antigen presenting cells	30
Figure 2.8 Uptake of 80×180 nm PEG(500)OVA particles by dendritic cells.....	30
Figure 2.9 Hydrogel NPs activate complement system.....	32
Figure 2.10 Analysis of LN DC subsets by flow cytometry.....	34
Figure 2.11 In vivo CD4 ⁺ OT-II T cell proliferation	36
Figure 2.12 Hydrogel vaccine elicits higher antibody titers than soluble antigen with or without Alum adjuvant.....	37
Figure 2.13 Size rather than PEG linker length dramatically influences IgG response..	39
Figure 3.1 Release profile for R848 from Me ₂ ProR848-NPs at varying pH.....	58
Figure 3.2 Release of R848 from Me ₂ ProR848-NPs at pH 5 vs. pH 7.4.....	59
Figure 3.3 Release profile for R848 from Me ₂ - and Et ₂ ProR848-NPs at pH 5.	60
Figure 3.4 Activity of Me ₂ - and Et ₂ ProR848 NPs compared to free R848.	61
Figure 3.5 Activation of RawBlue cells after dosing of R848 and silanol-R848 together.	63
Figure 3.6 Cytotoxicity of Me ₂ Pro-R848 particles and monomer.....	64
Figure 3.7 Serum cytokine profiles for soluble and particulate R848	65

Figure 3.8 R848-NPs significantly improve production of OVA-specific antibodies compared to soluble administration.	66
Figure 3.9 R848-NP formulation shows dose sparing effects for adjuvant dosage compared to soluble administration.	67
Figure 3.10 R848-NP formulation shows dose-sparing effects in antigen dosing compared to soluble R848 administration.	67
Figure 3.11 R848-NP dosage shows OVA-specific antibodies persisting in the blood out to at least 120 days.	68
Figure 4.1 DV2-specific IgG antibody response after prime and boost dose.	89
Figure 4.2 Antibody response to soluble DV2.	90
Figure A.1 MS spectrum of Me ₂ ProR848 dissolved in methanol.	115
Figure A.2 ¹ H NMR Spectrum of Me ₂ ProR848 dissolved in CD ₂ Cl ₂	116
Figure A.3 Two Dimensional NMR of Me ₂ ProR848 dissolved in CD ₂ Cl ₂	117
Figure A.4 MS spectrum of Et ₂ ProR848 dissolved in methanol.	118
Figure A.5 ¹ H NMR spectrum of Et ₂ ProR848 dissolved in deuterated methanol.	119
Figure A.6 LC-MS analysis of Me ₂ ProR848-NP degradation products.	120
Figure A.7 Neutralizing antibody assay of DV2 study.	122

LIST OF TABLES

Table 1.1 Toll-Like Receptors and their mode of action	5
Table 2.1 Characterization of bare NPs	20
Table 2.2 Characterization of OVA-conjugated NPs	25
Table 2.3 Composition of hydrogel particles.....	40
Table 3.1 Composition of Pro-Adjuvant NPs and Blank NPs	56
Table 3.2 Characterization of ProAdjuvant NPs	56
Table 3.3 Half-life of Me ₂ ProR848-NPs <i>in situ</i>	59
Table 3.4 Half maximal effective concentration (EC ₅₀) for R848 and ProR848 formulations	62
Table 4.1 Low OVA:NP ratio reactions	87
Table 4.2 Composition of PRINT NPs	94
Table A.1 Dengue conjugation reaction conditions.....	121

LIST OF SCHEMES

Scheme 3.1 Synthesis of R ₂ ProR848	55
Scheme 3.2 Two-step degradation mechanism of R848 from Me ₂ ProR848-NPs	57

LIST OF ABBREVIATIONS AND SYMBOLS

1k, 5k	molecular weight 1000 g/mol, 5000 g/mol
14k	1,400
ADE	antibody-dependent enhancement
AEM	2-aminoethyl methacrylate
Alum	aluminum salts
APC	antigen presenting cell
BCA assay	bicinchoninic acid assay
BMDC	bone marrow derived dendritic cell
°C	degrees Celsius
CD ₂ Cl ₂	deuterated dichloromethane
CD ₃ OD	deuterated methanol
c-di-GMP	cyclic dimeric guanosine monophosphate
CLR	C-type lectin receptor
CpG	CpG Oligodeoxynucleotide
CSM	cure-site monomer
CYD	yellow fever 17D
DEET	diethyltoluamide
DENV	dengue virus
DC	Dendritic cell
DLN	draining lymph node
DMF	Dimethylformamide
DNA	Deoxyribonucleic acid

DV2	dengue virus, serotype 2
E	dengue virus envelope protein
EC ₅₀	Half maximal effective concentration
ECM	extracellular matrix
EDC	(1-ethyl-3-(3-dimethylaminopropyl)carbodiimide
ELISA	enzyme-linked immunosorbent assay
Et ₂ ProR848	diethyl bis-silyl ether acrylate R848
FBS	fetal bovine serum
FDA	USA Food and Drug Administration
flu	influenza
GBS	group B <i>Streptococcus</i> antigen
GLA	Glucopyranosyl Lipid Adjuvant
GMP	good manufacturing practice
h	hour
HA	influenza hemagglutinin A protein
HEA	Hydroxyethyl acrylate
HIV	human immunodeficiency virus
HP(250)A	hydroxy tetraethylene glycol acrylate, molecular weight = 250 g/mol
HPLC	high performance liquid chromatography
HPV	human papillomavirus
HRMS	high resolution mass spectrometry
ICMV	interbilayer-crosslinked multilamellar vesicles
Ig	immunoglobulin, antibody

IL	interleukin
ISCOM	immunostimulating complex
LA	live attenuated
LC-MS	liquid chromatography-mass spectrometry
LN	Lymph node M1, M2 influenza matrix proteins
LPS	lipopolysaccharide
LTQFT	Linear ion trap – Fourier transform mass spectrometry
MeOH	methanol
Me ₂ ProR848	dimethyl bis silyl ether acrylate R848
MHz	megahertz
mL	milliliter, 10 ⁻³ liters
mM	millimolar
min	minute
MP	microparticle
MPLA	monophosphoryl lipid A
MPS	mononuclear phagocyte system
MS	mass spectrometry
MS	microsphere
MW	molecular weight
NA	influenza neuraminidase protein
NHS	N-Hydroxysuccinimide
NLR	nod-like receptor
nm	nanometer; 10 ⁻⁹ meters

NMR	nuclear magnetic resonance
NP	nanoparticle
OCT	optimal cutting temperature
OD	optical density
OVA	ovalbumin
PAMP	pattern associated molecular pattern
PC	dioleoylphosphatidylcholine
PEG	Poly(ethylene glycol)
PEGDA	poly(ethylene glycol) diacrylate, molecular weight = 700 g/mol
PFPE	perfluoropolyether
PLGA	poly(lactic- <i>co</i> -glycolic acid)
PLN	Popliteal lymph node
Poly(I:C)	polyinosinic:polycytidylic acid
PRINT	particle replication in non-wetting templates
prM	dengue virus premembrane protein
PRR	pattern recognition receptor
psi	pounds per square inch
PVOH	poly(vinyl alcohol)
R	any alkyl group
recE	recombinant dengue virus envelope protein
RLR	Rig-1-like receptor
RPM	rotations per minute
SEM	scanning electron microscopy

SiO ₂	silicon dioxide
TLR	toll like receptor
TMB	3,3',5,5'-tetramethylbenzidine
TNF	tumor necrosis factor
TPO	2,4,6 trimethylbenzoyl diphenylphosphine oxide
UV	ultra-violet
VLP	virus-like particle
μL	microliter, 10 ⁻⁶ liters
μm	micron; 10 ⁻⁶ meters
λ _{max}	maximum emission of ultra violet radiation

CHAPTER 1 VACCINATION AND THE PROMISE OF PARTICLE MEDIATED IMMUNITY

1.1 Modern Vaccination Strategies and Subunit Vaccines

Vaccination has revolutionized preventative medicine, providing the opportunity to avert deadly diseases rather than scrambling to treat them once they have infected a patient or community. The tremendous success of vaccination, however, has humble origins. Although a process known as variolation was practiced as least as early as the eleventh century in China and India,¹ true vaccination was not developed until Edward Jenner's work in the late 1790s.² Jenner discovered that inoculating a person with material from the cowpox infection of a milk maid would result in immunity against smallpox. Advances on this initial discovery paved the way for further development of the vaccine, eventually leading to the total eradication of smallpox in 1980.²

Since the time of Jenner, vaccines have been developed against nearly thirty different diseases.³ Most vaccines fall into one of two categories of whole-pathogen vaccines: inactivated or live attenuated. Live attenuated vaccines are synthesized by growing a virus in cell culture or another host organism (eggs are widely used) and passaging it through multiple generations until the virus has adapted to growing in non-human cells. The attenuated virus is rendered less capable of infecting humans, but is still able to replicate, though to a much lesser extent.¹ Because they are still able to replicate in the body, attenuated vaccines are very immunogenic, often providing protection after a single dose.⁴ Attenuated vaccines, however, are often

contraindicated for immunocompromised patients because they carry the risk for the attenuated pathogen to revert back to its original, infectious form.^{5,6}

Inactivated virus vaccines are fabricated by taking a virus and totally inactivating it by exposure to heat, ultra-violet radiation, or chemicals such as formaldehyde. The killed virus is unable to replicate *in vivo* but still contains the virus capsid structure, which is recognized by immune cells.¹ Inactivated vaccines are non-replicating, thereby avoiding the risk of infection, but are also less immunogenic, requiring regular booster doses.⁴ They are, however, safer for dosing in immunocompromised patients.

The next generation of vaccines is based on dosing pathogen subunits rather than whole pathogens. The subunits used represent the antigenic portions of the pathogen – surface proteins, DNA, polysaccharides, lipids – recognized by the immune system, instructing it to mount an immune response. Subunits can be either purified from the whole pathogen or synthesized in a lab. Purified subunits rely on growing large amounts of the pathogen, as with whole pathogen vaccines, leading to a reliance on the supply chain of cell or animal culture as well as being limited by the time it takes to grow the pathogen. They are potentially safer than whole pathogen vaccines, as the majority of the pathogen has been discarded. On the other hand, synthetic subunits can be made relatively quickly and easily without having contact with infectious material. Synthetic subunits can be expressed in high quantities in cell culture or fabricated *de novo* by different instruments.

As vaccines become less and less similar to the original pathogen, their immunogenicity wanes. When dosed alone, soluble subunits are not well recognized by the immune system and

are quickly cleared and degraded by the body. Different formulation and delivery techniques are being investigated to boost the immunogenicity of protein subunits as will be discussed below.

1.2 Activating Toll-Like Receptors as Vaccine Adjuvants

In order to improve the immunogenicity of vaccines, whole pathogens and antigen subunits are often formulated with one or more adjuvant. The purpose of an adjuvant is to modulate the response against a vaccine antigen while reducing the amount of antigen required to induce immunity.⁷ The most widely used category of adjuvants is aluminum salts – (Al(OH)₃), aluminum phosphate (AlPO₄) or alum (AlK(SO₄)₂·12H₂O).^{8,9} Aluminum salts, generally referred to as Alum, have been in use in vaccines since the 1920s. The mechanism of action for Alum is not well known, but studies have shown that adsorption of antigens to Alum helps to create a depot effect at the site of vaccine administration, allowing for prolonged release of antigen.¹⁰ Additionally, Alum may facilitate the production of other pro-inflammatory signals, leading to immune cell recruitment and enhanced uptake and presentation of antigen.¹⁰

Current adjuvant development strategies have focused on the rational design of molecules to mimic biologically conserved pathogen associated molecular patterns (PAMPs). PAMPs are molecular “danger signals” that are common to viruses and bacteria but are not found in higher organisms, indicating to the immune system that they belong to a non-self invader. PAMPs are recognized by a broad class of immune cell receptors called pattern recognition receptors (PRRs), trans-membrane proteins found on the cell surface, in endosomal compartments, and in the cytosol. PRRs are further broken down into toll-like receptors (TLRs), C-type lectin receptors (CLRs), nod-like receptors (NLRs), and Rig-1-like receptors (RLRs) depending on the type of pattern they recognize and the structure of the receptor. While all of these may be viable targets for vaccine adjuvant development, the scope of this work will focus on TLRs.

There are ten TLRs that have been identified in humans and thirteen in mice, each recognizing a different PAMP.¹¹ Table 1.1 outlines some of the TLRs that have been studied for vaccine applications, the PAMP recognized, and the adjuvant(s) used as ligands for those TLRs. When incorporating TLR ligands into vaccine formulations, these molecules activate the immune system by mimicking the danger signals presented by pathogens, augmenting the immune response against weakly immunogenic antigens. This strategy has been used in only a few vaccines available in the USA: human papillomavirus vaccine (Cervarix[®], GlaxoSmithKline) and hepatitis B virus vaccine (Fendrix[®], GlaxoSmithKline), which include a combined adjuvant, AS04, made up of MPLA (monophosphoryl lipid A) and Alum.¹² Many other TLR adjuvants and adjuvant systems have been examined at various stages of pre-clinical and clinical trials.^{7,13,14} Wide spread adoption of these vaccine adjuvants has been delayed due to the potential side effects and toxicity associated with systemic exposure to these potent compounds.¹⁵⁻¹⁸ Formulating adjuvants into particulate delivery vehicles, thereby directing uptake and release towards immune cells, may mitigate the effects of systemic exposure to both adjuvants and the pro-inflammatory cytokines they elicit from immune cells.¹³

Table 1.1 Toll-Like Receptors and their mode of action^{13,19,20}

Toll-Like Receptor	PAMP recognized	Adjuvant/Ligand
TLR1/TLR2	Gram-positive and gram-negative bacteria components: di- and triacetylated lipoproteins, peptidoglycans, lipopolysaccharides	PAM ₃ CAG
TLR2/TLR6		FSL-1 (synthetic diacetylated lipoprotein)
TLR3	Viral double stranded RNA, tRNA, siRNA	Poly (I:C)
TLR4	Structural component of gram-negative bacteria: lipopolysaccharides	LPS, MPLA
TLR5	Gram-positive and gram-negative bacterial flagellum	Flagellin
TLR7	Single stranded RNA, Imidazoquinolines, guanosine analogs	R848, imiquimod, loxoribine, 3M-019, 3M-052
TLR8	Single stranded RNA, Imidazoquinolines	R848
TLR9	Bacterial DNA	CpG ODN

1.3 Current Strategies for Particle-Based Delivery Vehicles for Subunit Vaccines

As detailed above, dosing soluble protein antigens and adjuvants both present challenges. By allowing these pathogen subunits to distribute throughout the body, as opposed to targeting them to the immune system, the bioavailability for uptake by immune cells declines and potential for off-target inflammatory effects grows. In order to formulate these subunits in a manner resembling their natural presentation by pathogens, thereby facilitating a more robust immune response, many groups have investigated various particle formulation strategies. Some of the

major categories of vaccine delivery vehicles include virus-like particles (VLPs), lipid-based particles, and polymer-based particles.^{13,14,21}

Virus-like particles (VLPs) closely resemble natural pathogens. VLPs are self-assembled nanoparticles made up of the capsid proteins of non-pathogenic viruses or assemblies of the antigenic protein itself.²²⁻²⁴ The HPV vaccines Cervarix and Gardasil® (Merck) are based on proteins from several strains of HPV that self-assemble into VLPs.²⁵ Relatively few antigenic proteins self-assemble into VLPs, so non-immunogenic VLPs can be used to deliver vaccine subunits carried in their interior or displayed on their surface.²⁶ This second category of VLPs is more widely applicable, but carries the potential for “viral interference” where patients develop antibodies against the vaccine vector rather than or in addition to the target antigen.²⁷

Lipid-based particles include liposomes, immunostimulating complexes (ISCOMs), and interbilayer-crosslinked multilamellar vesicles (ICMVs). These particle types are made up of lipid bilayers, which provide the opportunity to trap hydrophilic cargo in the particle core or between the layers of the particle and incorporate hydrophobic cargo within the lipid bilayers. ISCOMs are cage-like particles that spontaneously form when cholesterol, phospholipids, and the saponin adjuvant Quil A are combined in the correct ratio and act as antigen carriers as well as adjuvants.^{14,24} ICMVs have the additional benefit of having crosslinks between lipid bilayers, increasing the long term stability of the particles.²⁸ These versatile lipid-based particles have been used to deliver multiple different antigens for diseases ranging from influenza to malaria to cancer.^{13,29}

There is a wide variety of polymers that have been studied for use as vaccine delivery vehicles. Broadly, polymeric particles for vaccine delivery have been made from biopolymers

(e.g. chitosan, heparin), biodegradable polymers (e.g. poly(lactic-*co*-glycolic acid), poly(ϵ -caprolactone)), and non-degradable, biocompatible polymers (e.g. poly(ethylene glycol)), poly(methyl methacrylate)).^{21,30,31} Each category of polymers has different properties that can be exploited depending on the needs of a delivery system. For example, hydrophobic polymers like PLGA (poly(lactic-*co*-glycolic acid)) can be used to efficiently encapsulate hydrophobic antigens and adjuvants while hydrophilic polymers like PEG (poly(ethylene glycol)) can be used to encapsulate hydrophilic vaccine components. Additionally, polymeric systems can be modified with various functional handles for post-fabrication chemistries. Biopolymers and biodegradable polymers can be degraded by changes in pH, reducing environments found within the endosome and cytosol, or enzymes in the body; non-degradable particles are often cleared more slowly by the liver or kidneys.

Several major techniques are used for fabricating polymeric nano- and microparticles. One of the most utilized techniques is emulsion polymerization.^{14,21,32–35} Emulsion polymerization uses hydrophobic monomers and polymerizes them within amphipathic surfactant micelles.^{34,36} Hydrophobic cargos can be physically entrapped or covalently conjugated into the polymer core while the corona of surfactant molecules provide additional stability. Hydrophilic antigens and adjuvants may also be conjugated to the surface of the particles via the hydrophilic portions of the surfactant molecules.³⁴ Other particle fabrication techniques include precipitation,³⁷ electrospray,³⁸ and dendrimer formation.³⁹ Unique among the available particle fabrication technologies, PRINT – Particle Replication in Non-wetting Templates – allows for fabrication of nano- and microparticles with discrete size, shape, composition, and surface properties.^{40,41}

1.4 Fabrication of Nanoparticles via PRINT Technology – Controlling Size, Shape, Composition, and Surface Properties

PRINT (Particle Replication in Non-wetting Templates) is a unique particle molding technique combining lithographic methods from the semiconductor industry with the non-wetting properties of fluorinated polymers. Previous research on nano- and microparticle delivery vehicles for vaccine applications has been limited by particle fabrication methods that are often incapable of yielding homogeneous particles and are incompatible with industrial scale-up. The use of PRINT technology avoids these issues, allowing for precise control over particle size, shape, composition, and surface characteristics.⁴¹ In addition, PRINT is a highly scalable, GMP compliant process.

PRINT was first developed in the DeSimone Group in the mid-2000s and has led to the subsequent formation of Liquidia Technologies, a start-up company focused on commercializing PRINT technology. As pictured below in Figure 1.1, fabrication of particles via PRINT begins with a silicon wafer patterned with the feature size and shape of interest using traditional photolithography techniques. Low-surface energy perfluoropolyether (PFPE) is then applied to the silicon master template and chemically cross-linked to create a flexible elastomeric film with nano- or micron-sized cavities, known as a PRINT mold. The low surface energy of the PFPE allows for it to wet the entire surface of the mater template, resulting in faithful reproduction of the features. Additionally, the chemical resistance of PFPE prevents deformation of the PRINT mold when exposed to the organic solutions used in making monomer and polymer films, aiding in the fidelity of the produced particles to the original master template.⁴² The PRINT mold is then filled using a thin film of the monomer or polymer solution of the desired composition for the final particles. The versatility of PRINT technology allows for particles to be fabricated from essentially any material that can be made into a film, including PEG based hydrogels, PLGA and

other FDA approved materials, proteins, and chemotherapeutics.^{40,41,43-45} Capillary action is harnessed to fill nano-sized cavities while mechanical force aids in filling larger features. The non-wetting nature of PFPE prevents excess monomer or polymer from creating an interconnecting flash layer or scum layer, resulting in individual particles. When using a monomer solution, the monomer filled mold is photocured by brief irradiation by ultra-violet light, resulting in cross-linked particles. Particles can be removed from the PRINT mold by mating the filled mold with a sacrificial harvesting layer made of water soluble polymer capable of forming hydrogen bonds with the newly fabricated PRINT particles. Common harvesting layers are composed of poly(vinyl alcohol) (PVOH) and Plasdone™. Running the mold and harvesting layer through a heated laminator allows for the transfer of particles to the harvesting layer, leaving an array of particles on the sacrificial harvesting layer and an empty mold. The harvesting layer is then dissolved away using water or another appropriate solvent, yielding a dispersion of nearly monodisperse particles.

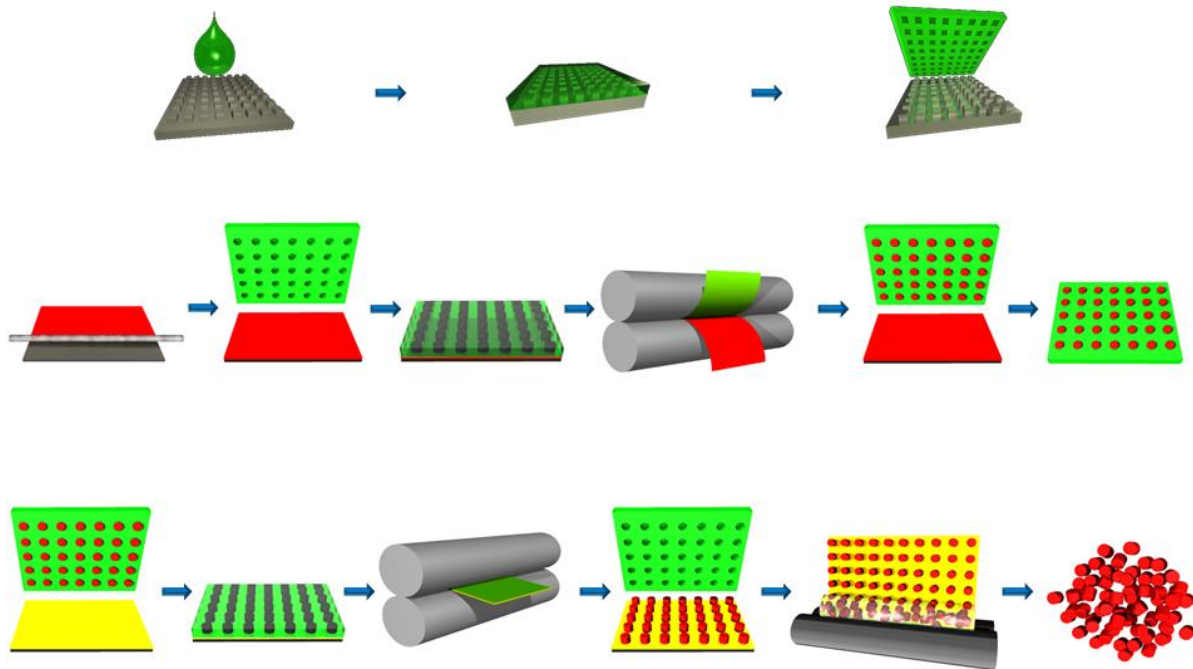


Figure 1.1 Particle Replication in Non-wetting Templates. A silicon wafer (gray) is patterned with nano- or micron-sized features through photolithography methods. PFPE (green) is dispersed across the silicon wafer and chemically cross-linked, yielding an elastomeric PRINT mold. A monomer or polymer thin film (red) is spread across a sheet of poly(ethylene terephthalate) (PET) and mated to the PRINT mold. Upon passing the mold and film through a laminator nip, the mold is filled with the particle material of choice. The filled mold is cured if necessary before being mated to a sacrificial harvesting layer (yellow) and passed again through a heated laminator. The mold is then removed from the harvesting sheet, revealing an array of individual particles. The sacrificial harvesting layer is then dissolved in a bead of water, revealing a nearly monodisperse solution of PRINT particles.

For vaccine applications, PRINT allows for imitation of natural pathogens in particle size, shape, and surface display of vaccine subunits. Previous work has shown that PLGA-based PRINT particles can be used to effectively adsorb influenza antigen, leading to an increased immune response compared to dosing the trivalent inactivated virus vaccine.⁴⁶ Investigation into this promising strategy is ongoing; however, changing the particle matrix from PLGA to a PEG based hydrogel system presents new opportunities for vaccine subunit delivery. The functional diversity of monomers that can be incorporated into the hydrogel particles affords the opportunity to conjugate vaccine subunit cargos throughout the particle matrix as well as conjugate cargos to the surface of the particles. The inert hydrogel matrix results in particles that are non-immunogenic, averting an immune response against the delivery vehicle.⁴⁷ Beyond

mirroring pathogen presentation of antigens and adjuvants, PRINT provides an opportunity to explore the relationship between particle size, shape, and surface characteristics, antigen and adjuvant trafficking and presentation, and the subsequent immune response. How these characteristics work together to stimulate the immune system, toward the goal of formulating safer, more effective subunit vaccines, will be explored in this work.

1.5 References

- (1) Plotkin, S. A. *Nat. Med.* **2005**, *11*, S5–11.
- (2) Riedel, S. *Proc. (Bayl. Univ. Med. Cent.)*. **2005**, *18*, 21–25.
- (3) Vaccines and Preventable Diseases <http://www.cdc.gov/vaccines/vpd-vac/> (accessed Sep 10, 2014).
- (4) Vaccines <http://www.niaid.nih.gov/topics/vaccines/understanding/pages/typesvaccines.aspx> (accessed Sep 12, 2014).
- (5) Zbinden, D.; Manuel, O. *Immunotherapy* **2014**, *6*, 131–139.
- (6) Ison, M. G.; Michaels, M. G. *Am. J. Transplant* **2009**, *9 Suppl 4*, S166–72.
- (7) Levast, B.; Awate, S.; Babiuk, L.; Mutwiri, G.; Gerdt, V.; van Drunen Littel-van den Hurk, S. *Vaccines* **2014**, *2*, 297–322.
- (8) Baylor, N. W.; Egan, W.; Richman, P. *Vaccine* **2002**, *20 Suppl 3*, S18–23.
- (9) Gupta, R.; Rost, B.; Relyveld, E.; Siber, G. *Vaccine Des.* **1995**, *6*, 229–248.
- (10) Marrack, P.; McKee, A. S.; Munks, M. W. *Nat. Rev. Immunol.* **2009**, *9*, 287–293.
- (11) Kawai, T.; Akira, S. *Cell Death Differ.* **2006**, *13*, 816–825.
- (12) Didierlaurent, A. M.; Morel, S.; Lockman, L.; Giannini, S. L.; Bisteau, M.; Carlsen, H.; Kielland, A.; Vosters, O.; Vanderheyde, N.; Schiavetti, F.; Larocque, D.; Van Mechelen, M.; Garçon, N. *J. Immunol.* **2009**, *183*, 6186–6197.
- (13) Demento, S. L.; Siefert, A. L.; Bandyopadhyay, A.; Sharp, F. A.; Fahmy, T. M. *Trends Biotechnol.* **2011**, *29*, 294–306.
- (14) de Temmerman, M.-L.; Rejman, J.; Demeester, J.; Irvine, D. J.; Gander, B.; De Smedt, S. *C. Drug Discov. Today* **2011**, *16*, 569–582.
- (15) Ahmed, S. S.; Plotkin, S. A.; Black, S.; Coffman, R. L. *Sci. Transl. Med.* **2011**, *3*, 93rv2.
- (16) Fife, K. H.; Meng, T.-C.; Ferris, D. G.; Liu, P. *Antimicrob. Agents Chemother.* **2008**, *52*, 477–482.
- (17) Szeimies, R.-M.; Bichel, J.; Ortonne, J.-P.; Stockfleth, E.; Lee, J.; Meng, T.-C. *Br. J. Dermatol.* **2008**, *159*, 205–210.

- (18) Dockrell, D. H.; Kinghorn, G. R. *J. Antimicrob. Chemother.* **2001**, *48*, 751–755.
- (19) Belz, G.; Smith, C.; Bharadwaj, M.; Rice, A.; Jackson, D. *Cytotherapy* **2004**, *6*, 88–98.
- (20) Storni, T.; Kündig, T. M.; Senti, G.; Johansen, P. *Adv. Drug Deliv. Rev.* **2005**, *57*, 333–355.
- (21) Ferreira, S. A.; Gama, F. M.; Vilanova, M. *Nanomedicine* **2013**, *9*, 159–173.
- (22) Noad, R.; Roy, P. *Trends Microbiol.* **2003**, *11*, 438–444.
- (23) Grgacic, E. V. L.; Anderson, D. A. *Methods* **2006**, *40*, 60–65.
- (24) Zhao, L.; Seth, A.; Wibowo, N.; Zhao, C.-X.; Mitter, N.; Yu, C.; Middelberg, A. P. J. *Vaccine* **2014**, *32*, 327–337.
- (25) Kang, S.-M.; Song, J.-M.; Quan, F.-S.; Compans, R. W. *Virus Res.* **2009**, *143*, 140–146.
- (26) Tissot, A. C.; Renhofa, R.; Schmitz, N.; Cielens, I.; Meijerink, E.; Ose, V.; Jennings, G. T.; Saudan, P.; Pumpens, P.; Bachmann, M. F. *PLoS One* **2010**, *5*, e9809.
- (27) Khanam, S.; Rajendra, P.; Khanna, N.; Swaminathan, S. *BMC Biotechnol.* **2007**, *7*, 10.
- (28) Moon, J. J.; Suh, H.; Bershteyn, A.; Stephan, M. T.; Liu, H.; Huang, B.; Sohail, M.; Luo, S.; Um, S. H.; Khant, H.; Goodwin, J. T.; Ramos, J.; Chiu, W.; Irvine, D. J. *Nat. Mater.* **2011**, *10*, 243–251.
- (29) Moon, J. J.; Suh, H.; Li, A. V.; Ockenhouse, C. F.; Yadava, A.; Irvine, D. J. *Proc. Natl. Acad. Sci. U. S. A.* **2012**, *109*, 1080–1085.
- (30) Socha, M.; Bartecki, P.; Passirani, C.; Sapin, A.; Damgé, C.; Lecompte, T.; Barré, J.; El Ghazouani, F.; Maincent, P. *J. Drug Target.* **2009**, *17*, 575–585.
- (31) Passirani, C.; Barratt, G.; Devissaguet, J.-P.; Labarre, D. *Life Sci.* **1998**, *62*, 775–785.
- (32) Hirosue, S.; Kourtis, I. C.; van der Vlies, A. J.; Hubbell, J. A.; Swartz, M. A. *Vaccine* **2010**, *28*, 7897–7906.
- (33) Ilyinskii, P. O.; Roy, C. J.; O’Neil, C. P.; Browning, E. A.; Pittet, L. A.; Altreuter, D. H.; Alexis, F.; Tonti, E.; Shi, J.; Basto, P. A.; Iannacone, M.; Radovic-Moreno, A. F.; Langer, R. S.; Farokhzad, O. C.; von Andrian, U. H.; Johnston, L. P. M.; Kishimoto, T. K. *Vaccine* **2014**, *32*, 2882–2895.
- (34) Hubbell, J. A.; Thomas, S. N.; Swartz, M. A. *Nature* **2009**, *462*, 449–460.

- (35) Akagi, T.; Baba, M.; Akashi, M. In *Polymers in Nanomedicine*; Kunugi, S.; Yamaoka, T., Eds.; Springer Berlin Heidelberg, 2012; pp. 31–64.
- (36) Rehor, A.; Tirelli, N.; Hubbell, J. A. *Macromolecules* **2002**, *35*, 8688–8693.
- (37) John, A. L. S.; Chan, C. Y.; Staats, H. F.; Leong, K. W.; Abraham, S. N. *Nat. Mater.* **2012**, *11*, 1–8.
- (38) Duong, A. D.; Sharma, S.; Peine, K. J.; Gupta, G.; Satoskar, A. R.; Bachelder, E. M.; Wyslouzil, B. E.; Ainslie, K. M. *Mol. Pharm.* **2013**, *10*, 1045–1055.
- (39) Kaminskas, L. M.; Porter, C. J. H. *Adv. Drug Deliv. Rev.* **2011**, *63*, 890–900.
- (40) Perry, J. L.; Herlihy, K. P.; Napier, M. E.; Desimone, J. M. *Acc. Chem. Res.* **2011**, *44*, 990–998.
- (41) Rolland, J. P.; Maynor, B. W.; Euliss, L. E.; Exner, A. E.; Denison, G. M.; DeSimone, J. M. *J. Am. Chem. Soc.* **2005**, *127*, 10096–10100.
- (42) Rolland, J. P.; Hagberg, E. C.; Denison, G. M.; Carter, K. R.; De Simone, J. M. *Angew. Chemie* **2004**, *116*, 5920–5923.
- (43) Kelly, J. Y.; DeSimone, J. M. *J. Am. Chem. Soc.* **2008**, *130*, 5438–5439.
- (44) Perry, J.; Reuter, K.; Kai, M.; Herlihy, K. *Nano Lett.* **2012**, 1–16.
- (45) Enlow, E. M.; Luft, J. C.; Napier, M. E.; DeSimone, J. M. *Nano Lett.* **2011**, *11*, 808–813.
- (46) Galloway, A. L.; Murphy, A.; DeSimone, J. M.; Di, J.; Herrmann, J. P.; Hunter, M. E.; Kindig, J. P.; Malinoski, F. J.; Rumley, M. A.; Stoltz, D. M.; Templeman, T. S.; Hubby, B. *Nanomedicine* **2013**, *9*, 523–531.
- (47) Roberts, R. A.; Shen, T.; Allen, I. C.; Hasan, W.; DeSimone, J. M.; Ting, J. P. Y. *PLoS One* **2013**, *8*, e62115.

CHAPTER 2 MANIPULATING PHYSICOCHEMICAL PROPERTIES OF POLYMERIC HYDROGEL PARTICLES TO ENHANCE LYMPHATIC TRAFFICKING AND IMMUNOGENICITY OF A MODEL SUBUNIT VACCINE

2.1 Introduction

Draining lymph nodes (LNs) are the primary site of action for initiating adaptive immunity, where cells that initiate adaptive immune responses (T and B cells) meet antigen or antigen-loaded antigen presenting cells (dendritic cells, macrophages).^{1,2} To activate B cells and generate a robust humoral response, two signals are required: direct crosslinking of B cell receptors by antigens, and co-stimulatory signals from CD4⁺ T cells (e.g. cytokines and CD40/CD40L binding).^{3,4} Antigen presenting cells, especially dendritic cells (DCs) are critical in priming T cells to provide helper signals to B cells.⁴⁻⁹ Because of the myriad activities of the immune system that take place in the lymph nodes, recent literature has focused on delivering vaccines directly to the draining LNs.^{4,6,7,9,10} By targeting the draining LNs vaccine uptake by antigen presenting cells (APCs), APC maturation, and cross presentation to T and B cells may all occur in close proximity, thus increasing the potency of the resulting response.

Utilizing purified and synthetic pathogen subunits (peptides, polysaccharides, lipids, DNA, etc.) for vaccination has become an increasingly attractive option due to significantly improved safety profiles compared to whole pathogen-based vaccines. However, limited clinical success of subunit vaccines has been achieved, e.g. HPV vaccines (Gardasil[®] from Merck and Co., Cervarix[®] from GlaxoSmithKline) and seasonal influenza vaccines (Fluvirin[®] from Novartis). Purified antigens are usually poor immunogens. Soluble pathogen subunits are not

efficiently captured by immune cells, are susceptible to non-specific degradation and metabolism *in vivo* and are subject to rapid clearance.¹⁰⁻¹³ Particle mediated delivery has shown great potential for subunit vaccine development and has gained increasing attention.^{6,10-12,14-23} Size, shape, and surface properties of particle vectors can be manipulated to target key APCs and promote cell uptake of antigens via phagocytosis, or facilitate self-drainage and direct delivery of vaccine to lymph node-resident immune cells.^{10-13,24} Surface display of antigens on particle carriers may allow multivalent interaction with B cells that mimics presentation by natural pathogens, enabling more efficient cross-linking of cognate B cell receptors, thereby increasing potency of these agents^{10,17,25} and achieving dose sparing effects.^{14,25}

Many parameters of particulate vaccine carriers (charge, size, and surface properties) may all contribute to the quality of the resulting immune response. Previous work on lymphatic trafficking of nanoparticles (NPs) has focused on delivery of cancer therapeutics or diagnostic molecules to aid in LN imaging;^{21,26-31} only recently have the effects of lymphatic trafficking on the efficacy of novel, particulate vaccines been examined.^{16,19,20,23,32,33} Cationic NPs have been found to have higher uptake *in vitro* and facilitate a more favorable endosomal pH environment, mitigating premature degradation of acid-sensitive antigens.³⁴ Conversely, *in vivo* results favor anionic NPs for higher rates of NP trafficking and subsequent uptake by APCs. This critical difference between *in vitro* and *in vivo* results may be due to the composition of the extracellular matrix (ECM) in the interstitial space of the lymphatic system: collagen fibers and highly anionic glycosaminoglycans.³⁵ The high density of negative charge may lead to aggregation of cationic NPs at the injection site while the electrostatic repulsion allows anionic NPs to move through the interstitial fluid.³⁶ This has been observed in various NP systems such as liposomes,³⁷ dendrimers,²⁹ star polymers,³⁰ and PLGA based NPs.²⁸

Size plays perhaps the largest role in the trafficking of NPs from the site of injection through the lymphatic system. Lymphatic trafficking of many sizes and compositions of spherical NPs have been examined including PLGA NPs (size 50 – 200 nm),³⁸ liposomes (single and multi-lamellar),³⁷ dendrimers (size 5 – 15 nm),²⁹ star polymers (size 10 – 25 nm),³⁰ polystyrene beads (size 20 – 2000 nm),¹⁹ and other polymeric NPs (size 25 – 3700 nm)^{32,39} (all sizes reported as diameter). The ideal NP size to harness interstitial flow and passively target the LNs appears to be between 20 nm, under which NPs are likely to enter directly into systemic circulation,^{29,38} and 100 nm, above which size NPs become stuck at the site of injection and rely on cell-mediated trafficking to the LNs.¹⁰ Within this size range, the optimal NP size appears to be widely system dependent.^{19,21,36,39}

PEGylation (surface conjugation or coating with chains of poly(ethylene glycol)) is commonly used to conjugate various cargos to nanoparticles, polymers, and biologics. For the purpose of developing a vaccine carrier, the level of PEGylation used to attach the vaccine cargo to the nanoparticle carrier should take in to consideration the effects PEG length and PEGylation density may have on lymphatic drainage and uptake by immune cells. PEGylation has been studied extensively in the search for long-circulating NPs, capable of avoiding detection and clearance by the mononuclear phagocyte system (MPS). Studies have found that while a dense layer of long PEG chains is necessary to maximize circulation time, the desired effects of low protein binding and decreased phagocytic uptake are seen at even low PEG densities and chain lengths.^{40,41} PEGylation has also been studied for applications in mucosal penetration for intranasal delivery of therapeutics:⁴² PEG coating is believed to interact with the mucus layer in a way that prevents NP aggregation, facilitating NP transport. This finding may be applied to the gel-like environment of the ECM, increasing NP drainage from the site of injection.²² Previous

findings agree that PEGylation increases lymphatic drainage from the injection site throughout various densities and molecular weights of PEG,^{20–23,27,31,33,43} but findings are conflicting regarding how this affects uptake of PEGylated NPs in the LNs. A study with 300 nm liposomes indicated that PEGylation can not only increase drainage and uptake, but facilitate deeper NP penetration into all regions of the LNs.²⁰ Others have found that PEGylation actually decreases retention of NPs in the LNs and uptake by APCs.^{21,33} Further examination of the effects of PEGylation on vaccine delivery would be greatly beneficial in the design of future vaccine delivery vehicles.

In addition to PEGylation, other surface characteristics can have dramatic effects on how the body interacts with NP vaccine carriers. The complement system is the body's first line of defense against invading pathogens, linking innate and adaptive immunity and playing an important role in peripheral lymph nodes to enhance B and T cell responses.⁵² Hubbell and co-workers reported that nanoparticles can be engineered to activate the complement system and improve immune responses to vaccines.^{53,54} By utilizing a hydroxyl-terminated monomer versus a methoxy-terminated monomer as the primary component of NPs, particles can be designed to activate the complement system and facilitate a stronger immune response against antigen.

Herein we present a versatile vaccine delivery platform based on hydrogel particles made of hydroxy-poly(ethylene glycol) (PEG) via PRINT technology (Particle Replication in Non-Wetting Templates),^{44–46} a unique mold-based particle fabrication process. The highly tunable nature of PRINT allows for a great degree of control over NP size, aspect ratio, charge, and surface functionality, facilitating a systematic study of these effects on NP trafficking through the lymphatic system and the subsequent immune response. We have demonstrated that this

vaccine carrier has the capacity to deliver subunit vaccine components to the draining LNs in a sustained manner and elicit robust antigen-specific humoral immune response.

2.2 Results and Discussion

Nanoparticle delivery of protein subunit vaccines to the lymph nodes allows antigens to interact directly with the immune system. Additionally, surface display of protein antigens similar to antigen presentation by natural pathogens may boost therapeutic efficacy of these subunits to the levels associated with whole pathogen vaccines without the related safety concerns.^{4,8,47} This study aimed to evaluate PRINT nanoparticles of various size, aspect ratio, and surface characteristics for their ability to traffic through the lymphatic system and explore their use for antigen delivery in vaccine applications.

2.2.1 Lymphatic Trafficking of Bare Particles

A delivery vector that traffics quickly and efficiently to the draining lymph nodes would be beneficial for delivering antigens and/or adjuvants to B cells and other antigen presenting cells (APCs) resident in the lymph nodes. A panel of rod/cylindrical PRINT NPs of different size, aspect ratio, and surface charge (Table 2.1) were injected subcutaneously in mice and screened for their ability to drain to the popliteal lymph nodes (PLNs). Rod shaped NPs may have added benefits over traditional spherical NPs in terms of cellular uptake as well as an increased surface area for cargo loading.⁴⁵ An 80×180 nm rod has over 3 times the volume of a spherical NP with the same diameter and 2.75 times the surface area. Consistent with literature, we found that sub-100 nm diameter,^{16,19,36,48–50} anionic^{28–30,37,50} NPs were able to traffic quickly to the PLN, with an increase in NP concentration over 48 hours (Figure 2.1). In contrast, all other NPs, regardless of size and charge, generally remained at the site of injection with less than 0.2% of the injected dose trafficking to the PLN. Histology analysis of the resected PLNs revealed that large amounts

of anionic 80×180 nm NPs populated the B cell-follicular area, which may provide opportunity for antigen presentation to B cells and development of a humoral immune response (Figure 2.2).

Larger and cationic NPs showed little accumulation in the LNs.

Table 2.1 Characterization of bare NPs

Mold Dimensions	Size (d.nm)	PDI	Zeta Potential (mV)
80×180 nm (-)	200.8 ± 11.6	0.025	-24.6 ± 0.3
80×320 nm (-)	254.7 ± 6.8	0.061	-31.9 ± 0.2
80×2000 nm (-)	595.7 ± 2.6	0.133	-28.7 ± 0.5
200×200 nm (-)	251.2 ± 2.1	0.128	-29.8 ± 0.3
1x1 μm (-)	1292 ± 189	-	-30.0 ± 0.8
80×180 nm (+)	183.8 ± 2.4	0.126	42.0 ± 1.5
80×320 nm (+)	229.0 ± 2.9	0.045	44.4 ± 0.3
80×2000 nm (+)	370.2 ± 27.7	0.069	32.6 ± 1.4
200×200 nm (+)	256.2 ± 21.8	0.104	43.1 ± 1.8
1x1 μm (+)	2581 ± 6.6	-	22.0 ± 0.7

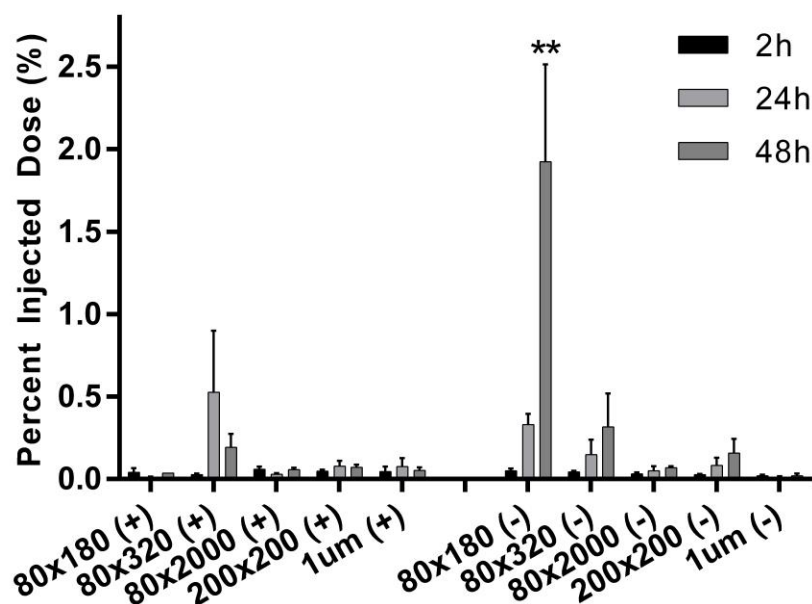


Figure 2.1 Lymphatic drainage and cell uptake of bare hydrogel particles. Mice were injected with 50 µg NPs in hind footpads. Draining PLNs were resected at indicated time points and examined for particle fluorescence by IVIS imaging. Error bars stand for SEM, N ≥ 4. **, p < 0.01 by one-way ANOVA compared to all other groups at 48 hours time point.

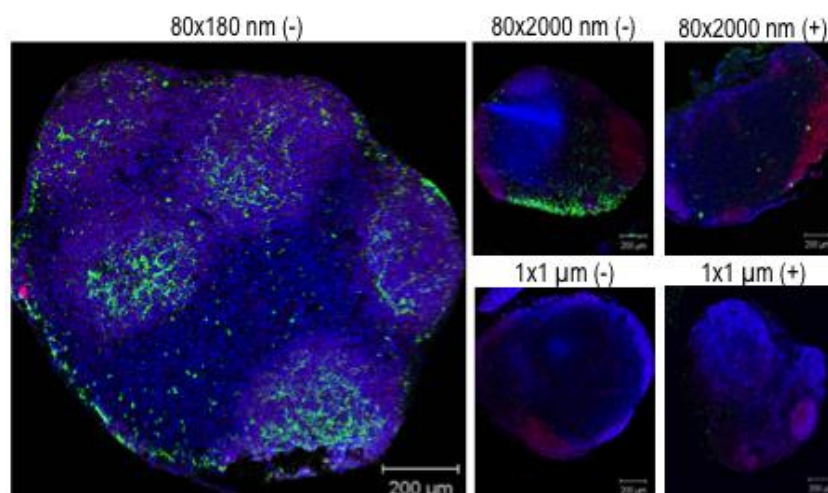


Figure 2.2 Localization of NPs in the PLNs was confirmed by confocal microscopy at 48 hours (80×180 nm NPs) or 72 hours (80×2000 nm and 1×1 µm NPs) post subcutaneous injections of different size and charge NPs. Blue: nuclei (DAPI); red: B cell (B220⁺); green: particles.

Flow cytometry was performed to determine which cell populations within the PLNs took up NPs. For all examined APC types (dendritic cells (DCs), macrophages, B cells, and plasmacytoid DCs) the anionic 80×180 nm NPs showed the highest uptake, i.e. percent of each

cell population that took up NPs (Figure 2.3). For all NP types, anionic NPs were present in a higher percentage of cells than their cationic counterpart. Similar to total lymphatic drainage, size dependence was observed with 80×180s being most efficiently internalized by all cell types examined. Strikingly, although less than 2% of total injected 80×180 nm NPs trafficked to the PLNs at 48 hours, an average of 20% of DCs in the LNs took up anionic 80×180 NPs, confirming that particle of this size, charge, and aspect ratio is able to target DCs.

Anionic 80×180 nm NPs, the best self-draining particle type, was chosen for further vaccine delivery studies.

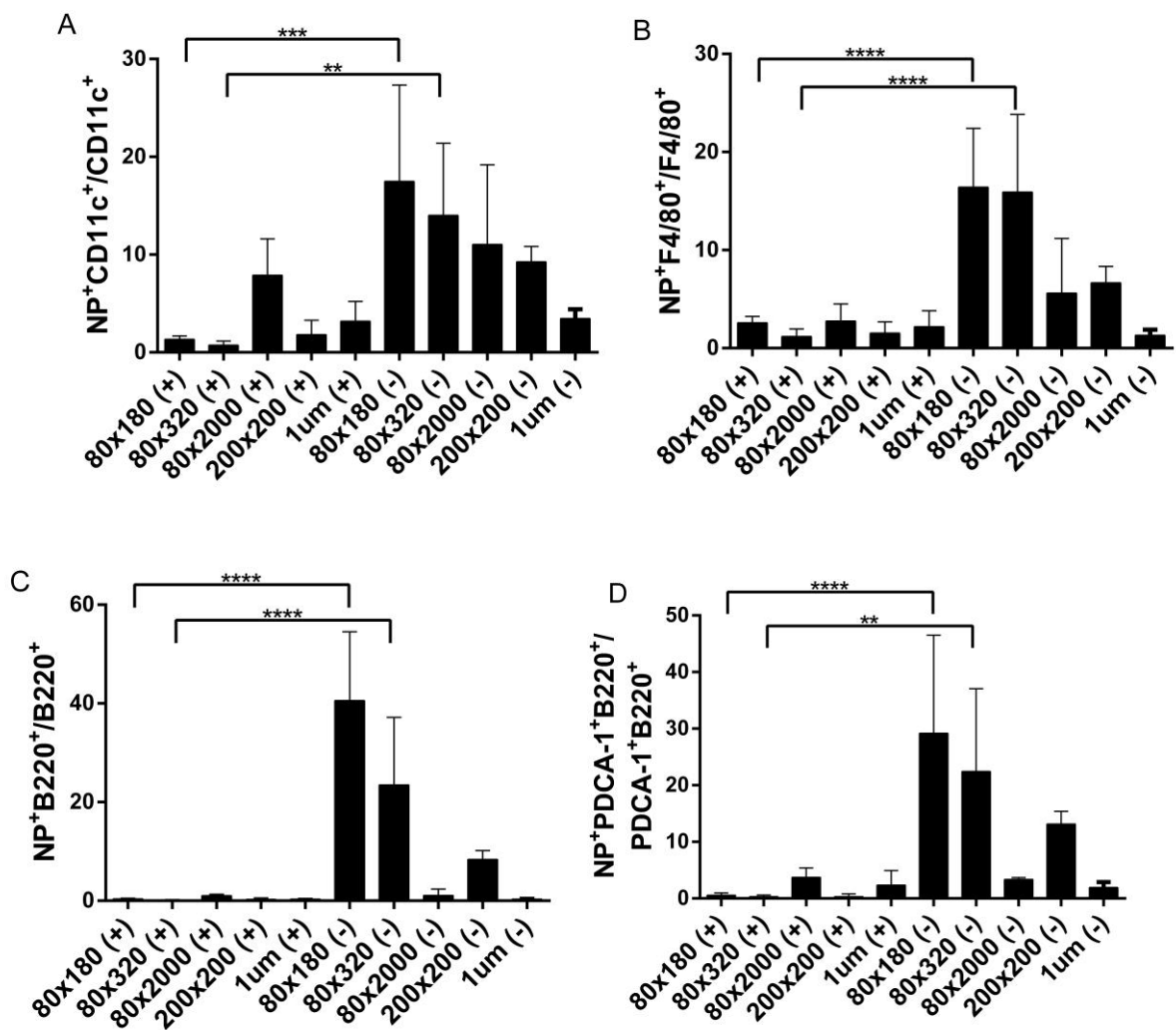


Figure 2.3 Flow cytometry of cells from lymph nodes resected 48 hours after injection. Data shown as NP positive cells/total cell population $\times 100$ to demonstrate percent of each cell type that had taken up NPs. A) Dendritic cells, DC11c⁺, B) macrophages, F4/80⁺, C) B cells, B220⁺, D) plasmacytoid DCs, PDCA-1⁺B220⁺. *, p < 0.05; **, p < 0.01; ***, p < 0.001; ****, p < 0.0001 by unpaired t test. N \geq 3.

2.2.2 Conjugation of Model Antigen and Surface Characteristics

Surface display of antigens greatly increases the chances of direct antigen presentation to B cells, facilitating a more robust antibody response. To test immunogenicity of antigen delivered by the hydrogel NP carrier, a model protein antigen ovalbumin (OVA) was covalently conjugated to the surface of 80 \times 180 nm NPs through various chemistries including poly(ethylene

glycol) (PEG)-based linkers, a common bioconjugation technique used to control the distance between ligands and NPs. PEGylation is frequently used to increase circulation half-life of small molecule drugs, biologics, and nanoparticles by decreasing the binding of serum proteins and opsonins, thus decreasing recognition by the mononuclear phagocyte system (MPS).⁵¹ For vaccine carriers, PEGylation may enhance drainage of NPs from the site of injection to the lymph nodes by blocking interactions with the extracellular matrix (ECM); however, a high level PEGylation, especially with high molecular weight PEG, could be undesirable as it may prevent NP uptake by phagocytic APCs.⁶ In order to examine the effect of PEG linker length on lymphatic drainage and cell uptake, OVA was conjugated to the surface of NPs via large, medium or small linkers: 5000 Da molecular weight PEG (PEG(5k)), 500 Da molecular weight PEG (PEG(500)), or a direct amide bond from protein to NP (PEG(0)) respectively. After conjugation of antigen, all NPs remained very well dispersed with polydispersity index (PDI) below 0.15 (Table 2.2). Forty-eight hours post-injection, significantly more PEG(500)OVA NPs reached PLNs as compared to the PEG(5k)OVA and PEG(0)OVA NPs (Figure 2.4). Surface modification with the long PEG(5k) linker was apparently not favorable for lymphatic drainage. Further comparison with bare NPs and no-OVA PEG(500) NPs indicated that the increase in trafficking for the PEG(500)OVA NPs came from the synergy between PEG(500) and OVA, rather than either component alone. PEGylation with a dense layer of short PEG(500) may stabilize the NPs under physiological conditions and decrease interactions with the ECM, while longer PEG(5k) may have a greater chance of becoming entangled with the biopolymers in the ECM.^{6,35} Additionally, compared to 80×180 nm PEG(500)OVA NPs, the 1 μm PEG(500)OVA NPs showed poor lymphatic trafficking on par with the bare 1 μm NPs (Figure 2.1); conjugation with PEG linker and OVA did not improve the drainage of 1 μm NPs. These results demonstrate

that the size of particles is an essential determinant for lymphatic drainage patterns of particle vectors, which can be further modulated by different lengths of PEG linkers.

Table 2.2 Characterization of OVA-conjugated NPs

Particle Type	Size (d.nm)	PDI	Zeta Potential (mV)	OVA Loading ($\mu\text{g}/\text{mg NP}$)
80 \times 180 nm bare	200.8 \pm 11.6	0.025	-24.6 \pm 0.3	–
80 \times 180 nm PEG(0)OVA	246.8 \pm 1.2	0.139	-33.6 \pm 1.2	30-100
80 \times 180 nm PEG(500)OVA	192.0 \pm 2.1	0.044	-39.3 \pm 1.6	30 – 90
80 \times 180 nm PEG(5k)OVA	191.3 \pm 0.6	0.076	-27.5 \pm 0.3	10 – 100
1 \times 1 μm PEG(500)OVA	1459 \pm 189.4	–	-7.0 \pm 0.5	10 – 100
1 \times 1 μm PEG(5k)OVA	1238 \pm 23.4	–	-9.6 \pm 0.4	10 – 100

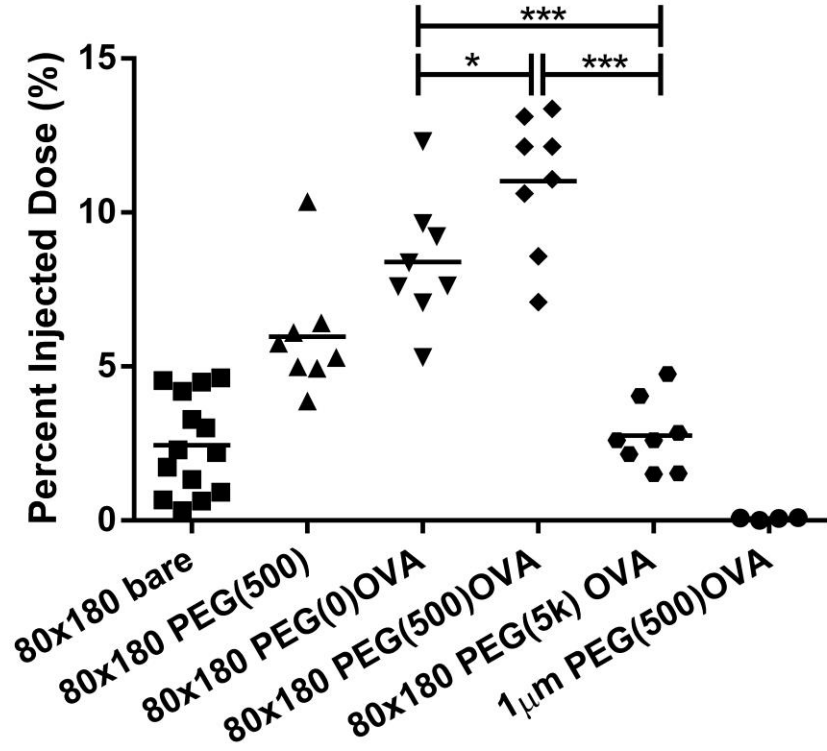


Figure 2.4 Total drainage OVA-loaded hydrogel of NPs in lymph nodes. 50 µg fluorescently labeled 80×180 nm hydrogels were subcutaneously injected into footpads of balb/c mice, and draining popliteal LNs were collected at 48 h, and imaged with IVIS Lumina. *, $p < 0.05$; ***, $p < 0.001$ by one-way ANOVA. N = 8-14.

The best draining particles, 80×180 nm PEG(500)OVA NPs, also showed rapid trafficking and were present in the PLN in as short as five minutes after injection, with the concentration of NPs in the PLN continuously increasing over forty-eight hours (Figure 2.5). At forty-eight hours, NP trafficking reached 10 % of total injected dose, 5× higher than bare anionic 80×180 nm NPs (2 %, Figure 2.1).

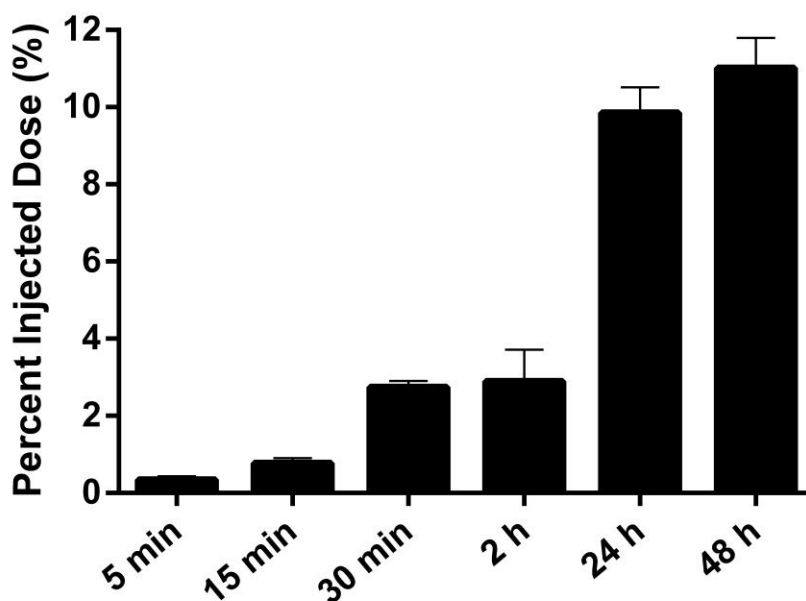


Figure 2.5 80×180 nm PEG(500)OVA NPs drained rapidly to the lymph nodes accumulated over 48 h. 50 µg fluorescently labeled 80×180 nm hydrogels were subcutaneously injected into footpads of balb/c mice. Draining popliteal LNs were collected at the indicated time points and imaged with IVIS Lumina. Error bars stand for SEM. N = 4-8.

In order to efficiently elicit an immune response, an effective NP delivery vector should ideally be able to ensure the antigen arrives at the site of action without being degraded or released prematurely. To compare the drainage of NP bound OVA to that of free OVA, we tagged the NPs and OVA with two different fluorophores. Free OVA (red) drained rapidly and was observed in the PLN two hours after injection, but was no longer detectable at twenty-four hours (Figure 2.6). This is consistent with literature indicating that soluble proteins are subject to quick lymphatic clearance.¹³ For 80×180 nm PEG(500)OVA NPs, particles and OVA (shown in yellow as overlapping of green NPs and red OVA) also drained quickly, as seen previously with the trafficking experiments, and were co-localized in the subcapsular regions of the PLN two hours after injection. NP-OVA (yellow) stayed in the PLN much longer than soluble OVA (red) and was still observed at 48 hours after injection (Figure 2.6), although the quantity of NP-OVA

(yellow) versus NPs alone (green) decreased over time, presumably due to OVA cleavage and degradation by proteases. More importantly, cleaved OVA (red) selectively accumulated in the B cell follicles and the presence of OVA in this region persisted for up to 15 days. A similar phenomenon was also observed for 80×180 nm PEG(0)OVA (Figure 2.6). This observation indicates that in general 80×180 nm hydrogel NPs are able to efficiently deliver antigen to the LNs and support sustained presentation of antigen to B cells. The longer residence time of NP-conjugated OVA in the PLN may help increase the interaction between antigen and B cells and LN-resident APCs compared to free OVA, resulting in an enhanced antibody response.

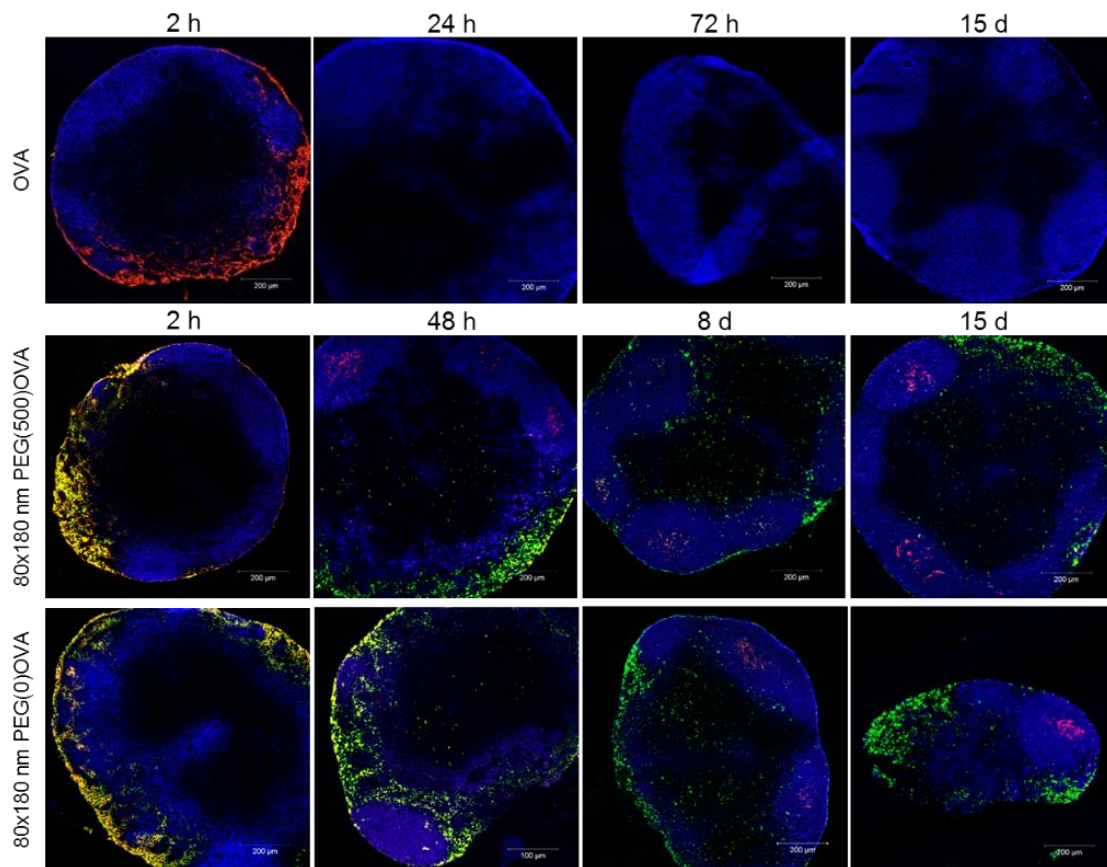


Figure 2.6 Persistent delivery of antigen to B cells in soluble form or by hydrogel NPs. Blue, B220 (B cells); green, NPs; red, OVA-AF555. Scale bar: 200 μm.

In addition to the delivery of antigens to B cells and crosslinking of cognate B cell receptors, eliciting a potent humoral response and B cell memory also requires help from CD4⁺ T cells,²⁴ therefore good vaccine carriers need to be able to deliver antigens to APCs and prime T cells efficiently. Analysis of draining LNs by flow cytometry showed that 48 hours post subcutaneous dosing, 80×180 nm hydrogels with OVA linked through all three linker lengths reached 10-20% of the DCs, and 10-35% of the macrophages in the PLNs while 1 μm PEG(500)OVA NPs were found in less than 2% of DCs or macrophages (Figure 2.7), indicating that the 80×180 nm NPs may efficiently deliver antigens to key APCs. Although the total drainage to LNs of these three NPs with various linker lengths (Figure 2.4) did not directly correlate with the uptake of NPs by cells in the PLNs, both results suggest that a long PEG linker is less favorable for antigen delivery to immune cells. The co-localization of the 80×180 nm PEG(500)OVA NPs with DCs was also observed by confocal microscopy analysis of sectioned draining LNs (Figure 2.8), indicating that these NPs are able to access all regions of the PLNs where B cell and T cell activation can occur, facilitating activation of both humoral and cellular immune responses.

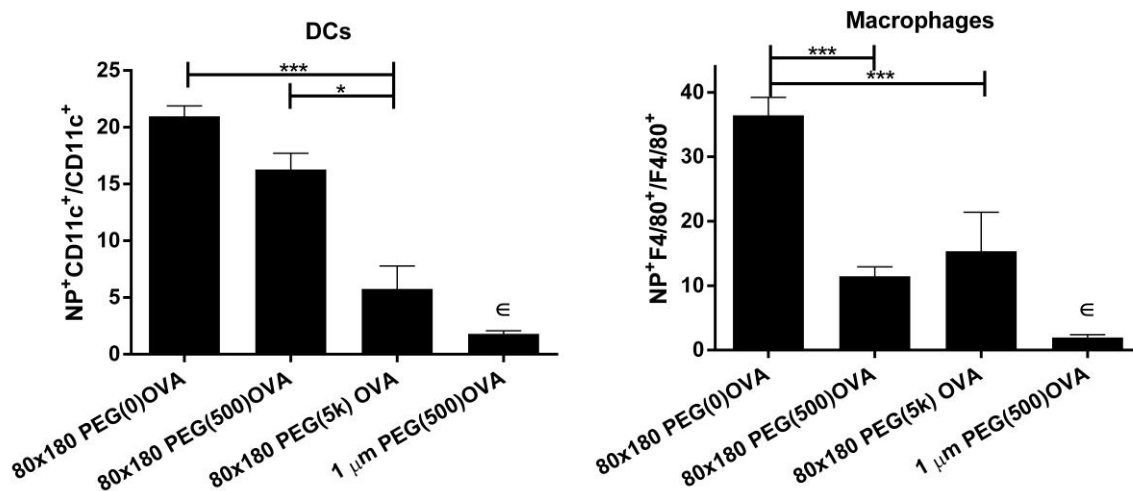


Figure 2.7 80×180 nm NPs are efficiently taken up by key antigen presenting cells (DCs and macrophages) in LNs 48 h post subcutaneous injection, as analyzed by flow cytometry. *, $p < 0.05$; **, $p < 0.01$; ***, $p < 0.001$; ε, $p < 0.001$ compared to all other groups, analyzed by unpaired t-test. $N \geq 4$.

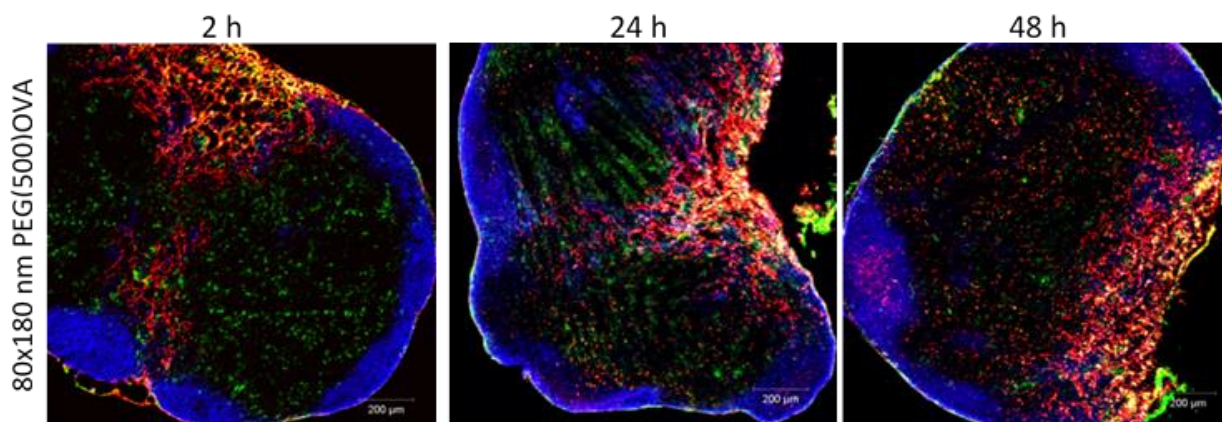


Figure 2.8 Uptake of 80×180 nm PEG(500)OVA particles by dendritic cells were confirmed by confocal microscopy at indicated time points post subcutaneous injections of particles. Blue: B cell (B220⁺); green: dendritic cells (CD11c⁺); red: particles.

The complement system acts not only as the first line of defense for the body, but also links innate and adaptive immunity and plays an important role in peripheral lymph nodes to enhance B and T cell responses.⁵² The complement system is activated by three different

pathways: classical, lectin, and alternative; however, all three pathways share a common step – activating the central component C3. Hubbell and co-workers reported that nanoparticles can be engineered to activate the complement system and improve immune responses to vaccines.^{53,54} Here we show that PRINT hydrogel NPs activate the complement system, as indicated by increase in the conversion of C3 to C3a (Figure 2.9a). Both bare and OVA-conjugated NPs promoted the conversion of C3 to C3a, suggesting that activation may result from the NP composition rather than post-fabrication modifications to the NPs. However, surface modification with long chain PEG may reduce the capacity of the NPs to activate the complement system, possibly due to a higher degree of shielding of the NP surface groups that would otherwise interact with components in the complement system. Furthermore, EDTA (ethylenediaminetetraacetic acid) but not EGTA (ethylene glycol tetraacetic acid) blocked the conversion of C3 to C3a (Figure 2.9b), indicative of complement activation via the alternative pathway rather than the classical pathway. These results demonstrate that in addition to the efficient LN targeted delivery of antigen, PRINT hydrogel NP vaccine vectors may potentially improve immune responses by activating the complement system.

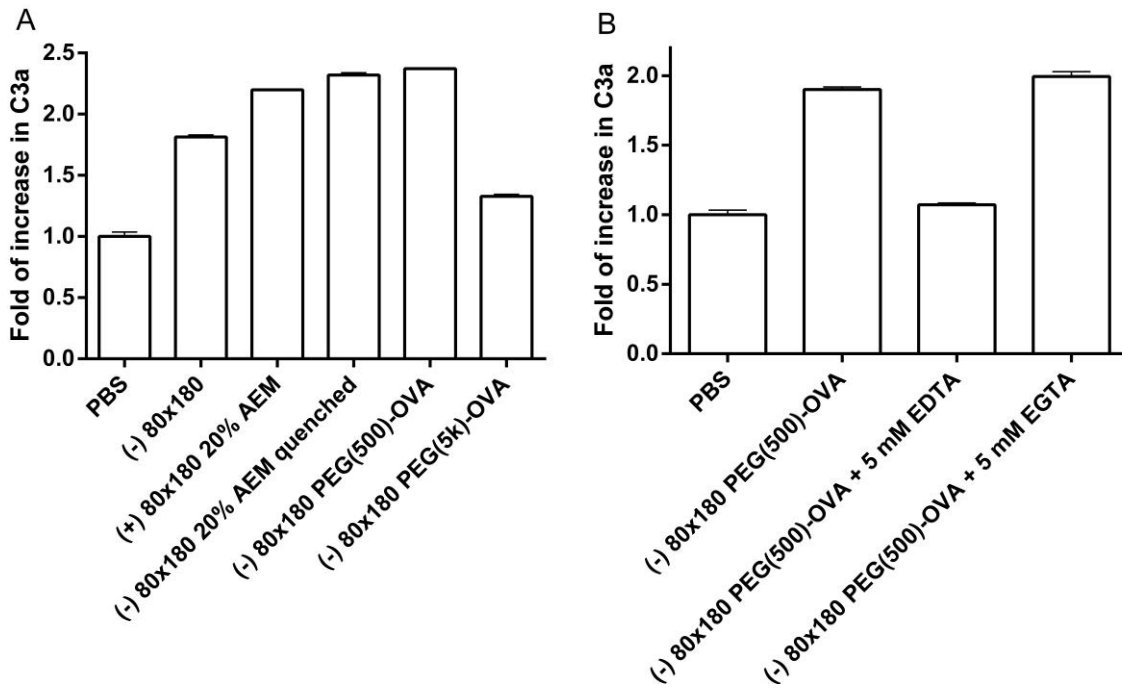


Figure 2.9 Hydrogel NPs activate complement system. Serum from C57BL/6 mice was incubated with a) 0.5 mg/ml NPs and b) 1.2 mg/ml NPs for 50 min at 37°C. Conversion from C3 to C3a was assayed by ELISA. The data represent one of two similar individual experiments; bars are average of two replicate wells in each experiment.

Lymph nodes are home to a large population of DCs, especially CD8 α^+ DCs which have been shown to be the most efficient DCs in antigen cross-presentation.^{6,9,55} In addition, there are other major DC subsets including migratory Langerhans cells and dermal DCs, normally resident in distal areas of the body, as well as LN resident double negative DCs as defined by surface markers CD8 and DEC205²² (Figure 2.10a). Subsequent analysis of draining LNs showed that initially 80 \times 180 nm PEG(500)OVA NPs distributed in all four different subsets of DCs somewhat evenly with an increase in the percentage of LN resident CD8 α^+ DCs over a 30-minute period (Figure 2.10b). This suggests self-draining NPs may be efficiently taken up by LN resident CD8 α^+ DCs and dermal DCs, which are specialized in antigen cross-presentation.⁵⁶ At 27 hours after injection, the percentage of NP⁺ LN resident DCs decreased and the percentage of

NP⁺ migratory dermal DCs increased, likely due to continuous uptake of NPs by dermal DCs at the injection site followed by cell mediated transport to PLNs. This is further verified by the presence of NPs in the PLNs at as early as 5 minutes post injections (Figure 2.5): cell-mediated delivery of NPs has been shown to occur over several hours to days.^{3,49} These results demonstrate that the 80×180 nm hydrogel NPs can be taken up by various DC subsets, with a high percentage of CD8α⁺ DCs and dermal DCs internalizing NPs, potentially preparing them for T cell priming.

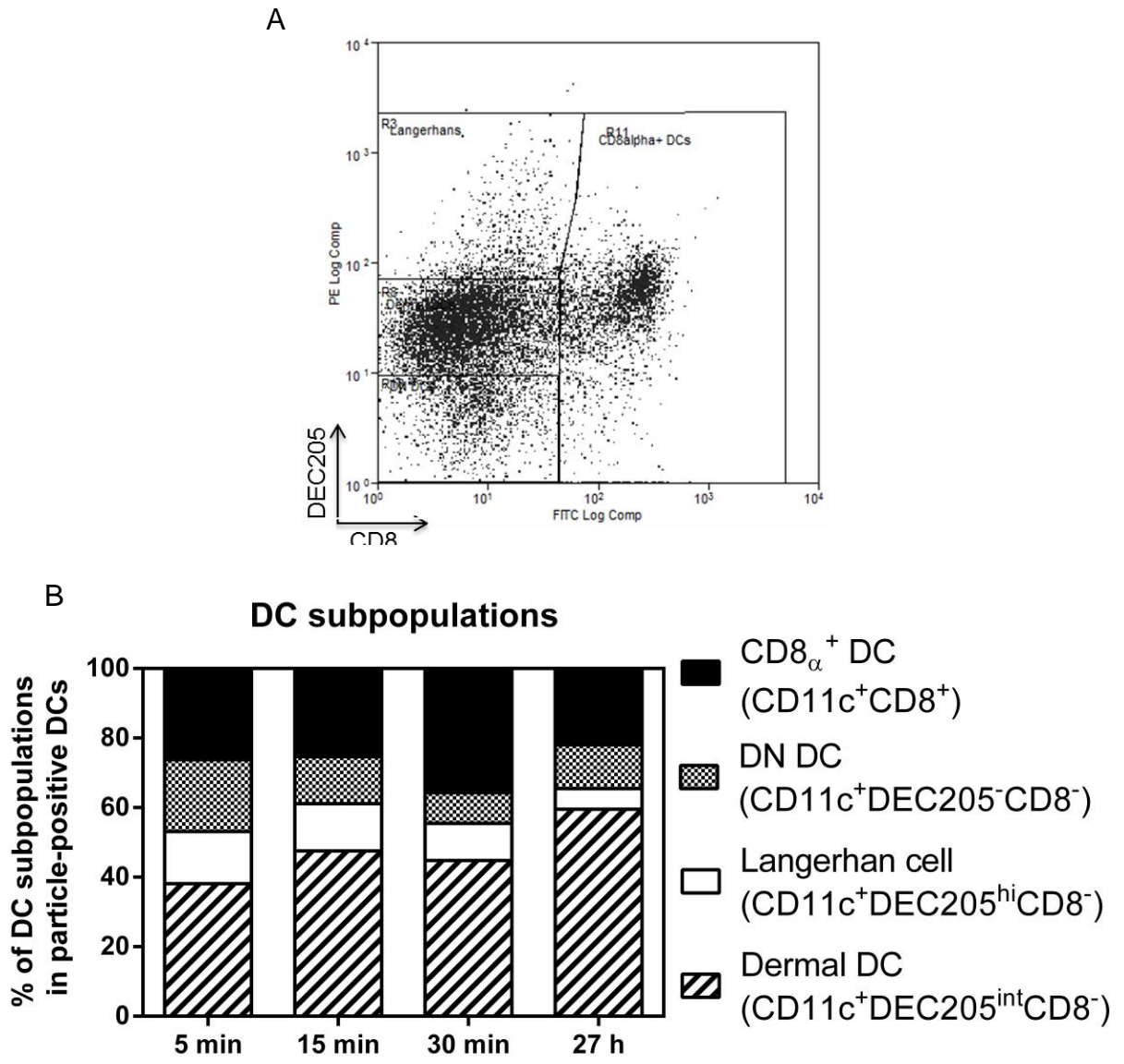


Figure 2.10 A) Analysis of LN DC subsets by flow cytometry. Single cell suspension of LNs was stained with anti-mouse CD11c, CD8 α and DEC205. Cells gated on CD11c⁺ were shown. The CD11c⁺ DC populations are defined as: CD8 α ⁺ DC (CD11c⁺CD8 α ⁺), DN DC (CD11c⁺DEC205⁻CD8 α ⁻), Langerhans cell (CD11c⁺DEC205^{hi}CD8 α ⁻), and dermal DC (CD11c⁺DEC205^{int}CD8 α ⁻). B) Uptake of NPs by various DC subsets in draining LNs, with an increase in the percentage of migratory DCs over time. 50 μ g fluorescently labeled 80 \times 180 nm hydrogels were subcutaneously injected into footpads of C57BL/6 mice. Draining popliteal LNs were collected at the indicated time points analyzed via flow cytometry.

2.2.3 Influence of Particle Drainage on Immune Response

The increased lymphatic drainage and the ability to access to key APCs present an opportunity for the 80×180 nm PEG(500)OVA particles to enhance immunogenicity of subunit vaccines.

To further explore the T cell priming ability of the 80×180 nm PEG(500)OVA NPs, an *in vivo* T cell proliferation assay was performed using CD4⁺ OT-II cells that recognize OVA-derived epitope OVA₃₂₃₋₃₃₉. As displayed in Figure 2.11, immunizations with 80×180 nm PEG(500)OVA NPs loaded with just 1 µg of OVA effectively stimulated the proliferation of CFSE (carboxyfluorescein diacrylate succinimidyl ester)-labeled CD4⁺ OT-II T cells, causing a dilution of the fluorescent dye, while no proliferation was seen in mice that were untreated or dosed with 1 µg soluble OVA. Together with the flow cytometry data (Figure 1.7. and 1.10b), we can deduce that the 80×180 nm PEG(500)OVA NPs are effectively taken up by APCs where they can deliver antigen cargo and activate helper T cells.

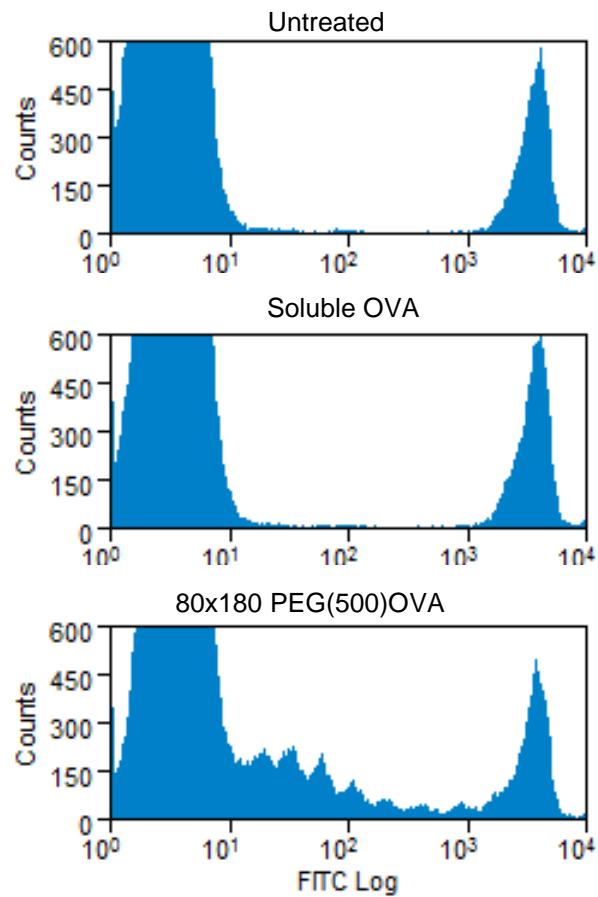


Figure 2.11 In vivo CD4⁺ OT-II T cell proliferation. Hydrogel-mediated delivery of antigen is more efficient in stimulating CD4⁺ T Cell proliferation than soluble antigen. N = 3-4.

To test immunogenicity of antigen delivered by this NP vector, mice were vaccinated against OVA delivered either in soluble form or conjugated to NPs as described previously. The display of antigen on the NP surface may increase the chance of direct present of antigen to B cells, although this strategy may be less protective to the antigen than encapsulation techniques. The immune response to free versus particulate OVA was evaluated following a prime-boost regimen. Seven days after the boost dose, mice immunized with 80×180 nm PEG(500)OVA NPs showed a tenfold increase in OVA-specific IgG production compared to free OVA and free OVA + bare NPs ($p < 0.05$, Figure 2.12a), whereas the NPs that were co-injected with free OVA did not augment the immune response. This data suggests that covalent conjugation to the NP vector

is necessary for enhanced immunity. NP-OVA was compared to free OVA plus the adjuvant alum, the standard of care for adjuvanted vaccines.⁵⁷ Free OVA + alum elicited higher antibody titers than NP-OVA; however, NP-OVA + alum gave a significant increase in antibody response compared to free OVA + alum (Figure 2.12b), indicating this NP-based vector for antigen delivery may be able to further improve the antibody response against protein antigen in adjuvanted vaccines. Previous work has shown that the PRINT hydrogel NPs induce no inflammatory response on their own;⁵⁸ therefore the major advantage of the NP vector most likely comes from its efficient delivery of antigen to immune system rather than direct immunomodulating ability.

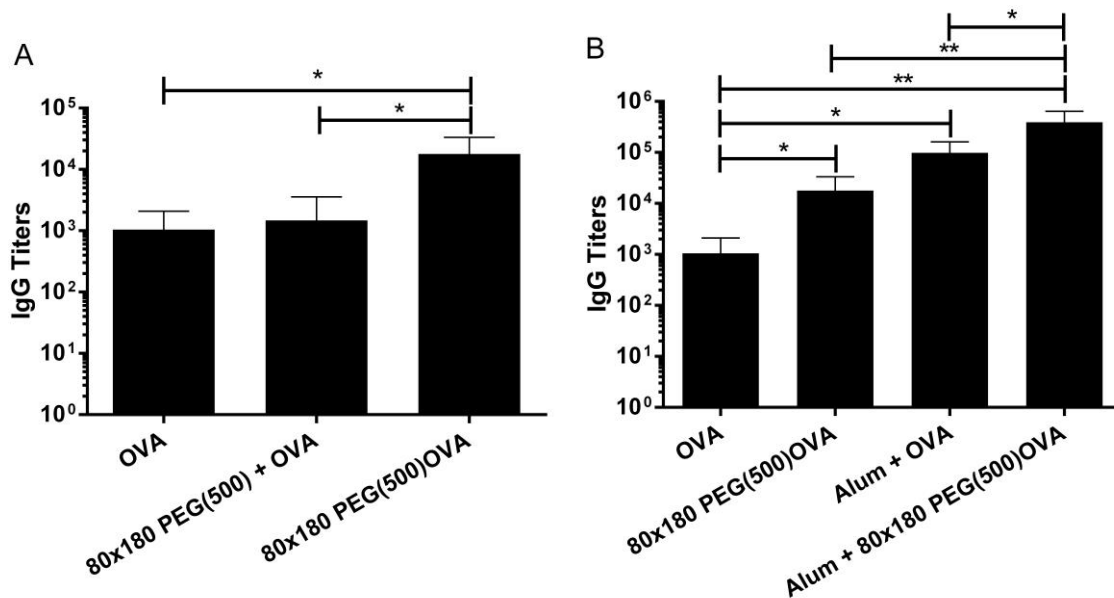


Figure 2.12 Hydrogel vaccine elicits higher antibody titers than soluble antigen with or without Alum adjuvant. Mice were immunized on day 0 and again on day 21 with 5 μ g OVA, soluble or conjugated to PRINT hydrogel NPs. OVA-specific IgG in plasma were examined by ELISA. *, $p < 0.05$; **, $p < 0.01$ by unpaired t-test. Error bars stand for SEM. N = 5.

To examine the correlation between trafficking and immune response, we investigated anti-OVA antibody production after OVA delivery via 80 \times 180 nm NPs with various PEG linker lengths as well as the 1 μ m NPs. Interestingly, despite the influence PEG linker length had on

NP trafficking (Figure 2.4), PEG linker length appeared to have no statistical effect on antigen-specific IgG production (Figure 2.13a). All linker lengths showed a tenfold increase in OVA-specific IgG production compared to free OVA, but the IgG levels were equivalent among the NP groups. However, the size of the NPs used to deliver OVA appeared to have a more dramatic effect on the total IgG. The antibody response against the 80×180 nm PEG(500)OVA NPs was over 1000 times higher than the response to the 1 µm PEG(500)OVA NPs ($p < 0.05$, Figure 2.13b). Remarkably, IgG response to 1 µm PEG(500)OVA NPs was even lower than soluble OVA, strongly suggesting that drainage of vaccine carrier and antigen interaction with LN-resident B cells are crucial to eliciting a humoral response. It is likely that there is a threshold amount of antigen needed in the lymph nodes for initiating a humoral immune response. This level may be sufficiently reached by the 80×180 nm NPs, including the relatively low self-draining 80×180 nm PEG(5k)OVA NPs, while the 1 µm NPs do not appear to deliver enough antigen to the LNs to do so.

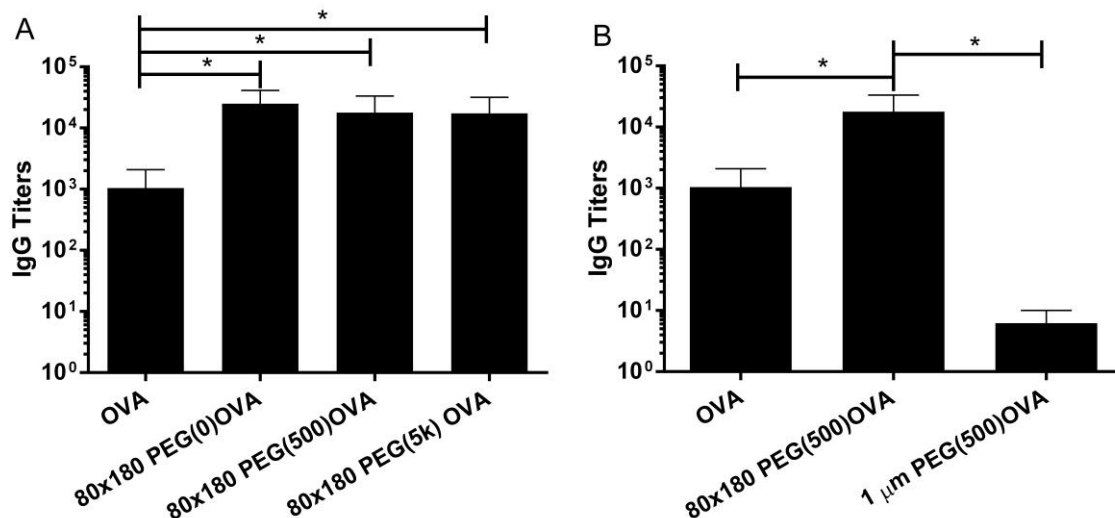


Figure 2.13 Size rather than PEG linker length dramatically influences IgG response. A, Length of PEG linker for OVA conjugation does not affect IgG response. B, Large 1 μm NPs elicit lower IgG production than soluble administration or smaller 80×180 nm NPs. Mice were immunized as in Figure 2.12 and plasma IgG was evaluated by ELISA. *, $p < 0.05$ by unpaired t-test. Data represent two or three individual experiments of $N = 4$. Error bars stand for SEM.

2.3 Conclusions

In conclusion, we have designed and optimized a versatile vaccine delivery platform based on PRINT NPs. We demonstrate that the size, aspect ratio, charge, and surface characteristics of NPs are all important in improving the lymphatic trafficking of NPs and their subsequent uptake by key APCs. Anionic sub-100 nm hydrogel NPs loaded with a model antigen showed high levels of self-drainage and were able to efficiently deliver antigen to B cells and major APCs, inducing antigen-specific humoral and cellular responses superior to free antigen alone. The simplicity of the chemistries used in antigen conjugation confers versatility to this delivery platform, allowing for potential application to many infectious diseases. Increasing the

efficacy of subunit vaccines through a particulate delivery platform is of great interest and may lead to a wide variety of safe and effective vaccines based on dosing pathogen subunits.

2.4 Materials and Methods

2.4.1 Materials

Alexa Fluor 488 maleimide was purchased from Invivogen, Inc. Maleimide-PEG(5k)-NHS and NHS-PEG(260)-OH were purchased from Creative PEGworks, Inc. Cell surface stains, antibodies, and ELISA reagents were purchased from eBioscience, Inc. TissueTek[®] OTC media, DyLight 680 maleimide, maleimide-PEG(500)-NHS, BCA assay, s-NHS (N-hydroxysulfosuccinimide), EDC (1-Ethyl-3-[3-dimethylaminopropyl]carbodiimide hydrochloride), and general solvents were purchased from Thermo Fisher Scientific, Inc. Tetraethylene glycol monoacrylate (HP(250)A) was synthesized in-house. All other chemicals and reagents were obtained from Sigma Aldrich, Inc. unless otherwise noted.

Cure-site monomer (CSM) solution was prepared by weighing out solid and liquid monomers into a conical tube and dissolving them in dry methanol to a final total of 2.5 weight % solids. The composition of solids was (weight %): hydroxy tetraethylene glycol acrylate (HP(250)A) (67-79), methoxy polyethylene glycol dimethacrylate, MW = 750 Da (10), 2-aminoethyl methacrylate HCl (AEM) (0-20), 2,4,6 trimethylbenzoyl diphenylphosphine oxide (TPO) (1), Alexa Fluor 488 maleimide or DyLight 680 maleimide (0-2) (Table 2.3). When utilizing fluorescent dyes, the dye took the place of 2% of the HP(250)A. A custom-built double-nip laminator was used for preparing hydrogel particles. Harvesting layers were synthesized in-house from poly(vinyl alcohol), MW = 2000 Da. PRINT molds were supplied by Liquidia Technologies.

Table 2.3 Composition of hydrogel particles

Monomer	Cationic Weight %	Anionic Weight %
2-aminoethyl methacrylate HCl (AEM)	10-20	0
PEG(700) diacrylate (PEGDA)	10-20	10-20
Hydroxy PEG(250) acrylate (HP(250)A)	67	77-87
2,4,6 trimethylbenzoyl diphenylphosphine oxide (TPO)	1	1
*DyLight 680 or AlexaFluor 488	2	2
Total	100	100

2.4.2 Animals

Female Balb/c, C57BL/6, and OT-II mice were purchased from Jackson Laboratory and used at age 6-12 weeks. All experiments involving mice were carried out in accordance with an animal use protocol approved by the University of North Carolina Animal Care and Use Committee.

2.4.3 Fabrication of Hydrogel NPs via the PRINT Process

The fabrication of nano- and micron-sized NPs was achieved by mold-based PRINT particle fabrication technology using a composition shown in Table 2.3.^{40,45,46} Briefly, cure-site monomer (CSM) solutions were prepared at 2.5 weight % solids in dry methanol. The film-split technique for preparing NPs was performed as described in the following: using a #5 Mayer rod, 350 μ L of CSM solution was cast on a sheet of corona treated poly(ethylene terephthalate) (PET), followed by brief evaporation of solvent with a heat gun to yield a transparent film (delivery

sheet). Patterned Fluorocur PRINT molds (Liquidia Technologies) were laminated against the delivery sheet with moderate pressure (40 psi) and delaminated at the same pressure. The filled mold was laminated against corona-treated PET and subsequently cured in a custom built UV-LED chamber (Phoseon, $\lambda_{\text{max}} = 395 \text{ nm}$) for 3.5 minutes. After photocuring, the mold was removed to reveal an array of NPs on PET. NPs were mechanically harvested off the PET with water (1 mL/40 in²). NPs were washed via centrifugation (15-30 min, 14,000 RPM, 4 °C), removal of supernatant, and resuspension in fresh solvent. NP yield was determined by thermogravimetric analysis (Q5000IR, TA Instruments). To conjugate OVA, NPs were first PEGylated by reacting 1 mg NPs with 1.6 μmol of maleimide-PEG(5k)-NHS or maleimide-PEG(500)-NHS using triethylamine (100 μL) in DMF at a final concentration of 1 mg NPs in 1.4 mL.⁴⁰ Reaction was run at room temperature overnight with shaking at 1400 RPM. NPs were then washed with fresh DMF. Residual amine groups on the surface of NPs were quenched with 13.5 μmol of NHS-PEG(260)-OH (Creative PEGworks) following the same PEGylation procedure above, or with 150 μmol of succinic anhydride, reacted in the presence of 186 μmol pyridine for 30 minutes with agitation at 1400 RPM. NPs were then washed into water. OVA was conjugated to the free maleimide groups by reacting NPs and OVA in a 1:1 weight ratio at a NP concentration of 4 mg/mL in Borate buffer pH 9.5 with 0.1 weight % PVOH, MW 2 kDa, overnight at room temperature with shaking at 1400 RPM. NPs were washed with buffer to remove unbound protein and washed with water to remove residual salt. For PEG(0) NPs, OVA was conjugated to the NP surface by first reacting the free amines on the NPs with succinic anhydride as used in quenching above, followed by reaction with OVA, EDC (1-ethyl-3-(3-dimethylaminopropyl)carbodiimide) and sulfo-NHS according to protocol by Thermo Scientific.

NPs were washed with buffer to remove unbound protein and washed with water to remove residual salt.

2.4.4 Nanoparticle Characterization

Scanning electron microscopy (SEM) enabled imaging of hydrogel NPs that were dispersed on a silicon wafer and coated with approximately 1.5 nm of Au/Pd (Hitachi S-4700, FEI Helios Nanolab 600). ζ -potential measurements were conducted on ~20 $\mu\text{g/mL}$ NP dispersions in water using a Zetasizer Nano ZS Particle Analyzer (Malvern Instruments Inc.). Particle concentrations were determined via thermogravimetric analysis (Q5000IR, TA Instruments). OVA conjugation was measured using a standard BCA Assay.

2.4.5 Lymphatic Drainage Studies

Mice were dosed with 50 μg of NPs in 20 μL of 9.25 weight % sucrose subcutaneously in the rear right footpad. To monitor OVA drainage, 5 μg OVA labeled with AlexaFluor 555 (Sigma), soluble or conjugated to NPs, was injected into the footpad. Mice were sacrificed at the indicated time points and draining popliteal LNs (PLNs) from both the dosed and contralateral control sides were resected. Resected PLNs were imaged for total fluorescence and/or homogenized into a single cell suspension for analysis of NP distribution in various cell types by flow cytometry. Additional dosed PLNs were frozen at $-80\text{ }^{\circ}\text{C}$ in OCT medium for histological analysis.

2.4.6 *Ex Vivo* Imaging

Imaging of resected LNs was done using an IVIS-Lumina II (PerkinElmer, Inc. Hopkinton, MA) with analysis done on Living Image[®] software, version 3.2 (PerkinElmer, Inc. Hopkinton, MA). For optimal performance of the DyLight 680 dye, excitation and emission filters were set to 675 nm and 720 nm, respectively.

2.4.7 Flow Cytometry

Draining LNs were resected at indicated time points post subcutaneous injections of 50 µg DyLight 680-labeled NPs. Single cell suspensions of LNs were made physically with frosted slides. Cells were stained with CD11c-eFluor450, F4/80-FITC, B220-PE, PDCA-PerCP-eFluor710 (eBioscience). Cells were then examined with Cyan ADP (Dako) and analyzed with Summit software. For DC subset analysis, LN cells were stained with CD11c-eFluor450, CD8α-FITC and DEC205-PE (eBioscience).

2.4.8 *In Vivo* CD4⁺ T Cell Proliferation

CD4⁺ T cells recognizing OVA323-339 were isolated from spleens of OT-II transgenic mice with a kit (Miltenyi Biotech). The purified T cells were labeled with 4 µM CFSE fluorescent dye for 10 min at 37 °C, and 10 million cells were adoptively transferred into each C57BL/6 mouse intravenously. The next day, mice were subcutaneously immunized with 1 µg OVA, soluble or NP-loaded. Spleens were harvested four days later and single cell suspensions were stained with CD4-PE-Cy7 and Vα2-eFluor450 (eBioscience). Cells were then examined with Cyan ADP (Dako) and analyzed with Summit software.

2.4.9 Complement Activation

A C3a sandwich ELISA was performed to measure complement activation in mouse serum following incubation with NPs. EIA plates (Corning 9018) were coated with an anti-mouse C3a monoclonal antibody (BD Biosciences, clone I87-1162) diluted 1:250 in coating buffer (eBioscience) overnight at 4 °C. Mouse serum was incubated 1:1 with either PBS or NPs at 37 °C for 50 min. Serial dilutions of purified mouse C3a protein (BD Biosciences) were included in each ELISA plate to establish a standard curve. Serum samples were added to wells in duplicate (50 µL total volume) and incubated for 3 hours. Anti-C3a-biotinylated detection

antibody (BD Biosciences, clone I87-419) was used at a 1:500 dilution in 1× assay diluent, and incubated for 40 min. Streptavidin-HRP (BD) was diluted 1:250 in 1× assay diluent for 30 min. 1× TMB substrate solution (eBioscience) was added to develop color. The reaction was stopped with 0.2 N H₂SO₄, and absorbance was read at 450 nm with a reference wavelength of 570 nm on a SpectraMax (Molecular Devices) plate reader.

2.4.10 Confocal Microscopy

Resected draining LNs were frozen in OCT medium without fixation. 10 μm sections were made with Leica cryostat, fixed with ice cold acetone, and stained with purified anti-mouse B220 (eBioscience) coupled with Goat anti-rat IgG-Alexa Fluor 488 or –Alexa Fluor 647 (Invitrogen), anti-mouse B220-biotin (eBioscience) coupled with Streptavidin-Alexa Fluor 555 (Invitrogen), or anti-mouse CD11c-biotin (eBioscience) coupled with Streptavidin-Alexa Fluor 633 (Invitrogen). Sections were examined with Zeiss 710 confocal microscope.

2.4.11 Immunizations and Antibody ELISA

C57BL/6 mice, 6-8 weeks old, were immunized with soluble OVA or NP-conjugated OVA at 5 μg per mouse, subcutaneously in the flank. Mice were primed on day zero and boosted on day 21. Plasma samples were collected by bleeding mice submandibularly on day 21 and day 28 post-prime and OVA-specific antibody production was examined by ELISA. Briefly, EIA plates (Corning) were coated with 10 μg/ml OVA in ELISA coating buffer (eBioscience) at 4 °C overnight. The wells were washed and blocked with 200 μL per well of 3% BSA in PBST (PBS with 0.05% Tween 20) for 2 hours. Plasma samples were diluted in blocking buffer and incubated for 2 hours. The wells were washed extensively with PBST and anti-OVA IgG were detected using HRP conjugated goat anti-mouse IgG (Invitrogen) and was visualized by adding 100 μL of TMB (eBioscience) to each well. The reaction was stopped after 11 min with 50 μL

0.2 M H₂SO₄. Optical densities (OD) were read at 450 nm and 570 nm. The antibody titer was determined as the highest dilutions with OD(450 nm – 570 nm) > 0.1.

2.5 References

- (1) Moon, J. J.; Huang, B.; Irvine, D. J. *Adv. Mater.* **2012**, *24*, 3724–3746.
- (2) Liu, H.; Moynihan, K. D.; Zheng, Y.; Szeto, G. L.; Li, A. V.; Huang, B.; Van Egeren, D. S.; Park, C.; Irvine, D. J. *Nature* **2014**, *507*, 519–522.
- (3) Bachmann, M. F.; Jennings, G. T. *Nat. Rev. Immunol.* **2010**, *10*, 787–796.
- (4) Pal, I.; Ramsey, J. D. *Adv. Drug Deliv. Rev.* **2011**.
- (5) Belz, G.; Smith, C.; Bharadwaj, M.; Rice, A.; Jackson, D. *Cytotherapy* **2004**, *6*, 88–98.
- (6) Hubbell, J. A.; Thomas, S. N.; Swartz, M. A. *Nature* **2009**, *462*, 449–460.
- (7) Cruz, L. J.; Tacke, P. J.; Rueda, F.; Domingo, J. C.; Albericio, F.; Figdor, C. G. *Targeting nanoparticles to dendritic cells for immunotherapy.*; 1st ed.; Elsevier Inc., 2012; Vol. 509, pp. 143–163.
- (8) De Temmerman, M.-L.; Rejman, J.; Demeester, J.; Irvine, D. J.; Gander, B.; De Smedt, S. C. *Drug Discov. Today* **2011**, *16*, 569–582.
- (9) Swartz, M. A.; Hubbell, J. A.; Reddy, S. T. *Semin. Immunol.* **2008**, *20*, 147–156.
- (10) Ferreira, S. A.; Gama, F. M.; Vilanova, M. *Nanomedicine* **2013**, *9*, 159–173.
- (11) Xiang, S. D.; Scholzen, A.; Minigo, G.; David, C.; Apostolopoulos, V.; Mottram, P. L.; Plebanski, M. *Methods* **2006**, *40*, 1–9.
- (12) Storni, T.; Kündig, T. M.; Senti, G.; Johansen, P. *Adv. Drug Deliv. Rev.* **2005**, *57*, 333–355.
- (13) Porter, C. J.; Charman, S. A. *J. Pharm. Sci.* **2000**, *89*, 297–310.
- (14) Kasturi, S. P.; Skountzou, I.; Albrecht, R. A.; Koutsonanos, D.; Hua, T.; Nakaya, H. I.; Ravindran, R.; Stewart, S.; Alam, M.; Kwissa, M.; Villinger, F.; Murthy, N.; Steel, J.; Jacob, J.; Hogan, R. J.; García-Sastre, A.; Compans, R.; Pulendran, B. *Nature* **2011**, *470*, 543–547.
- (15) Moon, J.; Suh, H.; Bershteyn, A.; Stephan, M. *Nat. Mater.* **2011**, *10*, 243–251.
- (16) Reddy, S. T.; van der Vlies, A. J.; Simeoni, E.; Angeli, V.; Randolph, G. J.; O’Neil, C. P.; Lee, L. K.; Swartz, M. A.; Hubbell, J. A. *Nat. Biotechnol.* **2007**, *25*, 1159–1164.
- (17) Rice-Ficht, A. C.; Arenas-Gamboa, A. M.; Kahl-McDonagh, M. M.; Ficht, T. A. *Curr. Opin. Microbiol.* **2010**, *13*, 106–112.
- (18) John, A. L. S.; Chan, C. Y.; Staats, H. F.; Leong, K. W.; Abraham, S. N. *Nat. Mater.* **2012**, *11*, 1–8.

- (19) Fifis, T.; Gamvrellis, A.; Crimeen-Irwin, B.; Pietersz, G. A.; Li, J.; Mottram, P. L.; McKenzie, I. F. C.; Plebanski, M. *J. Immunol.* **2004**, *173*, 3148–3154.
- (20) Zhuang, Y.; Ma, Y.; Wang, C.; Hai, L.; Yan, C.; Zhang, Y.; Liu, F.; Cai, L. *J. Control. Release* **2012**, *159*, 135–142.
- (21) Oussoren, C.; Storm, G. *Adv. Drug Deliv. Rev.* **2001**, *50*, 143–156.
- (22) Zhan, X.; Tran, K. K.; Shen, H. *Mol. Pharm.* **2012**.
- (23) Kaur, R.; Bramwell, V. W.; Kirby, D. J.; Perrie, Y. *J. Control. Release* **2012**, *164*, 331–337.
- (24) Johansen, P.; Mohanan, D.; Martínez-Gómez, J. M.; Kündig, T. M.; Gander, B. *J. Control. Release* **2010**, *148*, 56–62.
- (25) Bershteyn, A.; Hanson, M. C.; Crespo, M. P.; Moon, J. J.; Li, A. V.; Suh, H.; Irvine, D. J. *J. Control. Release* **2012**, *157*, 354–365.
- (26) Moghimi, S.; Hawley, A.; Christy, N.; Gray, T. *FEBS Lett.* **1994**, *344*, 25–30.
- (27) Illum, L.; Church, a E.; Butterworth, M. D.; Arien, A.; Whetstone, J.; Davis, S. *S. Pharm. Res.* **2001**, *18*, 640–645.
- (28) Rao, D.; Forrest, M. L.; Alani, A. W. G.; Kwon, G. S.; Robinson, J. R. *J. Pharm. Sci.* **2010**, *99*, 2018–2031.
- (29) Kaminskas, L. M.; Porter, C. J. H. *Adv. Drug Deliv. Rev.* **2011**, *63*, 890–900.
- (30) Bagby, T. R.; Duan, S.; Cai, S.; Yang, Q.; Thati, S.; Berkland, C.; Aires, D. J.; Laird Forrest, M. *Eur. J. Pharm. Sci.* **2012**.
- (31) Hawley, A.; Illum, L.; Davis, S. *Pharm. Res.* **1997**, *14*, 657–661.
- (32) Al Kobiasi, M.; Chua, B. Y.; Tonkin, D.; Jackson, D. C.; Mainwaring, D. E. *J. Biomed. Mater. Res. A* **2012**, *100*, 1859–1867.
- (33) Moghimi, S. M. *Biomaterials* **2006**, *27*, 136–144.
- (34) Thiele, L.; Merkle, H. P.; Walter, E. *Pharm. Res.* **2003**, *20*, 221–228.
- (35) Swartz, M. A. *Adv. Drug Deliv. Rev.* **2001**, *50*, 3–20.
- (36) Reddy, S. T.; Berk, D. A.; Jain, R. K.; Swartz, M. A. *J. Appl. Physiol.* **2006**, *101*, 1162–1169.
- (37) Patel, H. M.; Boodle, K. M.; Vaughan-Jones, R. *Biochim. Biophys. Acta.* **1984**, *801*, 76–86.
- (38) Rao, D. A.; Robinson, J. R. *J. Control. Release* **2008**, *132*, e45–e47.

- (39) Reddy, S. T.; Rehor, A.; Schmoekel, H. G.; Hubbell, J. A.; Swartz, M. A. *J. Control. Release* **2006**, *112*, 26–34.
- (40) Perry, J. L.; Reuter, K. G.; Kai, M. P.; Herlihy, K. P.; Jones, S. W.; Luft, J. C.; Napier, M.; Bear, J.E.; DeSimone, J. M. *Nano Lett.* **2012**, *12*, 5304–5310.
- (41) Gref, R.; Lück, M.; Quellec, P.; Marchand, M.; Dellacherie, E.; Harnisch, S.; Blunk, T.; Müller, R. *Colloids Surf. B. Biointerfaces* **2000**, *18*, 301–313.
- (42) Vila, A.; Gill, H.; McCallion, O.; Alonso, M. J. *J. Control. Release* **2004**, *98*, 231–244.
- (43) Oussoren, C.; Storm, G. *Pharm. Res.* **1997**.
- (44) Rolland, J. P.; Maynor, B. W.; Euliss, L. E.; Exner, A. E.; Denison, G. M.; DeSimone, J. M. *J. Am. Chem. Soc.* **2005**, *127*, 10096–10100.
- (45) Gratton, S. E. A.; Ropp, P. A.; Pohlhaus, P. D.; Luft, J. C.; Madden, V. J.; Napier, M. E.; DeSimone, J. M. *Proc. Natl. Acad. Sci. U. S. A.* **2008**, *105*, 11613–11618.
- (46) Gratton, S. E. A.; Williams, S. S.; Napier, M. E.; Pohlhaus, P. D.; Zhou, Z.; Wiles, K. B.; Maynor, B. W.; Shen, C.; Olafsen, T.; Samulski, E. T.; Desimone, J. M. *Acc. Chem. Res.* **2008**, *41*, 1685–1695.
- (47) Wilson, J. T.; Keller, S.; Manganiello, M. J.; Cheng, C.; Lee, C.-C.; Opara, C.; Convertine, A.; Stayton, P. S. *ACS Nano* **2013**.
- (48) Cohen, J. A.; Beaudette, T. T.; Tseng, W. W.; Bachelder, E. M.; Mende, I.; Engleman, E. G.; Fréchet, J. M. J. *Bioconjug. Chem.* **2009**, *20*, 111–119.
- (49) Manolova, V.; Flace, A.; Bauer, M.; Schwarz, K.; Saudan, P.; Bachmann, M. F. *Eur. J. Immunol.* **2008**, *38*, 1404–1413.
- (50) Hawley, A.; Davis, S.; Illum, L. *Adv. Drug Deliv. Rev.* **1995**.
- (51) Nel, A. E.; Mädler, L.; Velegol, D.; Xia, T.; Hoek, E. M. V.; Somasundaran, P.; Klaessig, F.; Castranova, V.; Thompson, M. *Nat. Mater.* **2009**, *8*, 543–557.
- (52) Carroll, M. C. *Nat. Immunol.* **2004**, *5*, 981–986.
- (53) Thomas, S. N.; van der Vlies, A. J.; O’Neil, C. P.; Reddy, S. T.; Yu, S. S.; Giorgio, T. D.; Swartz, M. A.; Hubbell, J. A. *Biomaterials* **2011**, *32*, 2194–2203.
- (54) Fine, D. P.; Marney, S. R.; Colley, D. G.; Sargent, J. S.; Prez, R. M. Des. *J. Immunol.* **1972**, *109*, 807–809.
- (55) Wilson, N. S.; El-Sukkari, D.; Belz, G. T.; Smith, C. M.; Steptoe, R. J.; Heath, W. R.; Shortman, K.; Villadangos, J. A. *Blood* **2003**, *102*, 2187–2194.
- (56) Paul, W. E. *Fundamental Immunology*; 7th ed.; Lippincott Williams & Wilkins, 2012; p. 385.

- (57) Baylor, N. W.; Egan, W.; Richman, P. *Vaccine* **2002**, *20 Suppl 3*, S18–23.
- (58) Roberts, R. A.; Shen, T.; Allen, I. C.; Hasan, W.; DeSimone, J. M.; Ting, J. P. Y. *PLoS One* **2013**, *8*, e62115.

CHAPTER 3 A PRO-ADJUVANT APPROACH TO ACHIEVE CONTROLLED DELIVERY OF VACCINE COMPONENTS VIA PRINT NANOPARTICLES

3.1 Introduction

Since the advent of vaccination in the late 1700s, the primary component of most vaccines has been either an attenuated or killed whole pathogen. As our understanding of immunity has matured, however, research has shifted toward subunit vaccines that utilize purified or synthetic immunogenic portions of pathogens (proteins, peptides, polysaccharides, and/or DNA). This vaccination strategy increases the safety of vaccines, especially for immunocompromised individuals.^{1,2} Conversely, ridding pathogens of the molecular machinery they use to infect the host organism usually decreases the body's recognition of the pathogen, resulting in a far less potent immune response than would be seen with a whole pathogen vaccine.³ As a response to this decrease in immunogenicity, one or more defined immunostimulatory molecules are often combined with subunit antigens as adjuvants to augment the immune response. Among these immunostimulators, many are agonists for toll-like receptors (TLRs), intra- and extracellular receptors that are able to recognize specific structural motifs that are present in a wide variety of pathogens, also known as pattern recognition receptors (PRRs).³ Both TLRs and PRRs are highly conserved among organisms and the pathogens that infect them, respectively.⁴

Resiquimod (also known as R848) is a synthetic imidazoquinoline-type molecule that is currently being studied in human clinical trials as a therapeutic treatment for diseases like hepatitis C virus, Leishmaniasis, HIV, and Kaposi's sarcoma.^{5,6} R848 activates both TLR 7 and 8 in humans and non-human primates, and TLR 7 in mice. Activation of TLR 7/8 prompts

dendritic cells (DCs) to migrate to the draining lymph nodes and produce pro-inflammatory cytokines⁷⁻⁹ while also promoting B cell secretion of antibodies and other pro-inflammatory cytokines.^{6,10} R848 has been found to be approximately 100 times more potent at activating the immune system when compared to imiquimod, an FDA approved imidazoquinoline and TLR 7 agonist currently used in the clinic.¹¹⁻¹⁴ Due to this dramatic increase in immune system activation, R848 has the potential for dose sparing effects and more efficient dosing.

R848 has been studied for the treatment of various skin diseases, including skin cancers and genital herpes, but dosing has been restricted to topical application due to side effects caused by systemic cytokine exposure¹⁵⁻¹⁷ and its short half-life *in vivo*.¹⁸ Additionally, topical cream dosing is typically up to 1000 times higher than subcutaneous injection dosing levels.

R848 has been examined in pre-clinical work as a vaccine adjuvant.¹⁸ A wide variety of studies in mice, rats, guinea pigs, and monkeys have shown the ability of R848 to activate antigen presenting cells (APCs) and to induce an adaptive immune response.¹⁹ Unlike the related imidazoquinoline-type molecule imiquimod, which is also used as an immunomodulator, R848 is water-soluble and has substantial oral bioavailability.⁶ This, however, also allows R848 to drain quickly through the lymphatics from subcutaneous or intramuscular injections into the circulatory system, leading to systemic exposure. Conjugating R848 to NPs may not only limit systemic exposure, but also increase bioavailability in lymphoid tissues and cells. Current techniques being studied to encapsulate R848 and decrease systemic exposure include various nanoparticle formulations via electrospray or emulsion techniques.²⁰⁻²³ Particles formed by electrospray or emulsion are often non-uniform, have variable encapsulation efficiency, and are prone to burst release of their cargo.^{21,22} Burst release in particular makes these strategies

ineffective in controlling systemic exposure and production of inflammatory cytokines, decreasing the benefits gained by encapsulating R848.

Several studies have also investigated modified imidazoquinoline type molecules. When modifying these TLR ligands, it is critical to maintain the original activity of the compound. Irreversible modifications have been shown to reduce adjuvanticity and/or remove activity for activation altogether.^{24,25} Reversible modification has been performed via covalent conjugation to a biodegradable polymer, PLGA, for use in synthetic vaccine particles (SVPs), fabricated through emulsion techniques.²³ Due to the biodegradable nature of PLGA, R848 can be cleaved over time from the PLGA backbone, maintaining the activity of R848 upon release.

The R848 encapsulation strategy presented here utilizes a pro-drug approach by modifying R848 in a way that allows for the molecule to revert to its original form *in vivo*. R848 is reversibly linked to a polymerizable acrylate group through acid labile bis-silyl ether bonds (Scheme 1). This strategy has been previously used to fabricate acid labile cross-linkers and chemotherapeutic pro-drugs with reproducible, tunable release profiles.^{26,27} In this work, the adjuvant R848 was modified into a pro-adjuvant and used in the fabrication of PRINT nanoparticles (Particle Replication in Non-Wetting Templates). These NPs were then examined for their ability to release active R848 under physiologically relevant pH conditions, for cytotoxicity and TLR 7/8 activation *in vitro*, and finally for their utility *in vivo* as vaccine adjuvants. Here we show that R848-NPs are an effective adjuvant with higher, sustained antibody response and lower systemic cytokine induction than free R848. R848-NP also exhibited potential for dose sparing effects in regard to both adjuvant and antigen levels. This pro-adjuvant approach harnesses the potency of R848 as a vaccine adjuvant while making it safer and more effective for clinical applications.

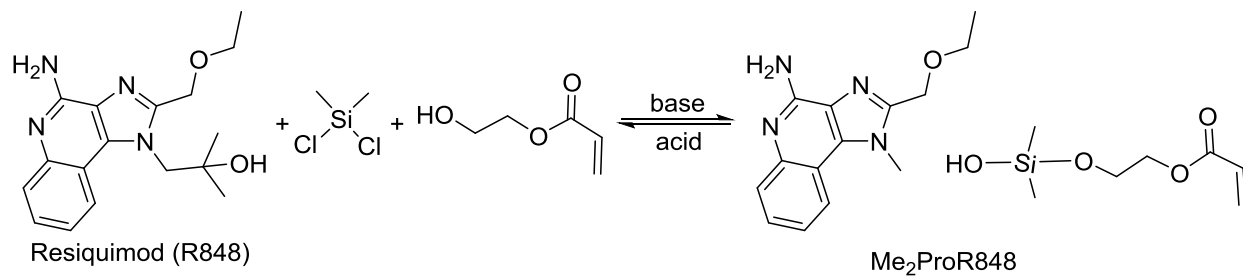
3.2 Results and Discussion

The molecular adjuvant resiquimod, also known as R848, has proven to be extremely potent in activating TLR 7/8 to the point that side effects from systemic exposure have outweighed potential benefits in clinical trials (clinicaltrials.gov). Here, we formulate R848 into an acid-labile ProR848 form, which can be covalently incorporated into PRINT nanoparticles (NPs). NP formulation can control how R848 interacts with the body, restricting release to the acidic environment of the endosome and limiting systemic exposure. We can in this way increase the potency of R848 as a vaccine adjuvant, boosting the immune response to subunit antigens while reducing the dose and limiting systemic side effects.

3.2.1 Synthesis and Characterization of R848 Pro-Adjuvant Monomer

Two derivatives of the ProR848 monomer were synthesized: dimethyl and diethyl bis-silyl ether acrylate R848, Me₂ProR848 and Et₂ProR848, respectively (Scheme 3.1). Structures were confirmed by ¹H NMR, ¹³C NMR, and LTQFT high-resolution mass spectrometry (Appendix Figure A.1 – A.6). Due to the larger alkyl groups on the bridging silicon atom, Et₂ProR848 was expected to have greater steric hindrance of the silyl ether bonds, slowing hydrolysis and resulting in a slower release of R848 from Et₂ProR848-NPs compared to Me₂ProR848-NPs. Differential degradation profiles allows for the release profile of the adjuvant to be tuned to the unique needs of each application and different particle characteristics (size, shape, composition). Larger or smaller alkyl groups may be employed to modify the release profile, as necessary.^{26,27}

Scheme 3.1 Synthesis of R₂ProR848. R groups represent two methyl or two ethyl groups, but could be substituted for various alkyl groups.



3.2.2 Release of R848 from R848-NPs

Me₂ProR848 and Et₂ProR848 were loaded into 80×320 nm PRINT NPs during the particle fabrication process by adding the ProR848 monomer to the cure-site monomer (CSM) solution at 10 weight % of the total solids (Table 3.1). ProR848-NPs remained well dispersed compared to blank NPs of similar composition (Table 3.2).

Table 3.1 Composition of Pro-Adjuvant NPs and Blank NPs

Monomer	ProR848 NPs	Blank NPs
	Weight %	Weight %
2-aminoethyl methacrylate HCl (AEM)	40	40
Methoxy PEG _{5k} acrylate	20	20
PEG _{1k} dimethacrylate	29	29
2,4,6 trimethylbenzoyl diphenylphosphine oxide (TPO)	1	1
Dimethyl or diethyl bis-silyl ether acrylate R848 (Me ₂ or Et ₂ ProR848)	10	0
Hydroxyethyl acrylate (HEA)	0	10
Total	100	100

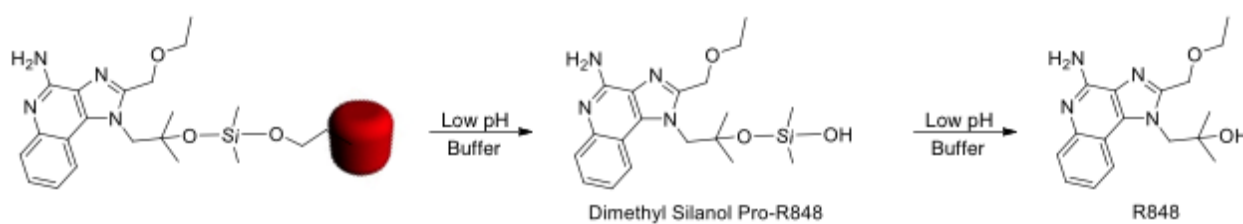
Table 3.2 Characterization of ProAdjuvant NPs

Cargo	Size (d.nm)	PDI	Zeta Potential (mV)
Pro-R848 (+)	294.5 ± 7.1	0.014	+30.0
Pro-R848 (-)	291.7 ± 8.7	0.021	-16.4
PEG(500)OVA	245.7 ± 6.8	0.061	-31.9

A release profile of R848 from R848-NPs was established at physiologically relevant conditions - 37°C (normal body temperature) at pH 5 (endosomal pH) or pH 7.4 (physiological

pH). R848 was found to be released from both Me₂- and Et₂ProR848-NPs through a 2-step degradation mechanism (Scheme 3.2): the silyl ether bridge degraded first between the silane and the NP, releasing Me₂- or Et₂silanol-R848, and second between the newly formed silanol and R848, releasing the free R848. This was confirmed via LC-MS (Appendix Figure A.6). At pH 5, the Me₂silanol-R848 was quickly released from the NPs, but converted steadily to free R848 over time. Within 11 hours, all of the cargo was released from the NPs, but the conversion of Me₂silanol-R848 to R848 increased steadily over 3 days (Figure 3.1a). After 7 days at pH 7.4, approximately 75% of the total cargo had been released (Figure 3.1b). The release of R848 at pH 5 was found to be almost 3 times faster than at pH 7.4 (Figure 3.2). The half-life of R848-NPs at pH 5 was found to be approximately 20 hours while the half-life at pH 7 was 55 hours, both calculated based on a one-phase exponential decay fit (Table 3.3). Et₂ProR848-NPs showed a much slower release profile compared to the dimethyl counterpart. At pH 5, only 10% of the loaded R848 was released after seven days (Figure 3.3).

Scheme 3.2 Two-step degradation mechanism of R848 from Me₂ProR848-NPs



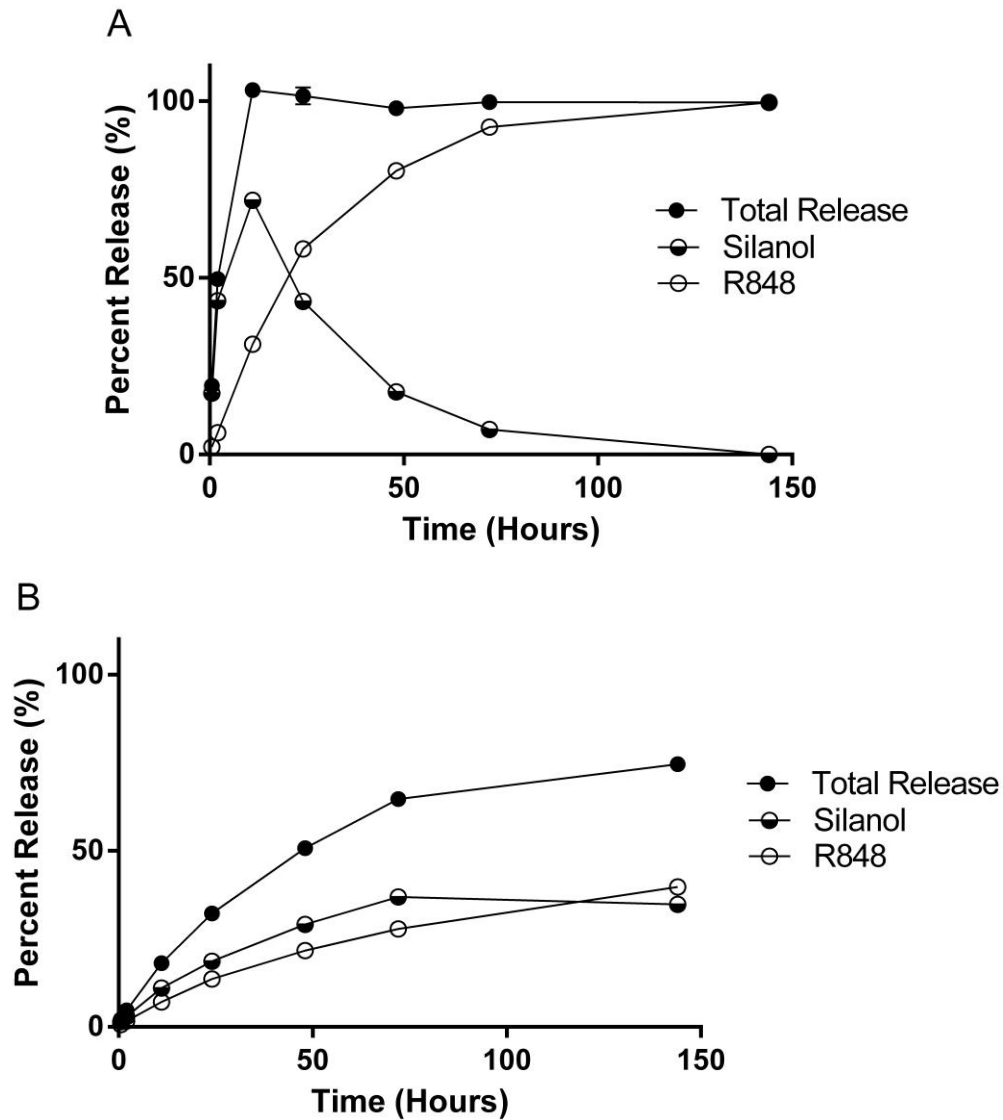


Figure 3.1 Release profile for R848 from Me₂ProR848-NPs at varying pH. A) At pH 5, NPs quickly release Me₂silanol-R848 which converts to free R848 steadily over time. B) At pH 7.4, Me₂silanol is slowly released and converts steadily to free R848 over time. Me₂ProR848-NP degradation plateaus at approximately 75% release. NPs were incubated in indicated buffer at a concentration of 1 mg/mL at 37 °C with agitation at 1400 RPM for seven days. Aliquots were taken from the NP solutions at the indicated time points. NPs were spun down and supernatant was tested by HPLC for R848 content. Values are reported as (amount released at given time point) ÷ (total amount released) × 100.

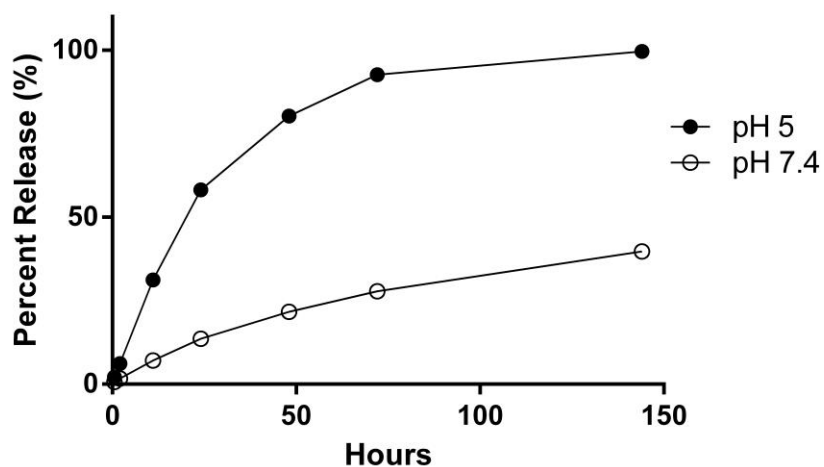


Figure 3.2 Release of R848 from Me₂ProR848-NPs at pH 5 vs. pH 7.4. R848 is released from NPs three times faster at pH 5 compared to pH 7.4. The half-life of Me₂ProR848-NPs at pH 5 is approximately 20 hours while at pH 7.4, half-life is 55 hours, both determined by fitting to a one phase decay, $R^2 > 0.999$.

Table 3.3 Half-life of Me₂ProR848-NPs *in situ*

pH	5	7.4
$t_{1/2}$ (hours)	19.85 ^a	54.79 ^a
Relative rate	1	2.76
^a Data fit to one phase decay, $R^2 > 0.999$		

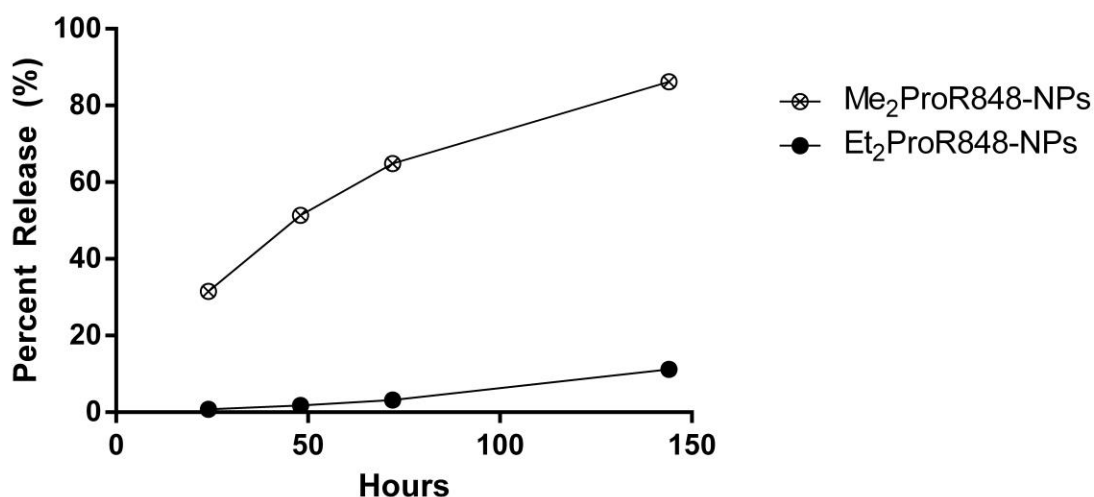


Figure 3.3 Release profile for R848 from Me₂- and Et₂ProR848-NPs at pH 5. R848 is fully released from Me₂ProR848 NPs over seven days at pH 5 while less than 20 % of R848 is released from the Et₂ProR848-NP formulation. The increased stability of Et₂ProR848-NP is due to the larger ethyl side groups on the bridging silicon atom.

3.2.3 *In Vitro* Analysis of R848

In vitro studies were performed to determine the activity of the Me₂- and Et₂ProR848-NPs compared to free, unmodified R848. Murine macrophage RawBlue reporter cells were dosed with R848, Me₂- and Et₂ProR848-NPs of various concentrations for 24 h at 37 °C. Me₂ProR848-NPs were found to be equally or slightly more efficient than free R848 at activating the TLR7 pathway *in vitro* while Et₂ProR848-NPs were less active by an order of magnitude (Figure 3.4a). These results indicate that Et₂ProR848-NPs do not release free R848 quickly enough to activate TLR7. While it is beneficial for the ProR848 to have long-term stability *in vivo* at pH 7.4, quick release of R848 upon endocytosis may be required in order to activate TLR7. After considering the *in situ* and *in vitro* results for Me₂- and Et₂ProR848-NPs, it was determined that the Me₂ProR848-NP formulation (hereafter “R848-NPs”) was the more promising candidate moving forward.

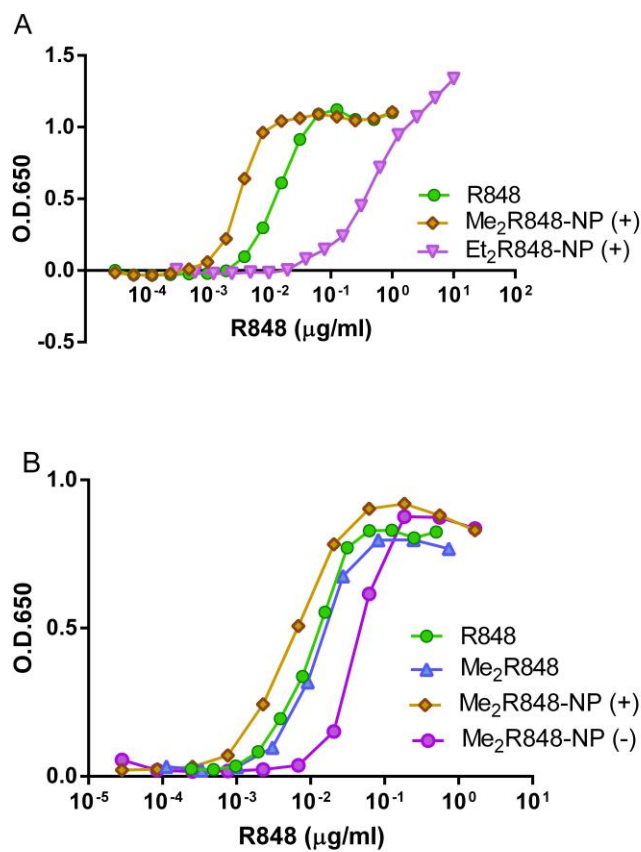


Figure 3.4 Activity of Me₂- and Et₂ProR848 NPs compared to free R848 on RawBlue macrophage cells. A) Me₂R848-NPs (+) elicit the production of alkaline phosphatase at lower concentrations than Et₂R848-NPs (+), indicating higher activation of TLR7. B) Cationic Me₂R848-NPs stimulate the production of alkaline phosphatase at lower doses than anionic Me₂R848-NPs, indicating the cationic NPs are more activating than the anionic counterpart. ProR848-NPs and soluble R848 were dosed on cells for 24 hours. After incubation, 50 µL medium was taken out from each well and added to 150 µL Quanti-Blue agent and incubated at 37 °C for 30 min to detect release of alkaline phosphatase as a measure for TLR 7 activation. Absorption was read at 650 nm. EC₅₀ values were calculated using a non-linear fit of the agonist dose response (Table 3.4). Figures are representative of three or more different experiments.

Soluble Me₂ProR848, and cationic and anionic R848-NPs were further compared for their activation of TLR pathway on RawBlue reporter cells (Figure 3.4b). Me₂ProR848 and cationic R848-NPs showed similar activity to free R848 as determined by EC₅₀ values (Table 3.4). Anionic R848-NPs showed lower activity than the other formulations with an EC₅₀ value approximately three times higher than soluble R848; however this may be due to the differential uptake of cationic versus anionic NPs *in vitro*.²⁸ Further experiments were done to determine the activity of the R848-silanol degradation intermediate compared to the free R848. Supernatants

from the degradation of cationic R848-NPs at pH 5 containing a known ratio of R848 to R848-silanol were dosed *in vitro*. Activation of RawBlue cells was determined at R848:silanol-R848 ratios of 1:4, 1:2, and 3:1 (Figure 3.5a). R848:silanol-R848 mixtures all showed similar cell activation to soluble R848 indicating that the silanol-R848 is still able to activate TLR 7. The above ProR848 formulations were dosed on both RawBlue cells and bone marrow derived DCs (BMDCs) to test for cytotoxicity. As shown in Figure 3.5 and Figure 3.6, there was no associated toxicity at any dosage of R848:silanol-R848, free R848, anionic or cationic Me₂ProR848-NPs, or the blank vehicle control. This result suggests that any activity seen through the reporter cell line or in subsequent experiments is due to the activity of R848 and not the NP vehicle.

Table 3.4 Half maximal effective concentration (EC₅₀) for R848 and ProR848 formulations

Formulation	EC ₅₀
Free R848	4.6 ng/mL
Me ₂ ProR848	6.75 ng/mL ± 2.33
R848-NPs (+)	6.8 ng/mL ± 4.2
R848-NPs (-)	39.8 ng/mL ± 4.6

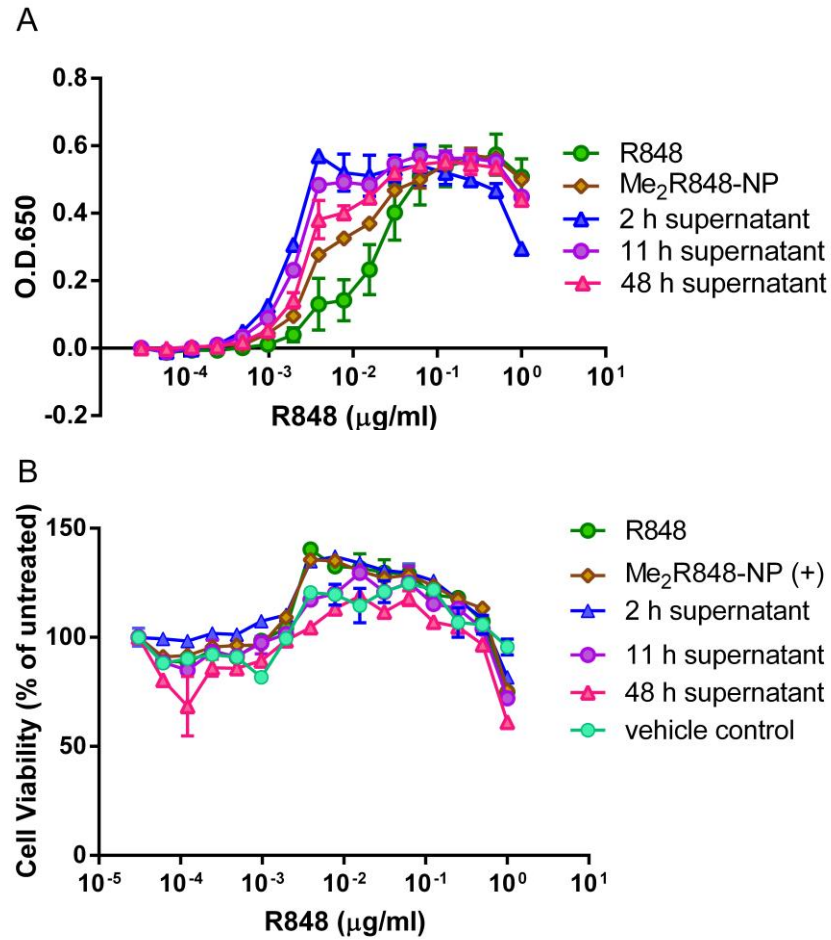


Figure 3.5 Activation of RawBlue cells after dosing of R848 and silanol-R848 together. R848:silanol-R848 mixture was collected from degradation of cationic R848-NPs at 12, 48, and 72 hours of incubation at pH 5. Cells were dosed with an equal amounts of total R848, shown as different R848:silanol-R848 ratios. R848:silanol-R848 mixture appeared to have negligible effect on cell activation compared to soluble R848 (A) and limited toxicity (B).

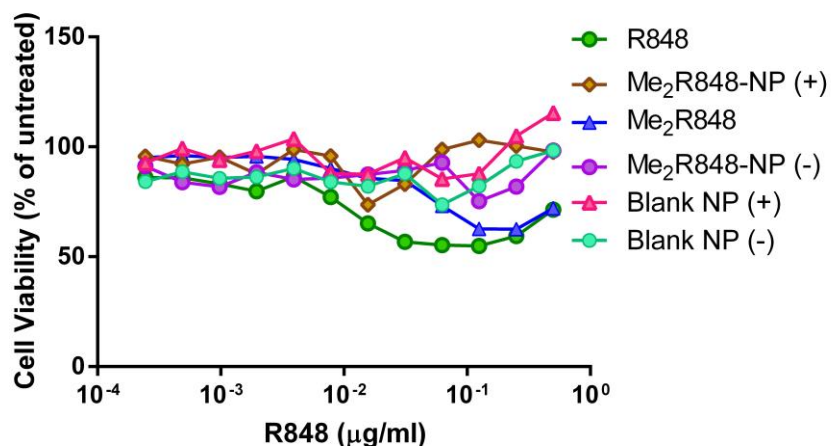


Figure 3.6 Cytotoxicity of Me₂Pro-R848 particles and monomer. R848 formulations were dosed on bone marrow derived DCs. Limited toxicity was observed for all formulations compared to an undosed control.

3.2.4 R848-NPs as a Vaccine Adjuvant *In Vivo*

Traditionally, R848 is able to boost antibody production with a skew towards a Th1 type response; however, the low molecular weight of R848 allows it to enter the blood stream and distribute throughout the body rather than going only to immune cells. This may lead to systemic inflammation, indicated by presence of TNF- α , IL-12, and other inflammatory cytokines. Systemic cytokine exposure is associated with the flu-like side effects seen after soluble administration of R848.²⁵ To determine if dosing R848 in particulate form would protect mice from systemic cytokine exposure, serum cytokine levels were tested after administration of soluble R848, cationic R848-NPs or anionic R848-NPs (Figure 3.7). Free R848 produced significant levels of both TNF- α and IL-12p40 in the blood at doses as low as 5ug R848/mouse. Anionic R848-NPs showed a modest reduction of TNF- α but not IL-12p40 production compared to soluble R848. Cationic R848-NPs significantly reduced both TNF- α and IL-12p40 production at doses lower than 8 μ g R848/mouse, indicating a therapeutically relevant window in which to dose R848 while reducing systemic cytokine exposure.

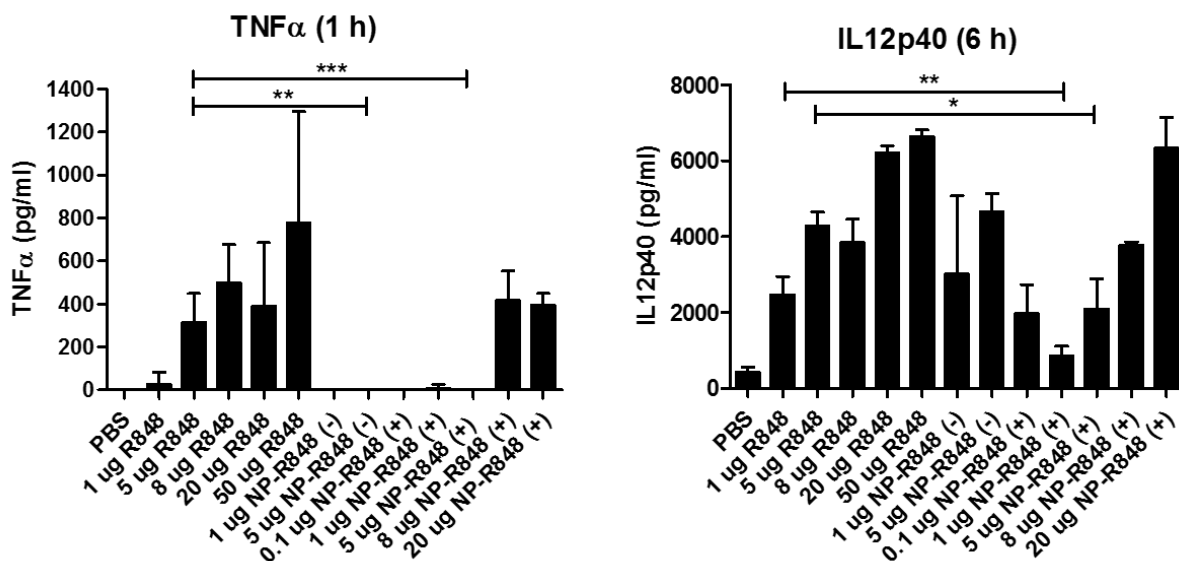


Figure 3.7 Serum cytokine profiles for soluble and particulate R848. Soluble R848 showed high levels of both TNF- α and IL12 with doses as low as 5 and 1 μ g R848 respectively. Cationic R848-NPs showed no TNF- α production for doses lower than 8 μ g R848. IL12 production after R848-NP dosage was significantly lower than soluble dosage as well. . N \geq 4. *, p < 0.05; **, p < 0.01; ***, p < 0.001 by unpaired t-test.

Based on the more favorable cytokine profile and *in vitro* activation of the cationic R848-NPs, only cationic R848-NPs were examined in the next stage of study.

It has been previously established that R848 can act as a vaccine adjuvant by increasing antibody production, especially IgG_{2a} type antibodies.^{29,30} Mice were dosed with R848-NPs or soluble R848 plus the model antigen ovalbumin (OVA) in order to determine how R848-NPs affect antibody production. OVA was dosed in either soluble form or conjugated to 80 \times 320 nm PRINT NPs (OVA-NP). Anti-OVA IgG and IgG_{2a} were tested one week after a boost dose. R848-NP + OVA-NP produced significantly higher antibody titers when compared all other formulations (p < 0.05, Figure 3.8), indicating that R848-NPs are not only as effective as a vaccine adjuvant as soluble R848, but are able to boost antibody production while also limiting systemic exposure.

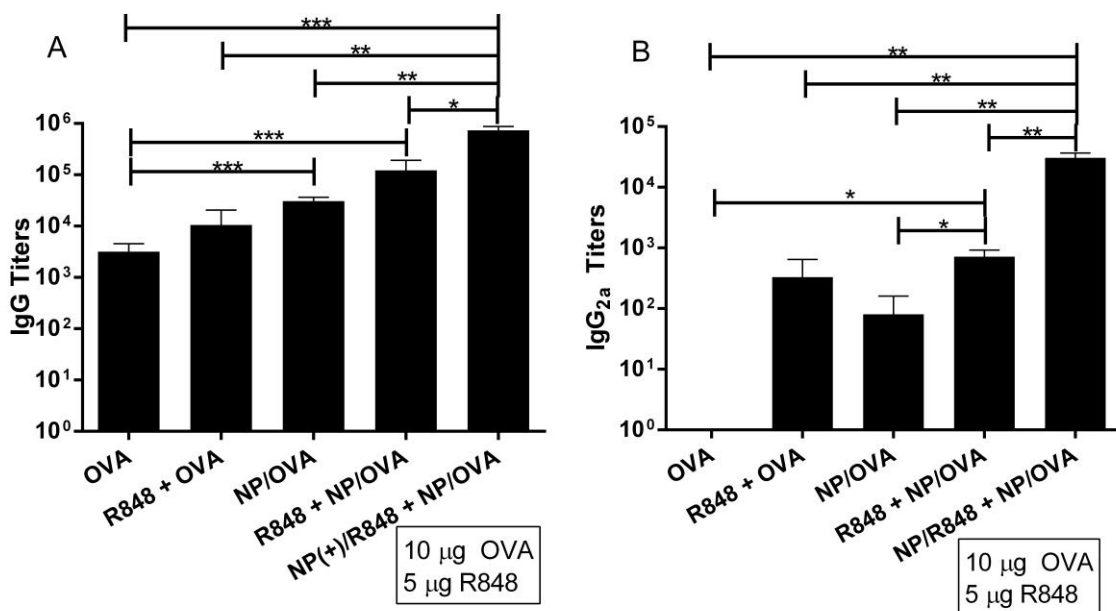


Figure 3.8 R848-NPs significantly improve production of OVA-specific antibodies compared to soluble administration. Mice were dosed subcutaneously with 10 µg OVA, soluble or NP, along with 5 µg R848, soluble or NP. After a prime-boost regimen, sera were collected and tested by ELISA for OVA-specific total IgG and subtype IgG_{2a}. R848-NPs significantly improved antibody production as well as IgG_{2a} production compared to soluble and unadjuvanted formulations. N ≥ 4. *, p < 0.05; **, p < 0.01; ***, p < 0.001 by unpaired t-test.

The high potency of R848 in comparison to other imidazoquinoline-type molecules and the potential increase in bioavailability from NP formulation provide an opportunity for R848 to have dose sparing effects in the amount of adjuvant and/or antigen needed to elicit a robust immune response. With the amount of antigen (OVA-NPs) held constant, the dose of R848 or R848-NPs was varied from 1 to 20 µg per mouse. When only 1 µg of R848-NPs were dosed, the antibody production was significantly higher than the highest dose of soluble R848 (Figure 3.9). At a 1 µg dose of R848 or R848-NPs, the antigen dose was lowered from 10 µg to 1 µg per mouse. Similar to the results seen when reducing the adjuvant dose, the lowest dose antigen with R848-NPs was higher than the higher dose of antigen with soluble R848 (Figure 3.10). These results suggest that by incorporating R848 into PRINT NPs, the potency of the adjuvant is increased, most likely due to a higher and longer lasting availability of R848 in local tissue and/or in the draining lymph nodes.

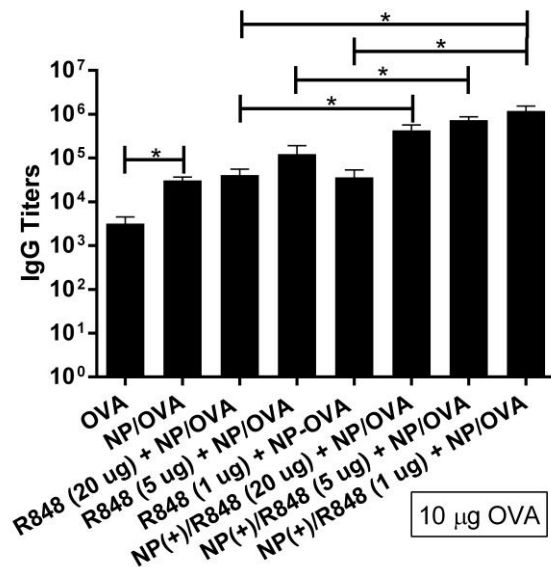


Figure 3.9 R848-NP formulation shows dose sparing effects for adjuvant dosage compared to soluble administration. Mice were dosed subcutaneously with the indicated dose of soluble or particulate R848 along with 10 µg soluble or particulate OVA. Sera were collected at day 28 after a prime-boost regimen and analyzed by ELISA for total IgG. N ≥ 4. *, p < 0.05; **, p < 0.01; ***, p < 0.001 by unpaired t-test.

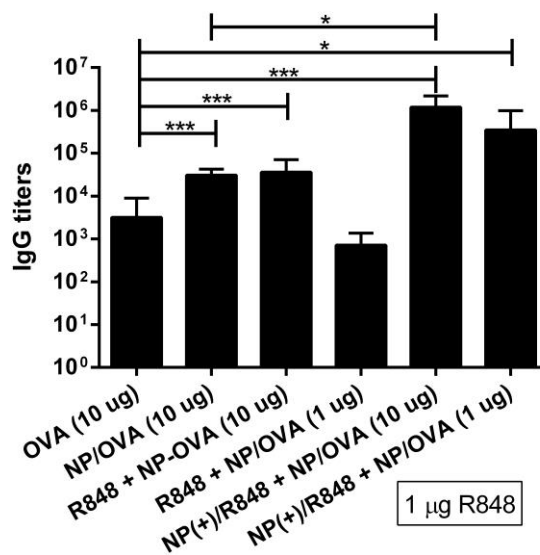


Figure 3.10 R848-NP formulation shows dose-sparing effects in antigen dosing compared to soluble R848 administration. Mice were dosed subcutaneously with the indicated dose of particulate OVA along with 1 µg soluble or particulate R848. Sera were collected at day 28 after a prime-boost regimen and analyzed by ELISA for total IgG. N ≥ 4. *, p < 0.05; **, p < 0.01; ***, p < 0.001 by unpaired t-test.

In addition to producing high levels of antigen-specific antibodies, an effective vaccine should elicit long lasting antibodies that remain for several months to several years. Mice that were immunized with the same prime-boost regimen above had blood drawn at regular increments to test for the persistence of OVA-specific antibodies. Mice dosed with R848-NP showed sustained high levels of IgG out to at least 120 days (Figure 3.11). This indicates that R848-NP formulation produce higher antibody levels than soluble administration and that the antibody response is robust enough to persist in the blood for an extended period of time.

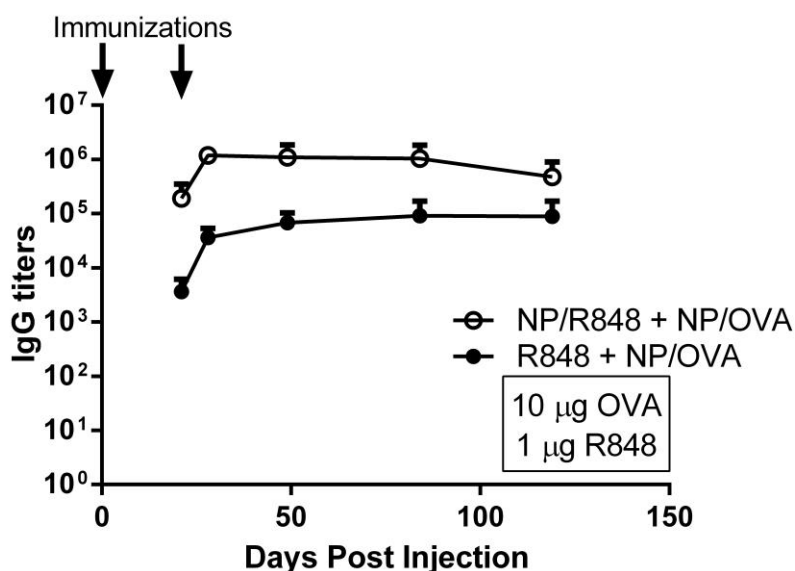


Figure 3.11 R848-NP dosage shows OVA-specific antibodies persisting in the blood out to at least 120 days. Mice were dosed subcutaneously with 10 μ g OVA-NP along with 1 μ g R848, soluble or NP. After a prime-boost regimen, blood was collected and serum was tested by ELISA for OVA-specific total IgG. R848-NPs significantly improved antibody production. Antibodies elicited by both formulations persisted out to at least 120 days after the first vaccination. The R848-NPs formulation showed a higher antibody response at all measured time points. Arrows represent immunizations at day 0 and day 21. $N \geq 4$.

FDA approval of R848 has stalled due to the high potency of this small molecule adjuvant producing unwanted side effects. By employing a pro-adjuvant strategy, we are able to covalently conjugate R848 into PRINT NPs with a controllable and reproducible release profile. Effective control of release of R848 at physiological pH limits systemic inflammation to a lower

dose window. By utilizing an acid-labile silyl ether linker to conjugate R848 to a polymerizable acrylate group, we are able to tune the release of R848 at endosomal pH, resulting in robust adjuvanticity without systemic exposure. Additionally, loading of R848 in particles greatly increase the adjuvanticity of R848 and lowers doses of both antigen and adjuvant that are necessary to achieve a robust antibody response. The antibodies produced were sustained in the blood for at least several months after only a prime and boost dose. These factors may be of critical importance for new vaccine technology, especially in times of epidemic diseases and in reducing costs for third world applications.

3.3 Conclusions

The potency of R848 in comparison to other imidazoquinoline molecules presents an interesting opportunity for vaccine applications. Utilizing R848 as a vaccine adjuvant can greatly increase the immune response produced, but may also result in more severe side effects often attributed to the inflammatory cytokine storm produced when the body is exposed to R848 and other potent immunostimulatory molecules.^{23,31} By conjugating R848 to PRINT nanoparticles through an acid-labile bond, we delivered R848 specifically to the endosomal compartment of antigen presenting cells, where TLR7/8 are found, with limited release at normal physiological pH. This resulted in reduced systemic exposure to R848 as indicated by low levels of serum cytokine production. In addition to decreasing systemic exposure, NP encapsulation also led to an increase in antigen-specific antibody production compared to soluble R848, likely because more of the R848 was available to the APCs of the lymph nodes rather than distributing throughout the body. Dose sparing effects were seen with both antigen and adjuvant dosing levels when dosed in particulate form compared to soluble form as well. Together, these data suggest that R848-NP formulation is a good candidate for a vaccine adjuvant, addressing the

concerns that have caused R848 to remain in the clinical testing stages rather than reaching FDA approval for normal use.

3.4 Materials and Methods

3.4.1 Materials

Resiquimod was purchased from Chemdea (Ridgewood, NJ). PRINT molds were supplied by Liquidia Technologies. All other chemicals and reagents were obtained from Sigma Aldrich, Inc., Fisher Scientific, Inc., Creative PEGworks, Inc., or eBioscience, Inc., unless otherwise noted.

3.4.2 Animals

Female C57BL/6 mice were purchased from Jackson Laboratory and used at age 6-12 weeks. All experiments involving the mice were carried out in accordance with an animal use protocol approved by the University of North Carolina Animal Care and Use Committee.

3.4.3 Synthesis of Pro-Adjuvant

R848 was modified into a pro-adjuvant by adding a polymerizable acrylate group to R848 through an acid-labile bis-silyl ether bond. 0.75 mmol R848, 6 mmol imidazole, and 1 mmol 4-dimethylaminopyridine were added to a flame dried scintillation vial with magnetic stir bar under an argon atmosphere and dissolved in 10 mL dry dimethylformamide (DMF). After stirring for 10 minutes until all reagents dissolved, 2 mmol of dimethyldichlorosilane was added drop-wise and allowed to react at room temperature for one hour. 2 mmol dry 2-hydroxyethyl acrylate (HEA) was added drop-wise and reaction was allowed to proceed for another hour. The product was extracted into ethyl acetate and dried by rotary evaporation. The product was purified by column chromatography with an eluent of 94% dichloromethane, 6% methanol. The

residual solvent was removed by rotary evaporation to yield a clear yellow oil with a yield above 80%. Structure was confirmed by $^1\text{H-NMR}$, $^{13}\text{C-NMR}$, and HRMS (Appendix Figures A.1-A.6).

3.4.4 Characterization of ProR848

Reverse phase high performance liquid chromatography (HPLC) was run on an Agilent 1200 series HPLC system using an Agilent C_{18} column. Due to solubility restrictions of R848, all samples were suspended in an aqueous solution (water, buffer) with 25% DMF. The mobile phase consisted of mixtures of H_2O with 0.1% trifluoroacetic acid (TFA) (solvent A) and acetonitrile with 0.1% TFA (solvent B). The elution protocol for R848 consisted of a gradient starting at 100:0 (A to B) and finishing at 0:100 (A to B) over 15 minutes followed by a hold at the final concentration for 5 minutes. The product was eluted at a flow rate of 1 mL/min and monitored at a wavelength of 260 nm.

Samples were prepared for NMR (nuclear magnetic resonance) by dissolving a small amount of the compound in CD_2Cl_2 or CD_3OD (deuterated methanol). NMR measurements were performed using a Bruker AVANCE III spectrometer at room temperature. ^1H NMR measurements were collected at 600 MHz and ^{13}C NMR measurements were collected at 150 MHz.

High resolution mass spectrometry (HRMS) was performed on a Thermo LTqFT (linear ion trap, Fourier transform mass spectrometry) with 7.0 Tesla magnet or a TriVersa Nanomate[®] ESI Micromass Quattro II Triple Quadrupole Mass Spectrometer. Solutions were dissolved to < 0.5 mg/mL in methanol before direct injection into the instrument. HRMS (m/z) calculated for $\text{Me}_2\text{ProR848}$, $[\text{M}]^+ = 487.2299$; found $[\text{M}]^+ \text{ m/z} = 487.2347$. HRMS (m/z) calculated for $\text{Et}_2\text{ProR848}$, $[\text{M}]^+ = 515.2612$; found $[\text{M}]^+ \text{ m/z} = 515.26$.

LC-MS (liquid chromatograph mass spectrometry) was performed on an Agilent 1200 Series LC-MS using a 2.7 μ M HALO C₁₈ column in positive ion mode with electrospray ionization. LC-MS data were analyzed using Agilent ChemStation software. Samples were prepared by degrading R848-NPs in low pH buffer at 1mg/mL and collecting the supernatant for analysis. Separations were performed in a mobile phase of 0 to 20% B over 25 minutes where A = 95:5 water:acetonitrile 0.2% formic acid and B = 0:100 water:acetonitrile with 0.2% formic acid. The compounds were eluted at a flow rate of 0.3 mL/min and monitored at a wavelength of 260 nm.

3.4.5 Fabrication of Hydrogel NPs via the PRINT Process

The fabrication of nano-sized particles was achieved by mold-based PRINT particle fabrication technology using the compositions shown in Table 3.1.^{28,32} For pro-adjuvant loaded NPs, cure-site monomer (CSM) solutions were prepared at 3 weight % solids in dry DMF. The film-split technique for preparing NPs was performed as described in the following: using a #3 Mayer rod, 150 μ L of CSM solution was cast on a sheet of corona treated poly(ethylene terephthalate) (PET), followed by brief evaporation of solvent with a heat gun to yield a transparent film (delivery sheet). Patterned Fluorocur PRINT molds (Liquidia Technologies) were laminated against the delivery sheet with moderate pressure (40 psi) and delaminated at the same pressure. The filled mold cured in a UV chamber ($\lambda_{\text{max}} = 395$ nm) for 3.5 minutes under a nitrogen atmosphere. After photocuring, the mold was laminated onto a sacrificial harvesting layer of 2 kDa poly(vinyl alcohol) (PVOH) at 80 psi, 150 °C. NPs were harvested with 2mL sterile filtered pH 7.4 buffer (Fisher Sci.) per 0.5 foot \times 5 foot section NPs were washed via centrifugation (15 min, 14k RPM, 4 °C), removal of supernatant, and resuspension in fresh solvent. NP yield was determined by thermogravimetric analysis (Q5000IR, TA Instruments).

Blank NPs for post-fabrication antigen loading were fabricated by a roll-to-roll process based on the above fabrication method using the composition in Table 2.3, as previously described.³³

3.4.6 Characterization of R848-NPs

Scanning electron microscopy (SEM) enabled imaging of hydrogel NPs that were dispersed on a silicon wafer and coated with approximately 1.5 nm of Au/Pd (Hitachi S-4700, FEI Helios Nanolab 600). ζ -potential measurements were conducted on ~20 $\mu\text{g}/\text{mL}$ NP dispersions in water using a Zetasizer Nano ZS Particle Analyzer (Malvern Instruments Inc.). Antigen conjugation was measured using a standard BCA Assay (Fisher).

Total adjuvant loading in R848-NPs was determined by degrading a sample of R848-NPs at a concentration of 1 mg/mL in a buffer solution, pH 3, at 37 °C with agitation at 1400 RPM for 48 hours. The supernatant was tested by HPLC for R848 content. For each batch of R848-NPs, this method was used to determine the total loading and release percentage for release profiles. To establish a release profile of the R848 from R848-NPs, samples of R848-NPs were suspended at 1mg/mL in buffer solutions at pH 5 or pH 7.4. 100 μL samples were taken at indicated time points and the supernatant was isolated and tested for R848 content by HPLC. The concentration at the indicated time point was divided by the total adjuvant loading to determine the percent of R848 released at each time point. All samples were run in triplicate.

3.4.7 *In Vitro* Studies.

RawBlue macrophage cells (Invivogen) were maintained in DMEM high glucose supplemented with 10% FBS, 2 mM L-glutamine, 100 units/mL penicillin and 100 $\mu\text{g}/\text{mL}$ streptomycin, 1 mM sodium pyruvate, non-essential amino acids, 100 $\mu\text{g}/\text{mL}$ Normocin, and 200 $\mu\text{g}/\text{mL}$ Zeocin. RawBlue cells were plated in 96-well plates at 100,000/well and incubated overnight at 37 °C. Cells were then dosed with samples in complete medium without

Normocin/Zeocin at 37 °C for 24 h. After incubation, 50 µL medium was taken out from each well and added to 150 µL Quanti-Blue™ agent (Invivogen) and incubated at 37 °C for 30 min. Absorption at 650 nm was read by a SpectraMax M5 plate reader (Molecular Devices).

Bone marrow derived DCs (BMDCs) were harvested from the bone marrow of C57BL/6 mice. Briefly, femur and tibia were collected and bone marrow cells were flushed out with RPMI 1640 medium supplemented with 10% FBS, 2 mM L-glutamine, 100 units/mL penicillin and 100 µg/mL streptomycin, 50 µM β-mecaptoethanol, 10 ng/mL GM-CSF and 10 ng/mLIL-4. Cells were cultured at 37 °C and fed once on day three. Loosely adherent and non-adherent cells were harvested on day 6 and suspended in Hanks buffered salt solution (GIBCO). A 2.3 mL Opti-Preconcentrate (Sigma) was added to 9.7 mL Hanks buffer with 1 mM EDTA, 0.5% (wt./vol.) bovine serum albumin, 10 mM HEPES, pH 7.4. The cell suspension was gently layered on the top of 6 mL of the Opti-Prep mixture and centrifuged at 600×g for 5 min. The cells at the interface were collected, washed and used for experiments. For cytotoxicity assay, 100,000 per well BMDCs were treated with samples at indicated doses for 24 h at 37 °C. Cell viability was evaluated with Promega CellTiter 96® AQueous One Solution Cell Proliferation Assay following manufacturer's instruction. Absorption at 490 nm was measured by a SpectraMax M5 plate reader (Molecular Devices).

3.4.8 Serum Cytokine Study

C57BL/6 mice, 6-8 weeks old, were immunized with soluble or R848-NP subcutaneously in the flank with the indicated doses. Blood was drawn at 1, 6, or 24 hours after dosing. Serum cytokine levels were assayed via ELISA (BD Biosciences). IL12p40 was tested at six and twenty-four hour and TNF-α was tested at one hour post immunizations. Sera from 6 h were tested for IL6 as well.

3.4.9 Immunizations and Antibody ELISA.

C57BL/6 mice, 6-8 weeks old, were immunized with soluble or R848-NP and soluble or OVA-NP subcutaneously in the flank with the indicated doses. Mice were primed on day zero and boosted on day 21. Plasma samples were collected by bleeding mice submandibularly on day 28 and OVA-specific antibody production was examined by ELISA. Briefly, EIA plates (Corning) were coated with 10 µg/mL OVA in ELISA coating buffer (eBioscience) at 4 °C overnight. The wells were washed and blocked with 200 µL per well of 3% BSA in PBST (PBS with 0.05% Tween 20) for 2 hours. Plasma samples were diluted in blocking buffer and incubated for 2 hours. The wells were washed extensively with PBST and anti-OVA IgG was detected using HRP conjugated goat anti-mouse IgG (Invitrogen) and was visualized by adding 100 µL of TMB (eBioscience) to each well. The reaction was stopped after 11 min with 50 µL 0.2 M H₂SO₄. Optical densities (OD) were read at 450 nm and 570 nm. The antibody titer was determined as the highest dilutions with OD 450-570 nm > 0.1.

3.5 References

- (1) Zbinden, D.; Manuel, O. *Immunotherapy* **2014**, *6*, 131–139.
- (2) Kotton, C. N. *Expert Rev. Vaccines* **2008**, *7*, 663–672.
- (3) Bachelder, E. M.; Beaudette, T. T.; Broaders, K. E.; Fréchet, J. M. J.; Albrecht, M. T.; Mateczun, A. J.; Ainslie, K. M.; Pesce, J. T.; Keane-Myers, A. M. *Mol. Pharm.* **2010**, *7*, 826–835.
- (4) Medzhitov, R.; Janeway, C. A. *Cell* **1997**, *91*, 295–298.
- (5) Pockros, P. J.; Guyader, D.; Patton, H.; Tong, M. J.; Wright, T.; McHutchison, J. G.; Meng, T.-C. *J. Hepatol.* **2007**, *47*, 174–182.
- (6) Smith, K. J.; Hamza, S.; Skelton, H. *Expert Opin. Pharmacother.* **2003**, *4*, 1105–1119.
- (7) Steinhagen, F.; Kinjo, T.; Bode, C.; Klinman, D. M. *Vaccine* **2011**, *29*, 3341–3355.
- (8) Gibson, S. J.; Lindh, J. M.; Riter, T. R.; Gleason, R. M.; Rogers, L. M.; Fuller, A. E.; Oesterich, J. L.; Gorden, K. B.; Qiu, X.; McKane, S. W.; Noelle, R. J.; Miller, R. L.; Kedl, R. M.; Fitzgerald-Bocarsly, P.; Tomai, M. A.; Vasilakos, J. P. *Cell. Immunol.* **2002**, *218*, 74–86.
- (9) Lehner, M.; Morhart, P.; Stilper, A.; Petermann, D.; Weller, P.; Stachel, D.; Holter, W. *J. Immunother.* **2007**, *30*, 312–322.
- (10) Bishop, G. A.; Hsing, Y.; Hostager, B. S.; Jalukar, S. V.; Ramirez, L. M.; Tomai, M. A. *J. Immunol.* **2000**, *165*, 5552–5557.
- (11) Tomai, M. A.; Imbertson, L. M.; Stanczak, T. L.; Tygrett, L. T.; Waldschmidt, T. J. *Cell. Immunol.* **2000**, *203*, 55–65.
- (12) Wagner, T. L.; Ahonen, C. L.; Couture, a M.; Gibson, S. J.; Miller, R. L.; Smith, R. M.; Reiter, M. J.; Vasilakos, J. P.; Tomai, M. A. *Cell. Immunol.* **1999**, *191*, 10–19.
- (13) Tomai, M.; Gibson, S.; Imbertson, L. *Antiviral Res.* **1995**, *28*, 253–264.
- (14) Testerman, T. L.; Gerster, J. F.; Imbertson, L. M.; Reiter, M. J.; Miller, R. L.; Gibson, S. J.; Wagner, T. L.; Tomai, M. A. *J. Leukoc. Biol.* **1995**, *58*, 365–372.
- (15) Dockrell, D. H.; Kinghorn, G. R. *J. Antimicrob. Chemother.* **2001**, *48*, 751–755.
- (16) Fife, K. H.; Meng, T.-C.; Ferris, D. G.; Liu, P. *Antimicrob. Agents Chemother.* **2008**, *52*, 477–482.

- (17) Szeimies, R.-M.; Bichel, J.; Ortonne, J.-P.; Stockfleth, E.; Lee, J.; Meng, T.-C. *Br. J. Dermatol.* **2008**, *159*, 205–210.
- (18) Tomai, M. A.; Miller, R. L.; Lipson, K. E.; Kieper, W. C.; Zarraga, I. E.; Vasilakos, J. P. *Expert Rev. Vaccines* **2007**, *6*, 835–847.
- (19) Vasilakos, J. P.; Tomai, M. A. *Expert Rev. Vaccines* **2013**, *12*, 809–819.
- (20) Bachelder, E. M.; Beaudette, T. T.; Broaders, K. E.; Dashe, J.; Fréchet, J. M. J. *J. Am. Chem. Soc.* **2008**, *130*, 10494–10495.
- (21) Duong, A. D.; Sharma, S.; Peine, K. J.; Gupta, G.; Satoskar, A. R.; Bachelder, E. M.; Wyslouzil, B. E.; Ainslie, K. M. *Mol. Pharm.* **2013**, *10*, 1045–1055.
- (22) Schully, K. L.; Sharma, S.; Peine, K. J.; Pesce, J.; Elberson, M. A.; Fonseca, M. E.; Prouty, A. M.; Bell, M. G.; Borteh, H.; Gallovic, M.; Bachelder, E. M.; Keane-Myers, A.; Ainslie, K. M. *Pharm. Res.* **2013**, *30*, 1349–1361.
- (23) Ilyinskii, P. O.; Roy, C. J.; O’Neil, C. P.; Browning, E. A.; Pittet, L. A.; Altreuter, D. H.; Alexis, F.; Tonti, E.; Shi, J.; Basto, P. A.; Iannacone, M.; Radovic-Moreno, A. F.; Langer, R. S.; Farokhzad, O. C.; von Andrian, U. H.; Johnston, L. P. M.; Kishimoto, T. K. *Vaccine* **2014**, *32*, 2882–2895.
- (24) Shukla, N. M.; Salunke, D. B.; Balakrishna, R.; Mutz, C. A.; Malladi, S. S.; David, S. A. *PLoS One* **2012**, *7*, e43612.
- (25) Smirnov, D.; Schmidt, J. J.; Capecchi, J. T.; Wightman, P. D. *Vaccine* **2011**, *29*, 5434–5442.
- (26) Parrott, M. C.; Luft, J. C.; Byrne, J. D.; Fain, J. H.; Napier, M. E.; Desimone, J. M. *J. Am. Chem. Soc.* **2010**, *132*, 17928–17932.
- (27) Parrott, M. C.; Finniss, M.; Luft, J. C.; Pandya, A.; Gullapalli, A.; Napier, M. E.; DeSimone, J. M. *J. Am. Chem. Soc.* **2012**, *134*, 7978–7982.
- (28) Gratton, S. E. A.; Ropp, P. A.; Pohlhaus, P. D.; Luft, J. C.; Madden, V. J.; Napier, M. E.; DeSimone, J. M. *Proc. Natl. Acad. Sci. U. S. A.* **2008**, *105*, 11613–11618.
- (29) Velasquez, L. S.; Hjelm, B. E.; Arntzen, C. J.; Herbst-Kralovetz, M. M. *Clin. Vaccine Immunol.* **2010**, *17*, 1850–1858.
- (30) Vasilakos, J. P.; Smith, R. M.; Gibson, S. J.; Lindh, J. M.; Pederson, L. K.; Reiter, M. J.; Smith, M. H.; Tomai, M. A. *Cell. Immunol.* **2000**, *204*, 64–74.
- (31) Tacke, P. J.; Zeelenberg, I. S.; Cruz, L. J.; van Hout-Kuijter, M. A.; van de Glind, G.; Fokkink, R. G.; Lambeck, A. J. A.; Figdor, C. G. *Blood* **2011**, *118*, 6836–6844.

- (32) Gratton, S. E. A.; Williams, S. S.; Napier, M. E.; Pohlhaus, P. D.; Zhou, Z.; Wiles, K. B.; Maynor, B. W.; Shen, C.; Olafsen, T.; Samulski, E. T.; Desimone, J. M. *Acc. Chem. Res.* **2008**, *41*, 1685–1695.
- (33) Perry, J. L.; Reuter, K. G.; Kai, M. P.; Herlihy, K. P.; Jones, S. W.; Luft, J. C.; Napier, M.; Bear, J.E.; DeSimone, J. M. *Nano Lett.* **2012**, *12*, 5304-5310.

CHAPTER 4 PRINT BASED VACCINES FOR CLINICALLY RELEVANT DISEASE MODELS

4.1 Introduction

Infectious diseases are the second largest cause of death worldwide, responsible for nearly nine million deaths each year.¹ Of these deaths, over three million can be attributed to vaccine preventable diseases such as rotavirus, pneumonia, and influenza.² In addition to the almost thirty vaccines currently available in the USA, research is underway to develop vaccines against a host of other diseases such as Staphylococcal disease,³ Alzheimer's disease,⁴ and HIV⁵ (human immunodeficiency virus). Increasing attention has been paid to subunit-based vaccines in the development of new vaccines and improving on those already available. Nanoparticle delivery of pathogen subunits may further address some of the pitfalls of traditional whole-pathogen vaccines while boosting the immunogenicity of subunits alone. Nanoparticles have the potential to mimic the natural multivalent presentation of antigen and adjuvant to immune cells that is not likely to occur when these subunits are dosed in soluble form.⁶⁻⁹ Additionally, for diseases that present with several distinct strains, nanoparticles may be able to concurrently deliver antigens for multiple strains to the same immune cell, enhancing the immune response.

4.1.1 Dengue Virus as a Global Threat and Current Vaccine Strategies

Dengue virus is a mosquito borne virus that affects up to 50 million people each year.¹⁰ While dengue infection is uncommon in the United States, over 40% of the world lives in at-risk areas where *Aedes aegypti*, the disease carrying mosquitos, reside. Dengue virus is unique in that the virus has four distinct serotypes and protection against one serotype does not provide cross-

protection against the other serotypes.¹¹ In fact, infection by one serotype of dengue virus often results in a more severe response to dengue virus if infected by a second serotype, thought to be caused by antibody-dependent enhancement (ADE). ADE results when antibodies against a single serotype are weakly or non-neutralizing against other serotypes of a virus but are still cross-reactive, essentially protecting the virus from being recognized by neutralizing antibodies and allowing it to continue to replicate and infect the immune cells attempting to clear the virus.^{10,12} There is no approved treatment or vaccine against dengue virus and the best method of prevention is to avoid mosquito bites via DEET (diethyltoluamide) treated mosquito nets and personal use of 20-30% DEET bug spray, both of which may be challenging to access reliably in developing countries.¹³

Current efforts toward a vaccine against dengue virus have investigated live-attenuated (LA) dengue viruses, recombinant proteins, viral vectors, and DNA-based vaccines.^{10,11} In a phase III clinical trial, one LA dengue vaccine utilizing an inactivated yellow fever 17D virus (CYD) as a vector produced key antigenic proteins for each of the four dengue serotypes, eliciting neutralizing antibodies to all four serotypes in more than 60% of patients; however, the dosing schedule was spread over a period of 12 months before attaining this high level of immunity.¹³ DNA vaccines, recombinant virus vaccines, and subunit protein vaccines are currently being explored in the preclinical stages and early stage clinical trials. These non-replicating vaccine strategies have the benefit over a dengue-based LA vaccine in that they may be dosed to immunocompromised patients without risk of infection. DNA vaccines are often inexpensive, stable over a wide temperature range, and may be dosed on a condensed immunization schedule, although they are often less immunogenic than LA vaccines^{11,14-26}. Self-assembling adenovirus and alphavirus replicon vaccines are able to increase uptake into cells due

to their particulate nature compared to soluble DNA, thereby increasing their potency.^{11,27-32} This strategy, however, carries the risk of “viral interference” where patients develop antibodies against the vaccine vector rather than or in addition to the target antigen, decreasing the efficacy of subsequent doses.²⁹ Neutralizing antibodies in DENV infected patients recognize the serotype specific envelope protein (E protein), which has become the primary target for subunit protein vaccines, along with structural proteins, like the premembrane protein (prM).³³ Preserving the quaternary structure of E is critical to eliciting neutralizing antibodies against DENV, as the neutralizing human monoclonal antibodies that have been isolated appear to recognize the quaternary structure of two or more E proteins interacting rather than the sequence alone.^{34,35} The prM protein may assist E in this assembly, which presents a challenge for recombinant E protein (recE) vaccines in maintaining its native structure. Synthesis of an abbreviated recE formulated with the adjuvant alum has shown promise in presenting a “native-like” structure and research projects in this area were recently transferred from Hawaii Biotech, Inc. to the vaccine manufacturer Merck & Co. for clinical evaluation.³⁶ RecE and specific domains of recE present an opportunity for protection on a shortened dosing schedule, however, similar to DNA vaccines, these recombinant proteins face the challenge of efficient cell uptake and initiating a balanced immune response against all four serotypes of dengue virus.^{11,37-42}

Combining a recE protein-based subunit vaccine with PRINT nanoparticles, we may be able to overcome the challenges faced thus far by DENV subunit vaccines. Native DENV is a roughly spherical particle, 40–50 nm in diameter with prM and E proteins decorating the surface of the virus.¹⁰ By conjugating recE to nanoparticles of similar size and shape to native DENV, we may be able to induce stronger interaction with and uptake by immune cells than soluble E alone. Additionally, by either combining all four recE serotypes onto a single nanoparticle or

mixing nanoparticles with individual serotype recE, we can explore the relationship between antigen presentation to the immune system and the development of a balanced immune response. PRINT nanoparticles are biocompatible, non-immunogenic,⁴³ and have not shown any risk to date of eliciting viral interference type of effects against the particle matrix. Unlike other nanoparticle platforms, the unique tunability of PRINT offers the opportunity to explore the size, shape, composition, and surface charge of the particle vector, as well as the linker length between the particle and the protein, the density of the protein on the particle surface, and the ratios among different serotypes in a single formulation.

4.1.2 Influenza Virus: Overcoming Barriers Towards Total Immunization

Seasonal influenza (flu) affects between 5-10% of the adult population each year, resulting in up to 5 million severe cases of the flu and up to 500,000 deaths annually.⁴⁴ While current vaccine strategies are typically 60%-85% effective in healthy patients at preventing the flu, there are considerable drawbacks to current formulations, especially for immunocompromised patients. In healthy patients, both inactivated and live attenuated (LA) vaccine types may be utilized, though these may both be less effective in the elderly. LA vaccines are contraindicated for immunocompromised patients and inactivated vaccine formulations have shown to be less effective in these populations as well.^{45,46}

Immunocompromised patients, patients with HIV, those who have received organ or stem cell transplants, and those who take biologic agents (e.g. TNF- α blockers like adalimumab and infliximab for rheumatoid arthritis, Crohn's disease, and other inflammatory diseases), are at higher risk of developing severe complications from the flu, including pneumonia, other respiratory infections, hospitalization, and death, and therefore represent a group which could reap the greatest benefit from safe and effective vaccines against the flu. Unfortunately, the

immunosuppressed state of these individuals often results in a lower antibody response after vaccination, leading to inadequate protection against flu infection. For transplant patients especially and others taking immunosuppressive drugs, the flu vaccine may be ineffective up to six months after transplant and for heart and/or lung transplant patients, certain adjuvanted vaccines have been implicated in increased risk of transplant rejection.⁴⁷ For these patients, it is especially important to develop safer and more effective vaccines against influenza by utilizing an efficient delivery system to restrict exposure to strong immunostimulating molecules to local tissues and lymphoid organs.

Additional areas where current vaccination strategies are lacking include the time to manufacture, the reliance on a steady supply of eggs as a precursor of vaccines, lack of cross protection against changes in the antigen signature of the flu virus, and the short lifetime of the immune response.^{48,49} Several novel strategies are currently being explored to address these concerns. One interesting strategy being studied by several groups is the development of a universal vaccine against the flu.⁵⁰⁻⁵² This approach targets antigens with highly conserved epitopes rather than the HA and NA proteins, which are prone to antigenic drift year to year. Universal vaccines based on influenza matrix proteins (M1, M2) and nucleoproteins (NP) have been investigated in several clinical trials, but these conserved epitopes often require adjuvants or other “helper” sequences in order to elicit a robust immune response.⁵⁰ DNA vaccines have been investigated as well, in which the HA gene is inserted into a DNA plasmid which is then dosed to the patient. These vaccines induce host cells to express the HA antigen, allowing the hosts immune cells to interact with HA antigens that were produced internally rather than coming from the virus. As mentioned above, DNA vaccines have good stability and the potential for rapid production, however, they have shown limited immunogenicity in humans.⁵³ In 2013, a

recombinant HA influenza vaccine, FluBlok® (Protein Sciences, Meriden, CT), was approved in the USA for patients age 18-49.⁵⁴ Recombinant vaccines are made in the lab without reliance on eggs and do not come in contact with the native pathogen. While this strategy shows promise as well, FluBlok was shown to be only 44.6% effective in healthy adults, leaving much to be desired.⁵⁵

Recombinant protein antigen technology has spurred exploration of nanoparticle strategies for development of novel flu vaccines. Delivering protein subunits via nanoparticles offers advantages over soluble delivery such as protecting the antigen from premature degradation, delivery to professional antigen presenting cells (APCs), and co-delivery with other vaccine components like immunostimulatory molecules to the same APC.⁵⁶ Virus-like particles have been utilized to deliver both recombinant HA and NA proteins *in vivo*.^{57,58} Virus-like particles utilize structural proteins from inert viruses with the genetic material removed and replaced with a protein of interest; in this case, HA and/or NA proteins⁵⁸ or peptides.⁵⁷ This strategy has shown promising results and has led to several clinical trials, but utilizing foreign proteins to build the VLP structure has the potential to cause an anti-vector immune response, similar to viral interference, in addition to the desired immune response.^{29,59} Biodegradable, inorganic calcium phosphate core-shell particles have been investigated as vaccine delivery vehicles.⁵⁶ Recombinant HA and an immunomodifer, CpG, were encapsulated in the layers of calcium phosphate during particle fabrication, leading to particles that could steadily release their cargo as the particles degraded *in vivo*. The degradation products are found naturally in the body so present no opportunity for anti-vector immune responses. Organic nanoparticle systems have also been explored for development of new HA vaccines. In one study, liposomes were formed with dioleoylphosphatidylcholine (PC) with recombinant HA encapsulated within the

liposome.⁶⁰ Other studies have investigated the biodegradable/biocompatible polymer PLGA (poly(lactic-co-glycolic acid)) as the basis for fabricating nanoparticles for the delivery of recombinant HA.^{61,62}

Previous work by Liquidia Technologies (Research Triangle Park, NC) investigated the applications of PRINT technology for the development of a flu vaccine using HA.⁶¹ In this study, PRINT was used to fabricate cationic PLGA NPs, which could adsorb HA proteins from the commercial flu vaccine Fluvirin® (a purified subunit vaccine). NPs were mixed with varying amounts of Fluvirin to achieve protein adsorption. It was found that mice dosed with 20 µg NPs + 0.025 µg of Fluvirin elicited a higher immune response than 1 µg of Fluvirin alone, representing a forty times decrease in the amount of antigen dosed. This result demonstrates the potential in formulating an influenza vaccine using PRINT particles.

In this work, HA was covalently linked to the surface of 80×320 nm PRINT hydrogel nanoparticles (NPs) to formulate flu vaccines. This covalent linkage allows for a greater amount of HA to be delivered with a smaller amount of NPs when compared to adsorption strategies. Covalent conjugation also allows for a greater degree of stability to assure particle-mediated delivery of HA to APCs: when proteins are electrostatically adsorbed to NPs, a strong electrolyte solution may be able to disrupt the adsorption, resulting in premature release of cargo. With covalent conjugation, only chemical means, e.g. protease degradation of the peptide epitopes from the protein, will be able to remove HA from the NP surface. Additionally, covalent linkage allows for more precise investigation into the role of linker length and surface density of antigen in eliciting an immune response. Herein I describe the initial steps in developing a PRINT hydrogel-based vaccine for influenza.

4.2 Results and Discussion

4.2.1 Conjugation of Dengue Virus Envelope Protein to PRINT NPs

The dengue virus envelope protein (E) has been established as a major target of neutralizing antibodies against dengue virus^{33,34,63} and has been studied in previous work for the development of a vaccine against dengue virus.^{11,37-42} A recombinant form of this protein (recE) was expressed by host cells *in vitro* for use in the development of a PRINT NP-based dengue vaccine.

The E protein of dengue virus, serotype 2 (DV2) shares some chemical similarities to the model protein antigen ovalbumin (OVA). The two antigens are both 40-50 kDa in weight with many lysine (free amine functional group) and aspartic acid and glutamic acid (free carboxylic acid functional groups) residues exposed on the surface of the protein (DV2 E protein, Protein Data Bank ID: 1OAN). One important difference, however, is the isoelectric point (pI) of the two proteins. OVA has a pI of ~4.5, indicating that at neutral pH, the protein will have a net negative charge. RecE has a pI of 7, indicating that it will have a net neutral charge at neutral pH. This difference in pI may have a dramatic effect on the reactivity of the proteins under various reaction conditions.

Due to the high cost and low availability of recombinant E protein (recE), the conjugation reactions were first performed with OVA. Previous reactions with OVA used a 1:1 ratio of OVA to NPs (Chapter 2) so to better represent the available amount and concentration of recE, reactions were carried out either maintaining the NP concentration and attempting to conjugate as much of the OVA as possible to the NPs (Reaction 1) or maintaining the 1:1 ratio and overall NP and protein concentration (Reaction 2). Both reactions resulted in moderate to high levels of OVA conjugation, well above the limit of detection for the BCA assay (Table 4.1). These

reactions were carried out with both a short PEG linker (MW = 500) and a direct amide bond between the protein and the NP, resulting in similar protein conjugation levels with both linkers.

Table 4.1 Low OVA:NP ratio reactions

	Reaction 0 (Chapter 2)	Reaction 1	Reaction 2
NP:OVA ratio	1:1	5:1	1:1
Reaction volume	1.4 mL	1.4 mL	0.28 mL
Amount of NPs	1-4 mg	1 mg	0.2 mg
Amount of OVA	1-4 mg	0.2 mg	0.2 mg
Average OVA Conjugation	100 $\mu\text{g}/\text{mg}$ NP	50 $\mu\text{g}/\text{mg}$ NP	250 $\mu\text{g}/\text{mg}$ NP

In an attempt to translate this reaction directly to the DV2 recE, and achieve a modest level of DV2 conjugation, NPs were prepared and reacted as per reaction 1 above. The resulting NPs had 3.4 μg DV2/mg NP, tenfold lower than the OVA reaction. Extensive exploration of reaction conditions, buffer salts, buffer concentrations, and linker lengths was performed (Appendix Table A.1). The optimized protocol used the maleimide-PEG(500)-NHS linker with the DV2 reacted at pH 9-10 in a sodium borate/potassium borate buffer mixture. The optimized reaction conditions yielded approximately 10-15 μg DV2/mg NP, nearly tenfold lower than the average for the OVA reaction. The extreme difference in protein conjugation between OVA and DV2 may be partially attributed to the difference in pI, but the complex quaternary structure of DV2 may also play a role in the accessibility of the amine and carboxylic acid functional handles during reaction.

4.2.2 Vaccination with Soluble Versus Particulate Dengue Recombinant E Protein Antigen

80×320 nm PEG(500) DV2 NPs were used in a vaccination study in C57BL/6 mice comparing the immune response against soluble DV2 recE to DV2-NPs. Soluble DV2 was dosed alone or with an adjuvant (alum, soluble R848, or R848-NPs). DV2-NPs were dosed alone or with R848 in soluble or particulate form. After a twenty-eight day prime-boost dosing regimen, blood was collected and sera were tested for anti-DV2 antibodies. Disappointingly, soluble DV2 administration appeared to produce a stronger immune response than DV2-NP administration, regardless of adjuvants used (Figure 4.1). The results were interesting in that each soluble DV2 group had one or two high responding mice as well as several low-responding mice. The DV2-NP groups were more consistent with essentially no mice showing DV2-specific antibody production. Further testing on sera from the mice revealed that even mice that did produce higher levels of DV2-specific IgG did not generally produce neutralizing antibodies (Appendix Figure A.7).

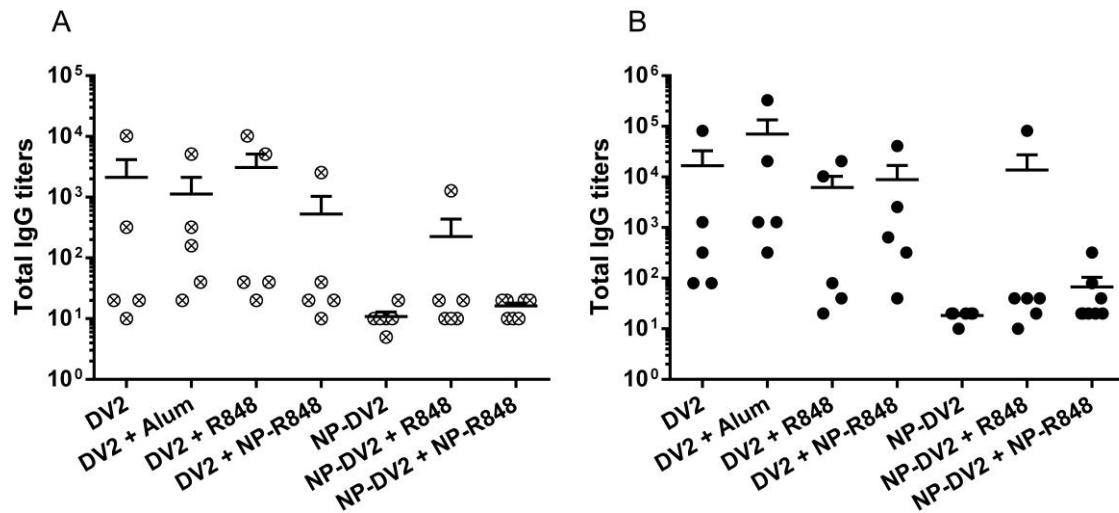


Figure 4.1 DV2-specific IgG antibody response after prime and boost dose. B157c/6 mice were injected subcutaneously with 1 μg soluble or particulate DV2 with or without adjuvant (3 mg Alum, 5 μg R848, or 5 μg R848-NP) on day 0 and again on day 21. After prime dose, several mice showed anti-DV2 antibody production after soluble DV2 administration, but essentially no response was seen from DV2-NP groups. One week after boost dose, mice receiving soluble DV2 showed higher antibody titers, while only one mouse receiving DV2-NPs showed anti-DV2 IgG production. The addition of adjuvants appeared to have minimal effect on antibody response to both soluble and particulate DV2. N = 5-7 mice per group.

While these preliminary results do not appear promising for a DV2-NP vaccine, they suggest areas for improvement in future studies. For soluble DV2 administration, DV2 alone and DV2 + alum showed similar responses, i.e. alum did not augment the immune response as expected from this potent adjuvant. This indicates that at the 1 μg dose of DV2 may be too low to be effective in the time frame studied. Clements *et. al.* used prime doses of 25 μg and boost doses of 12.5 μg DV2 for unadjuvanted, soluble administration.³⁸ At that higher dosing level, there were clear differentiations between study groups vaccinated with and without various adjuvants. Increasing the dose of DV2 protein to 10-20 μg per mouse may give a better picture as to the effects of NP formulation and the presence of different adjuvants. Additionally, other mouse models may be more suited for DV2 studies (balb/c¹¹, AG129⁶⁴).

As a preliminary experiment before comparing higher doses of DV2 versus DV2-NPs, higher doses of soluble DV2 were examined in balb/c mice with and without Alum adjuvant to determine an appropriate minimum antigen dose. Mice were vaccinated with 10 μ g soluble DV2 or 5 or 10 μ g DV2 plus 3 mg Alum (Figure 4.2). When compared to the results in Figure 4.1, there is a clear difference between the adjuvanted and unadjuvanted groups. Additionally, all mice in a given group showed more consistent responses rather than the grouping of high responders and low responders seen previously. Following this result, future studies will attempt to elucidate the difference in immune response for soluble DV2 versus DV2-NP at higher dosing level and with the balb/c mouse strain.

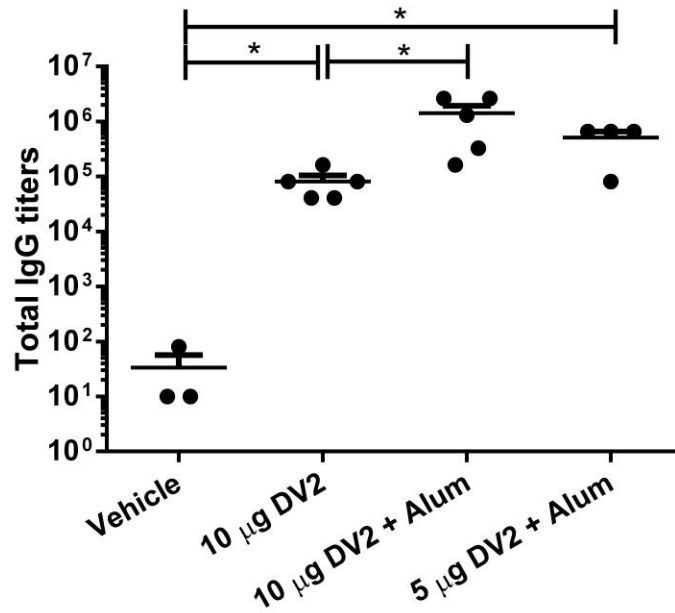


Figure 4.2 Antibody response to soluble DV2. Balb/c mice were injected subcutaneously with the indicated doses of DV2 with or without alum on day 0 and again on day 21. For all groups, mice showed narrower spread of responses than the previous study (Figure 4.1). There was a significant difference in the immune response for all study groups compared to a vehicle control as well as between an adjuvanted versus unadjuvanted dose of 10 μ g DV2. Further examination of the relationship between soluble DV2 administration and DV2-NPs will build upon this pilot dosing study. N = 3-5. *, p < 0.05 by unpaired t test.

4.2.3 PRINT-Based Vaccine Against Hemagglutinin Protein for Influenza Virus

Influenza hemagglutinin (HA) is an antigenic protein found on the surface of influenza viruses (flu). HA has been widely studied as an antigen target for subunit flu vaccines⁶⁵ and is utilized in the commercial flu vaccines FluBlok (recombinant) and Fluvirin (purified). It would be widely beneficial to have a flu vaccine delivery vehicle in which the protein antigens could be easily exchanged for others based on which strains of the flu were circulating in a given year or even at different times within the flu season, helping to compensate for antigenic shift and antigenic drift.⁶⁵ Due to the “plug and play” nature of PRINT technology and the ease of conjugating a variety of proteins to hydrogel NPs, HA was used as a second clinically relevant target that could harness the potential advantages of a PRINT NP-based vaccine.

HA was conjugated to 80×320 nm NPs through EDC chemistry, resulting in a direct amide bond between the HA protein and surface carboxylic acid groups on the NPs. The NPs were found to have 85 µg HA per milligram of NPs, on par with the conjugation levels seen for the model antigen ovalbumin. Future studies will explore the relationship between soluble versus particulate delivery of HA and the subsequent immune response as well as delivery of HA with various adjuvants

4.3 Conclusion

There are many diseases that are potentially preventable through novel vaccination strategies, which may also be used to further improve current vaccines in the clinic. PRINT nanotechnology has the potential for wide application across different types of vaccines, ranging from ground breaking new vaccines against growing disease threats like dengue virus to incremental improvements on already existing vaccine technology, as in the case of influenza vaccines. The versatility of PRINT and the antigen conjugation strategies presented here have the

potential to facilitate a “plug and play” vaccine platform, in which relevant antigen targets could easily be transitioned into viable vaccine candidates with a potentially lower barrier to entry for subsequent antigen formulations and without the safety concerns associated with whole pathogen vaccines and preservation additives

4.4 Materials and Methods

4.4.1 Materials

Dengue E protein was produced at the UNC Protein Expression and Purification core facility. Hemagglutinin recombinant influenza A, subtype H1N1 (A/California/04/2009) protein was purchased from Life Technologies. Methoxy PEG(5k) acrylate was purchased from Creative PEGworks, Inc. Cell surface stains, antibodies, and ELISA reagents were purchased from eBioscience, Inc. TissueTek[®] OTC media, maleimide-PEG(500)-NHS, BCA assay, s-NHS (N-hydroxysulfosuccinimide), EDC (1-Ethyl-3-[3-dimethylaminopropyl]carbodiimide hydrochloride), and general solvents were purchased from Thermo Fisher Scientific, Inc. Tetraethylene glycol monoacrylate (HP(250)A) was synthesized in-house. All other chemicals and reagents were obtained from Sigma Aldrich, Inc. unless otherwise noted. PRINT molds were supplied by Liquidia Technologies.

4.4.2 Dengue E Protein Characterization

E protein for dengue virus serotype 2 (DV2) were provided by the UNC Protein Expression and Purification core facility. Briefly, DV2 was expressed in Sf9 insect cells infected with a recombinant baculovirus and purified using a monoclonal antibody column charged with dengue specific 4G2 antibodies. Purified protein was eluted from the column using a low pH citrate buffer and quickly neutralized by pH 7-8 phosphate buffer with 15% w/v glycerol. Protein concentration was estimated by absorbance at 280nm as well as by ELISA and confirmed by gel

electrophoresis by comparison against a commercial DV2 standard of known concentration.

Protein was further concentrated using a 10 kDa cut off Amicon Ultra – 4 regenerated cellulose centrifugal filter unit (EMD Millipore). Protein used in experiments had a final concentration between 0.1 and 1 mg/mL.

4.4.3 Animals

Female balb/c and C57BL/6 mice were purchased from Jackson Laboratory and used at age 6-12 weeks. All experiments involving mice were carried out in accordance with an animal use protocol approved by the University of North Carolina Animal Care and Use Committee. In general, dengue studies were carried out on C57BL/6 mice while hemagglutinin studies were carried out on balb/c mice unless otherwise specified.⁶¹

4.4.4 Fabrication of Hydrogel NPs via the PRINT Process and Protein Conjugation

PRINT NPs size diameter = 80 nm by length = 320 nm were fabricated as described in Chapters 2 and 3⁶⁶⁻⁶⁸ using the compositions shown in Table 4.2.

Table 4.2 Composition of PRINT NPs

Monomer	Protein Conjugated NPs	ProR848 NPs
Cationic monomer	2-aminoethyl methacrylate; 20%	2-aminoethyl methacrylate; 40%
Cross-linker	PEG(700) diacrylate; 10%	PEG(1k) dimethacrylate; 29%
Monomer	Hydroxyl PEG(250) acrylate; 69%	Methoxy PEG(5k) acrylate; 20%
Photo initiator	2,4,6 trimethylbenzoyl diphenylphosphine oxide; 1%	
Cargo	n/a	ProR848; 10%

DV2 was conjugated to NPs through a PEG(500) linker. NPs were first PEGylated by reacting 1 mg NPs with 1.6 μ mol of maleimide-PEG(500)-NHS using triethylamine (100 μ L) in DMF at a final concentration of 1 mg NPs in 1.4 mL.⁶⁸ Reaction was run at room temperature overnight with shaking at 1400 RPM. NPs were then washed with fresh DMF. Residual amine groups on the surface of NPs were quenched with 150 μ mol of succinic anhydride, reacted in the presence of 186 μ mol pyridine for 30 minutes with agitation at 1400 RPM. NPs were then washed into water. DV2 was conjugated to the free maleimide groups by reacting NPs and DV2 in a 4:1 weight ratio at a NP concentration of 4 mg/mL in phosphate buffer pH 9.5 with 0.1 weight % glycerol, overnight at room temperature with shaking at 1400 RPM. NPs were washed with buffer to remove unbound protein and washed with water to remove residual salt. Final concentration was determined by thermogravimetric analysis (Q5000IR, TA Instruments) and protein conjugation was determined by BCA assay. Typical conjugation for DV2 was 10-15 μ g DV2 per 1 mg NPs, far lower than the conjugation efficiency seen with ovalbumin in Chapter 2.

Hemagglutinin was conjugated to PRINT NPs via EDC chemistry, described previously as PEG(0) in Chapter 2. Each milligram of NPs were first reacted with 150 μ mol of succinic

anhydride in the presence of 186 μmol pyridine for 30 minutes with agitation at 1400 RPM in order to convert free amines on the NP surface into carboxylic acid groups. NPs were then reacted with EDC (1-ethyl-3-(3-dimethylaminopropyl)carbodiimide) and sulfo-NHS according to protocol by Thermo Scientific. Finally, NPs were concentrated to 3 mg/mL and 0.695 mg of HA protein were added to activated NPs and allowed to react for two hours. NPs were washed with buffer to remove unbound protein and washed with water to remove residual salt. Final concentration was determined by thermogravimetric analysis (Q5000IR, TA Instruments) and protein conjugation was determined by BCA assay. Preliminary conjugation for HA was $\sim 85 \mu\text{g}$ HA per 1 mg NPs, similar the conjugation efficiency seen with ovalbumin in Chapter 2.

4.4.5 Nanoparticle Characterization

NPs were imaged via Scanning electron microscopy (SEM) ζ -potential measurements were conducted on $\sim 20 \mu\text{g/mL}$ NP dispersions in water using a Zetasizer Nano ZS Particle Analyzer (Malvern Instruments Inc.). Particle concentrations were determined via thermogravimetric analysis (Q5000IR, TA Instruments). Protein conjugation was measured using a standard BCA Assay (Fisher Scientific, Inc.).

4.4.6 Immunization and Antibody ELISA

Balb/c or C57BL/6 mice, 6-8 weeks old, were immunized with soluble antigen/adjuvant or NP-conjugated antigen/adjuvant at the indicated dose, subcutaneously in the flank. Mice were primed on day zero and boosted on day 21. Plasma samples were collected by bleeding mice submandibularly on day 21 and day 28 post-prime and antigen-specific antibody production was examined by ELISA. Briefly, EIA plates (Corning) were coated with $10 \mu\text{g/ml}$ OVA in ELISA coating buffer (eBioscience) at 4°C overnight. The wells were washed and blocked with $200 \mu\text{L}$ per well of 3% BSA in PBST (PBS with 0.05% Tween 20) for 2 hours. Plasma samples were

diluted in blocking buffer and incubated for 2 hours. The wells were washed extensively with PBST and anti-antigen IgG were detected using HRP conjugated goat anti-mouse IgG (Invitrogen) and was visualized by adding 100 μ L of TMB (eBioscience) to each well. The reaction was stopped after 11 min with 50 μ L 0.2 M H₂SO₄. Optical densities (OD) were read at 450 nm and 570 nm. The antibody titer was determined as the highest dilutions with OD (450 nm – 570 nm) > 0.1.

4.5 References

- (1) The top 10 causes of death
<http://www.who.int/mediacentre/factsheets/fs310/en/index2.html>.
- (2) Global Immunization: Diseases and vaccines - A World View. <http://www.chop.edu/>.
- (3) Botelho-Nevers, E.; Verhoeven, P.; Paul, S.; Grattard, F.; Pozzetto, B.; Berthelot, P.; Lucht, F. *Expert Rev. Vaccines* **2013**, *12*, 1249–1259.
- (4) Lambracht-Washington, D.; Rosenberg, R. *Discov. Med.* **2013**, *15*, 319–326.
- (5) Ross, A. L.; Bråve, A.; Scarlatti, G.; Manrique, A.; Buonaguro, L. *Lancet Infect. Dis.* **2010**, *10*, 305–316.
- (6) Bershteyn, A.; Hanson, M. C.; Crespo, M. P.; Moon, J. J.; Li, A. V.; Suh, H.; Irvine, D. J. *J. Control. Release* **2012**, *157*, 354–365.
- (7) Bachmann, M. F.; Rohrer, U. H.; Kündig, T. M.; Bürki, K.; Hengartner, H.; Zinkernagel, R. M. *Science* **1993**, *262*, 1448–1451.
- (8) Chackerian, B.; Lowy, D. R.; Schiller, J. T. *J. Clin. Invest.* **2001**, *108*, 415–423.
- (9) Dintzis, H.; Dintzis, R.; Vogelstein, B. *Proc. Natl. Acad. Sci. U. S. A.* **1976**, *73*, 3671–3675.
- (10) Guzman, M. G.; Halstead, S. B.; Artsob, H.; Buchy, P.; Farrar, J.; Gubler, D. J.; Hunsperger, E.; Kroeger, A.; Margolis, H. S.; Martínez, E.; Nathan, M. B.; Pelegriño, J. L.; Simmons, C.; Yoksan, S.; Peeling, R. W. *Nat. Rev. Microbiol.* **2010**, *8*, S7–16.
- (11) Durbin, A. P.; Whitehead, S. S. *Viruses* **2011**, *3*, 1800–1814.
- (12) McArthur, M. A.; Sztein, M. B.; Edelman, R. *Expert Rev. Vaccines* **2013**, *12*, 933–953.
- (13) Poo, J.; Galan, F.; Forrat, R.; Zambrano, B.; Lang, J.; Dayan, G. H. *Pediatr. Infect. Dis. J.* **2010**, *30*, 9–17.
- (14) Simmons, M.; Murphy, G. S.; Kochel, T.; Raviprakash, K.; Hayes, C. G. *Am. J. Trop. Med. Hyg.* **2001**, *65*, 420–426.
- (15) Simmons, M.; Murphy, G. S.; Hayes, C. G. *Am. J. Trop. Med. Hyg.* **2001**, *65*, 159–161.
- (16) Raviprakash, K.; Marques, E.; Ewing, D.; Lu, Y.; Phillips, I.; Porter, K. R.; Kochel, T. J.; August, T. J.; Hayes, C. G.; Murphy, G. S. *Virology* **2001**, *290*, 74–82.

- (17) Raviprakash, K.; Apt, D.; Brinkman, A.; Skinner, C.; Yang, S.; Dawes, G.; Ewing, D.; Wu, S.-J.; Bass, S.; Punnonen, J.; Porter, K. *Virology* **2006**, *353*, 166–173.
- (18) Raviprakash, K.; Ewing, D.; Simmons, M.; Porter, K. R.; Jones, T. R.; Hayes, C. G.; Stout, R.; Murphy, G. S. *Virology* **2003**, *315*, 345–352.
- (19) Raviprakash, K.; Kochel, T. J.; Ewing, D.; Simmons, M.; Phillips, I.; Hayes, C. G.; Porter, K. R. *Vaccine* **2000**, *18*, 2426–2434.
- (20) Raviprakash, K.; Porter, K. R.; Kochel, T. J.; Ewing, D.; Simmons, M.; Phillips, I.; Murphy, G. S.; Weiss, W. R.; Hayes, C. G. *J. Gen. Virol.* **2000**, *81*, 1659–1667.
- (21) Beckett, C. G.; Tjaden, J.; Burgess, T.; Danko, J. R.; Tamminga, C.; Simmons, M.; Wu, S.-J.; Sun, P.; Kochel, T.; Raviprakash, K.; Hayes, C. G.; Porter, K. R. *Vaccine* **2011**, *29*, 960–968.
- (22) Konishi, E.; Yamaoka, M.; Kurane, I.; Mason, P. W. *Vaccine* **2000**, *18*, 1133–1139.
- (23) Konishi, E.; Kosugi, S.; Imoto, J. *Vaccine* **2006**, *24*, 2200–2207.
- (24) Imoto, J.-I.; Konishi, E. *Vaccine* **2007**, *25*, 1076–1084.
- (25) Apt, D.; Raviprakash, K.; Brinkman, A.; Semyonov, A.; Yang, S.; Skinner, C.; Diehl, L.; Lyons, R.; Porter, K.; Punnonen, J. *Vaccine* **2006**, *24*, 335–344.
- (26) Lu, Y. *Vaccine* **2003**, *21*, 2178–2189.
- (27) Raja, N. U.; Holman, D. H.; Wang, D.; Raviprakash, K.; Juompan, L. Y.; Deitz, S. B.; Luo, M.; Zhang, J.; Porter, K. R.; Dong, J. Y. *Am. J. Trop. Med. Hyg.* **2007**, *76*, 743–751.
- (28) Raviprakash, K.; Wang, D.; Ewing, D.; Holman, D. H.; Block, K.; Woraratanadharm, J.; Chen, L.; Hayes, C.; Dong, J. Y.; Porter, K. *J. Virol.* **2008**, *82*, 6927–6934.
- (29) Khanam, S.; Rajendra, P.; Khanna, N.; Swaminathan, S. *BMC Biotechnol.* **2007**, *7*, 10.
- (30) Holman, D. H.; Wang, D.; Raviprakash, K.; Raja, N. U.; Luo, M.; Zhang, J.; Porter, K. R.; Dong, J. Y. *Clin. Vaccine Immunol.* **2007**, *14*, 182–189.
- (31) White, L. J.; Parsons, M. M.; Whitmore, A. C.; Williams, B. M.; de Silva, A.; Johnston, R. E. *J. Virol.* **2007**, *81*, 10329–10339.
- (32) White, L. J.; Sariol, C. A.; Mattocks, M. D.; Wahala M P B, W.; Yingsiwaphat, V.; Collier, M. L.; Whitley, J.; Mikkelsen, R.; Rodriguez, I. V.; Martinez, M. I.; de Silva, A.; Johnston, R. E. *J. Virol.* **2013**, *87*, 3409–3424.

- (33) Kaufman, B.; Summers, P.; Dubois, D.; Eckels, K. *Am. J. Trop. Med. Hyg.* **1987**, *36*, 427–434.
- (34) Fibriansah, G.; Tan, J. L.; Smith, S. A.; de Alwis, A. R.; Ng, T.-S.; Kostyuchenko, V. A.; Ibarra, K. D.; Wang, J.; Harris, E.; de Silva, A.; Crowe, J. E.; Lok, S.-M. *EMBO Mol. Med.* **2014**, *6*, 358–371.
- (35) De Alwis, R.; Smith, S. A.; Olivarez, N. P.; Messer, W. B.; Huynh, J. P.; Wahala, W. M. P. B.; White, L. J.; Diamond, M. S.; Baric, R. S.; Crowe, J. E.; de Silva, A. M. *Proc. Natl. Acad. Sci. U. S. A.* **2012**, 1–6.
- (36) Coller, B.-A. G.; Clements, D. E.; Bett, A. J.; Sagar, S. L.; Ter Meulen, J. H. *Vaccine* **2011**, *29*, 7267–7275.
- (37) Robert Putnak, J.; Coller, B.-A.; Voss, G.; Vaughn, D. W.; Clements, D.; Peters, I.; Bignami, G.; Hough, H.-S.; Chen, R. C.-M.; Barvir, D. A.; Seriwatana, J.; Cayphas, S.; Garçon, N.; Gheysen, D.; Kanesa-Thanan, N.; McDonell, M.; Humphreys, T.; Eckels, K. H.; Prieels, J.-P.; Innis, B. L. *Vaccine* **2005**, *23*, 4442–4452.
- (38) Clements, D. E.; Coller, B.-A. G.; Lieberman, M. M.; Ogata, S.; Wang, G.; Harada, K. E.; Putnak, J. R.; Ivy, J. M.; McDonell, M.; Bignami, G. S.; Peters, I. D.; Leung, J.; Weeks-Levy, C.; Nakano, E. T.; Humphreys, T. *Vaccine* **2010**, *28*, 2705–2715.
- (39) Hermida, L.; Bernardo, L.; Martín, J.; Alvarez, M.; Prado, I.; López, C.; Sierra, B. D. L. C.; Martínez, R.; Rodríguez, R.; Zulueta, A.; Pérez, A. B.; Lazo, L.; Rosario, D.; Guillén, G.; Guzmán, M. G. *Vaccine* **2006**, *24*, 3165–3171.
- (40) Valdés, I.; Bernardo, L.; Gil, L.; Pavón, A.; Lazo, L.; López, C.; Romero, Y.; Menendez, I.; Falcón, V.; Betancourt, L.; Martín, J.; China, G.; Silva, R.; Guzmán, M. G.; Guillén, G.; Hermida, L. *Virology* **2009**, *394*, 249–258.
- (41) Valdés, I.; Gil, L.; Romero, Y.; Castro, J.; Puente, P.; Lazo, L.; Marcos, E.; Guzmán, M. G.; Guillén, G.; Hermida, L. *Clin. Vaccine Immunol.* **2011**, *18*, 455–459.
- (42) Valdés, I.; Hermida, L.; Martín, J.; Menéndez, T.; Gil, L.; Lazo, L.; Castro, J.; Niebla, O.; López, C.; Bernardo, L.; Sánchez, J.; Romero, Y.; Martínez, R.; Guzmán, M. G.; Guillén, G. *Vaccine* **2009**, *27*, 995–1001.
- (43) Roberts, R. A.; Shen, T.; Allen, I. C.; Hasan, W.; DeSimone, J. M.; Ting, J. P. Y. *PLoS One* **2013**, *8*, e62115.
- (44) WHO. Vaccines: Influenza. <http://www.who.int/>.
- (45) Zbinden, D.; Manuel, O. *Immunotherapy* **2014**, *6*, 131–139.
- (46) Ison, M. G.; Michaels, M. G. *Am. J. Transplant* **2009**, *9 Suppl 4*, S166–72.

- (47) Schaffer, S. A.; Husain, S.; Delgado, D. H.; Kavanaugh, L.; Ross, H. J. *Am. J. Transplant* **2011**, *11*, 2751–2754.
- (48) Noh, J. Y.; Kim, W. J. *Infect. Chemother.* **2013**, *45*, 375–386.
- (49) Bateman, A. C.; Kieke, B. A.; Irving, S. A.; Meece, J. K.; Shay, D. K.; Belongia, E. A. *J. Infect. Dis.* **2013**, *207*, 1262–1269.
- (50) Zheng, M.; Luo, J.; Chen, Z. *Infection* **2014**, *42*, 251–262.
- (51) Wei, C.; Ekiert, D. C.; Nabel, G. J.; Wilson, I. A. In *Textbook of Influenza*; Webster, R. G.; Monto, A. S.; Braciale, T. J.; Lamb, R. A., Eds.; John Wiley & Sons, Ltd: Oxford, UK, 2013; pp. 327–336.
- (52) Lee, Y.-T.; Kim, K.-H.; Ko, E.-J.; Lee, Y.-N.; Kim, M.; Kwon, Y.-M.; Tang, Y.; Cho, M.-Y.; Lee, Y.-J.; Kang, S.-M. *Clin. Exp. Vaccine Res.* **2014**, *3*, 12–28.
- (53) Ellebedy, a H.; Webby, R. J. *Vaccine* **2009**, *27 Suppl 4*, D65–8.
- (54) Goldenberg, M. M. *Pharm. Ther.* **2009**, *33*, 362–363.
- (55) Treanor, J. J.; El Sahly, H.; King, J.; Graham, I.; Izikson, R.; Kohberger, R.; Patriarca, P.; Cox, M. *Vaccine* **2011**, *29*, 7733–7739.
- (56) Knuschke, T.; Sokolova, V.; Rotan, O.; Wadwa, M.; Tenbusch, M.; Hansen, W.; Staeheli, P.; Epple, M.; Buer, J.; Westendorf, A. M. *J. Immunol.* **2013**, *190*, 6221–6229.
- (57) Patterson, D. P.; Rynda-Applé, A.; Harmsen, A. L.; Harmsen, A. G.; Douglas, T. *ACS Nano* **2013**, *7*, 3036–3044.
- (58) Kang, S.-M.; Song, J.-M.; Quan, F.-S.; Compans, R. W. *Virus Res.* **2009**, *143*, 140–146.
- (59) Bråve, A.; Ljungberg, K.; Wahren, B.; Liu, M. A. *Mol. Pharm.* **2007**, *4*, 18–32.
- (60) Smirnov, D.; Schmidt, J. J.; Capecchi, J. T.; Wightman, P. D. *Vaccine* **2011**, *29*, 5434–5442.
- (61) Galloway, A. L.; Murphy, A.; DeSimone, J. M.; Di, J.; Herrmann, J. P.; Hunter, M. E.; Kindig, J. P.; Malinoski, F. J.; Rumley, M. A.; Stoltz, D. M.; Templeman, T. S.; Hubby, B. *Nanomedicine* **2013**, *9*, 523–531.
- (62) Kasturi, S. P.; Skountzou, I.; Albrecht, R. A.; Koutsouanos, D.; Hua, T.; Nakaya, H. I.; Ravindran, R.; Stewart, S.; Alam, M.; Kwissa, M.; Villinger, F.; Murthy, N.; Steel, J.; Jacob, J.; Hogan, R. J.; García-Sastre, A.; Compans, R.; Pulendran, B. *Nature* **2011**, *470*, 543–547.

- (63) Messer, W. B.; de Alwis, R.; Yount, B. L.; Royal, S. R.; Huynh, J. P.; Smith, S. A; Crowe, J. E.; Doranz, B. J.; Kahle, K. M.; Pfaff, J. M.; White, L. J.; Sariol, C. A; de Silva, A. M.; Baric, R. S. *Proc. Natl. Acad. Sci. U. S. A.* **2014**, *111*, 1939–1944.
- (64) Murrell, S.; Wu, S.-C.; Butler, M. *Biotechnol. Adv.* **2011**, *29*, 239–247.
- (65) Kirchenbaum, G. A; Ross, T. M. *Curr. Opin. Immunol.* **2014**, *28*, 71–76.
- (66) Gratton, S. E. A.; Williams, S. S.; Napier, M. E.; Pohlhaus, P. D.; Zhou, Z.; Wiles, K. B.; Maynor, B. W.; Shen, C.; Olafsen, T.; Samulski, E. T.; Desimone, J. M. *Acc. Chem. Res.* **2008**, *41*, 1685–1695.
- (67) Gratton, S. E. A; Ropp, P. A; Pohlhaus, P. D.; Luft, J. C.; Madden, V. J.; Napier, M. E.; DeSimone, J. M. *Proc. Natl. Acad. Sci. U. S. A.* **2008**, *105*, 11613–11618.
- (68) Perry, J. L.; Reuter, K. G.; Kai, M. P.; Herlihy, K. P.; Jones, S. W.; Luft, J. C.; Napier, M.; Bear, J.E.; DeSimone, J. M. *Nano Lett.* **2012**, *12*, 5304-5310.

CHAPTER 5 FUTURE DIRECTIONS AND SUMMARY

5.1 Future Directions

5.1.1 Combining Vaccine Antigens and Adjuvants into a Single Particle Formulation

As demonstrated in this work, nanoparticle delivery of antigens and adjuvants can have a dramatic effect on the immune response elicited by these potent compounds. While our focus thus far has been on the delivery of each component individually, other works have shown synergistic benefits from combining antigens and adjuvants onto the same micro- or nanoparticle. This enables both vaccine components to be delivered to the same immune cell, activating toll-like receptors (TLRs) as well as presenting the immunogenic antigen, thereby more closely mimicking how immune cells interact with native pathogens.

Several different strategies have been employed to combine antigens and adjuvants in the same delivery vehicle. CpG is a single stranded oligonucleotide that is known to activate TLR9, an intracellular TLR that recognizes unmethylated CpG motifs, commonly found in microbial DNA, but not in vertebrate DNA sequences. CpG is able to boost both innate and humoral immune responses. CpG has been used as a vaccine adjuvant in several studies looking at the immune response when antigen and adjuvant are delivered together in a single particle formulation versus when dosed in soluble form. In one study, Hunter *et al.* encapsulated CpG and a group B *Streptococcus* antigen (GBS) into PLGA microspheres.¹ The microsphere-encapsulated formulation outperformed administration of soluble GBS + soluble CpG as well as soluble GBS alone.

In another study, CpG was covalently modified for incorporation into an acid-labile polymer nanoparticle.² When irreversibly modifying immunostimulatory molecules, there is a chance of decreasing or eliminating their activity. When CpG was modified at the 5' end of the oligonucleotide, the CpG-NPs elicited lower IL-12 production while modification at the 3' end had no effect on the activity of the CpG-NPs when compared to soluble CpG. NPs loaded with OVA and CpG (3'CpG/OVA particles) were compared to OVA particles administered with soluble CpG and soluble administration of both OVA and CpG. It was found that the 3'CpG/OVA particles were able to more effectively enhance the cytotoxic T lymphocyte (CTL) response against OVA-expressing cancer cells and increase survival time compared to other formulations, demonstrating protective immunity from co-administration of antigen and adjuvant in a single particle formulation.

Flagella, an adjuvant for TLR5, have been incorporated into a recombinant bacteria-based vaccine against the HIV-1 Gag antigen (Gag).³ TLR5 is found on the surface of several types of immune cells including macrophages and DCs and specifically detects bacterial flagellin. *Lactobacillus acidophilus*, an inert bacterium found in the gastrointestinal tract of humans and animals, was modified to express the Gag protein and/or flagellin from *Salmonella enterica* (FLiC) on the surface of the bacteria. By combining both Gag and FLiC on the same bacteria, higher levels of IgA were detected in key mucosal surfaces of the digestive and reproductive tracts in mice compared to dosing Gag expressing recombinant lactobacilli alone.

One of the few FDA approved vaccine adjuvants, monophosphoryl Lipid A (MPLA), boosts immunity through TLR4. TLR4 naturally recognizes lipopolysaccharide (LPS), a component of the outer membrane of bacteria. MPLA is a truncated, less toxic version of LPS. Lipid A, also known as endotoxin, is responsible for the activity of LPS and MPLA. Moon *et al.*

have investigated the incorporation of MPLA into interbilayer-crosslinked multilamellar vesicles (ICMV) when delivering OVA as well as the malaria antigen VMP001.⁴ Combining MPLA into the bilayers of ICMVs increased the immune response against OVA, which was especially apparent at lower doses of antigen.

A second FDA approved adjuvant, imiquimod (R837), has been investigated in particulate delivery of vaccines. R837 activates TLR7/8 in humans (TLR7 in mice) and is an imidazoquinoline-type molecule like resiquimod (R848). These imidazoquinoline molecules mimic motifs found in viral single stranded RNA. R837 was investigated in combination with MPLA in PLGA nanoparticles.⁵ PLGA particles were fabricated with OVA, MPLA + R837, or all three components. When PLGA(OVA/MPLA/R837) particles were compared to PLGA(OVA) + PLGA(MPLA/R837) particles, interestingly separating the antigen and adjuvant onto different particles greatly increased the antibody response.

Overall, these works compare antigen and adjuvant combined into a single particle formulation to soluble administration, and have shown that co-delivery of antigen and adjuvant in the same particle vehicle greatly enhances antigen-specific immune responses. Kasturi *et al.* looks into the potential of utilizing antigen particles + adjuvant particles as an alternative to combining both components on a single particle while maintaining particulate dosing for both components.⁵ They found that it was preferable to formulate their antigen and adjuvant on separate PLGA-based particles, mixed before injection. A study by Kazzaz *et al.* found different results, indicating that the immune response against separate antigen and adjuvant particles was comparable to a single antigen + adjuvant particle.⁶ Notably, combining both the antigen and adjuvant in particles, whether together or separate, elicited a significantly higher antibody response compared to using soluble adjuvant with a particulate antigen.

Formulating antigen particles and adjuvant particles separately and co-administering the two particle types allows for more flexibility in the ratio of adjuvant and antigen, potentially allowing the vaccine to be tuned to the needs of each patient at the time of injection. This may be beneficial in personalizing vaccines and decreasing the dosage of adjuvant needed when patients are receiving multiple vaccines in a single doctors visit, as is the case with many childhood vaccinations. While this presents an interesting opportunity in exploring personalized vaccination, there has been limited and conflicting information about the benefits of dosing antigens and adjuvants in a single particle formulation versus two separate particle formulations.

PRINT based vaccines could help fill this knowledge gap by investigating administration of antigen and adjuvant on a single particle, on different particles, or in different combinations of soluble and particulate dosing. The strategies presented here for fabrication of R848-NPs (Chapter 3) could be combined with the post-fabrication antigen conjugation strategies presented in Chapter 2 and Chapter 4 to create OVA-R848-NPs. Additional conjugation strategies could be explored as well. Thiol functionalized CpG could be utilized to reversibly (disulfide bond) or irreversibly (thiol to maleimide reaction) conjugate this adjuvant to NPs through commercially available PEG linkers prior to protein conjugation. Further adjuvants could be promising candidates for this type of chemistry as well, given they retain their adjuvanticity after chemical modification.^{2,7} Combining antigens and adjuvants into a single particle formulation could further boost the immunogenicity of subunit vaccines, leading to lower doses, fewer side effects, and greater access to important vaccines, especially in developing countries.

5.1.2 Exploring the Synergy Between Multiple Adjuvants in Augmenting Vaccine Efficacy

The major cells of the immune system, APCs like dendritic cells, macrophages, and B cells, often contain a mix of pattern recognition receptors (PRRs) like TLRs, NOD-like receptors

(NLRs), and RIG-1-like receptors (RLRs), each responsible for recognizing different types of pathogen associated molecular patterns (PAMPs). Combining different TLR, NLR, and RLR agonists with antigens into a single vaccine formulation may stimulate multiple PRRs on a single cell, leading to a more authentic immune response compared to dosing antigen alone or single adjuvants, especially when the adjuvants act through different mechanisms of activation.⁸⁻¹⁰ Many combinations of adjuvants have been examined in soluble dosing form, but few have been examined in particulate form, which may augment the immune response elicited by these compounds.

An extensive study by Matthews *et al.* compared combinations agonists for TLRs 1/2, TLR3, TLR4, and TLRs 7/8 to determine if dual-TLR activation would enhance immunogenicity of adjuvants.¹¹ They examined individual TLR activation alone as well as TLR7/8+TLR3, TLR7/8+TLR4, TLR1/2+TLR3, and TLR4+TLR3 in combination. They found that stimulation of TLR7/8 plus either TLR3 or TLR4 led to higher cytokine production as well as higher levels of antibody production compared to single TLR agonist administration or the other combo therapies. These combinations also aided in polarizing the immune response toward a Th1 response, which is particularly important for eliciting cellular immunity. These studies help to establish the basic knowledge of effects from combining immune modulators in dispersed in solutions. Further knowledge is needed for particle-mediated delivery of multiple immune modulating agents, which requires stable association of these molecules to particle vectors.

The benefits of adsorbing antigens and adjuvants to alum prior to administration, thus creating a depot that can trap antigens and adjuvants at the injection site for prolonged release rather than allowing them to clear via lymphatic drainage, were further explored by Xiao *et al.*¹⁴ When alum was pre-treated with phosphate buffer, blocking alum from adsorbing other

compounds, vaccination with a dual adjuvant vaccine produced a lower antibody response against recombinant poxvirus L1 (V1L). While the phosphate treated alum groups still provided some protection against a lethal challenge, the groups receiving untreated alum + CpG +L1V showed 100% survival after challenge. When the second adjuvant CpG was excluded, the immune response against the single adjuvant formulation was lower than that of the phosphate treated or untreated dual-adjuvant therapy, indicating a synergy between the alum and CpG in building immunity.

Silica nanoparticles (SiO_2) have also been studied for their adjuvant properties.^{15,16} Similar to alum, SiO_2 particles may be able to form a depot at the site of administration, leading to prolonged stimulation of the immune system. SiO_2 particles were combined with bis-(3',5')-cyclic dimeric guanosine monophosphate (c-di-GMP), a mucosal adjuvant, and recombinant hemagglutinin (HA) antigen HAC1 in an attempt to design a better intranasally delivered vaccine against influenza. Alum+HAC1 elicited higher sera IgG, but the dual adjuvant SiO_2 +c-di-GMP+HAC1 produced higher levels of IgG and IgA in the lung. When HAC1 was dosed with SiO_2 alone, sera IgG levels were high but lung IgG levels were low. When HAC1 was dosed with c-di-GMP alone, the opposite happened and lung IgG levels were high and sera levels were low. The synergy between SiO_2 and c-di-GMP promoted robust mucosal and systemic immunity.¹⁶

Co-administration of adjuvants via different nanoparticle formulations has been investigated using both PLGA microspheres¹⁷ as well as nano-emulsions.¹⁸ Combinations of TLR agonists and mucosal adjuvants were examined for synergistic adjuvant effects when encapsulated into PLGA microspheres (MS) with bovine serum albumin (BSA) as a model antigen. Single and double adjuvant MS were compared to soluble administration of single and

double adjuvant combinations. All MS formulations elicited high levels of IgG, indicating a strong humoral response, but only the MPLA (TLR4 agonist) + α -galactosylceramide (mucosal adjuvant) combination led to the high levels of splenocyte proliferation and IFN- γ secretion after stimulation of T cells, demonstrating a strong cellular immune response as well.¹⁷

In an effort to create a tuberculosis vaccine, synthetic TLR4 adjuvant Glucopyranosyl Lipid Adjuvant (GLA) was combined with TLR9 agonist CpG in a nanoemulsion with tuberculosis recombinant fusion protein ID93. Both adjuvants individually increased cytokine production *in vivo* and provided some reduction in viral load in the lung after a challenge study, but the combination of the two adjuvants in a single nanoemulsion resulted in cytokine production higher than the additive value of the two adjuvants alone as well as a greater reduction in viral burden when mice were challenged in as little as four weeks after immunization.

Alum has been used as an adjuvant in clinical vaccines since the mid-1920s,¹⁹ but recently a dual adjuvant system has been introduced in the clinic. Adjuvant System 04 (AS04) is a combination adjuvant consisting of MPLA adsorbed onto particulate Alum.²⁰ AS04 is a component of the human papillomavirus (HPV) vaccine Cervarix (Glaxo Smith Kline) as well as the hepatitis B virus vaccine Fendrix (Glaxo Smith Kline). The co-administration of MPLA with Alum led to higher innate and adaptive immune responses.^{20,21}

The successes discussed here demonstrate the promise of dual-adjuvant vaccines, but further improvements may be made in a more mechanistic approach to studying the impact of combining adjuvants. Many of the studies on combined adjuvant vaccines have examined soluble adjuvants rather than particulate adjuvants, with high potential for systemic exposure to

these molecules. By anchoring these adjuvant molecules to nanoparticles, they can be targeted to the lymphatics directly, preventing whole-body distribution, increasing bioavailability to cells of interest, and potentially decreasing the dose needed to elicit a robust immune response.

Using PRINT nanoparticles, single or multiple adjuvants can be targeted to the lymph nodes. The ratio of adjuvants can be controlled on a single particle and compared to combinations of multiple single-adjuvant particles to determine the benefits of activating multiple TLRs in a single cell versus activating multiple cells through different TLRs. While activating multiple TLRs in a single cell would more closely resemble natural infection, having multiple single-adjuvant particles would offer more freedom in dosing these compounds in a way personalized to the patient. The strategy detailed in Chapter 3 for the conjugation of resiquimod (R848) could be combined with a post-fabrication approach to conjugate TLR9 agonist CpG to the surface of particles reversibly or irreversibly. Previous work has shown the potential for synergy between R848 and CpG,^{12,13} and it would be interesting to further investigate this adjuvant combination and determine an ideal ratio between the components to maximize adjuvanting effects without dosing an excess of these potent and costly molecules.

5.2 Summary

5.2.1 Manipulating Physicochemical Properties of Polymeric Hydrogel PRINT Nanoparticles to Enhance Lymphatic Trafficking and Immunogenicity of a Model Subunit Vaccine

As research has shifted from whole pathogen vaccines to the safer subunit vaccines, it has become apparent that the immunogenicity of the antigen used is not the only factor in eliciting a robust immune response. The way in which the cells of the immune system interact with the antigen plays a critical role in the type of response generated. By delivering vaccine antigens via PRINT nanoparticles, we can begin to investigate how different characteristics of the vaccine delivery system effect the interactions with the immune system and ultimately change the

immune response. In this investigation, sub-100 nm anionic hydrogel NPs were found to have the highest level of trafficking to the lymph nodes and greatest uptake in key APCs. These NPs were subsequently loaded with a model antigen through simple and straightforward conjugation strategies that could be applied to a wide variety of other protein and peptide antigens. Antigen conjugation to this nanoparticle platform resulted in high levels of NP-antigen self-drainage, delivery of antigen to B cells, and robust antigen-specific humoral and cellular responses superior to free antigen alone. These findings may find application to a wide variety of infectious diseases, increasing the efficacy of subunit-based vaccines.

5.2.2 A Pro-Adjuvant Approach to Achieve Controlled Delivery of Vaccine Components via PRINT Nanoparticles

Resiquimod (R848) is a potent TLR 7/8 agonist that has been studied as a vaccine adjuvant. While system exposure to R848 can have negative side effects, when delivered to antigen presenting cells, it is able to greatly increase the immune response against less immunogenic subunit antigens. The pro-adjuvant approach allows for R848 to be conjugated into PRINT nanoparticles for delivery to APCs, but upon acidification of the endosomal compartment, R848 is released in its original, unmodified form allowing it to activate TLR 7/8. Formulating R848 into particulate form mitigated systemic exposure, as indicated by minimal serum cytokine production, while boosting antigen-specific antibody production against a model antigen. NP formulation also decreased the amount of antigen and adjuvant necessary to elicit a robust immune response, which could translate into protective immunity against infectious diseases with lower doses of expensive vaccine components.

5.2.3 PRINT Based Vaccines for Clinically Relevant Disease Models

The development of a new vaccine delivery vehicle ultimately must be tested using clinically relevant antigens to determine its efficacy compared to the current standard of care for

a given disease. The simplicity of the conjugation chemistries used in designing a PRINT NP based vaccine may allow for wide application to many diseases with a constantly decreasing barrier to entry for subsequent diseases. By combining this versatile delivery platform with discovery of new target antigens, vaccines may be quickly developed against new strains of known diseases as well as orphan diseases with minimal financial incentive for commercial research and development. Dengue virus (DENV) has been chosen as a good candidate for development of a PRINT based vaccine due to the conformation-specific presentation of the antigenic E protein of DENV as well as the need for a balanced response against four distinct DENV serotypes. Influenza has also been investigated for development of a PRINT vaccine. The ever-changing nature of the influenza virus necessitates quick turn around in development of new vaccines and could benefit from the “plug and play” approach presented with PRINT NPs as a vaccine delivery platform. Investigations into these clinically relevant diseases are in the preliminary stages, but early results show that this technique is very promising in increasing the safety and efficacy of vaccines.

5.3 References

- (1) Hunter, S. K.; Andracki, M. E.; Krieg, M. *Am. J. Obstet. Gynecol.* **2001**, *185*, 1174–1179.
- (2) Beaudette, T. T.; Bachelder, E. M.; Cohen, J. A.; Obermeyer, A. C.; Broaders, K. E.; Fréchet, J. M. J.; Kang, E.; Mende, I.; Tseng, W. W.; Davidson, M. G.; Engleman, E. G. *Mol. Pharm.* **2009**, *6*, 1160–1169.
- (3) Kajikawa, A.; Zhang, L.; Long, J.; Nordone, S.; Stoeker, L.; LaVoy, A.; Bumgardner, S.; Klaenhammer, T.; Dean, G. *Clin. Vaccine Immunol.* **2012**, *19*, 1374–1381.
- (4) Moon, J.; Suh, H.; Bershteyn, A.; Stephan, M. *Nat. Mater.* **2011**, *10*, 243–251.
- (5) Kasturi, S. P.; Skountzou, I.; Albrecht, R. A.; Koutsonanos, D.; Hua, T.; Nakaya, H. I.; Ravindran, R.; Stewart, S.; Alam, M.; Kwissa, M.; Villinger, F.; Murthy, N.; Steel, J.; Jacob, J.; Hogan, R. J.; García-Sastre, A.; Compans, R.; Pulendran, B. *Nature* **2011**, *470*, 543–547.
- (6) Kazzaz, J.; Singh, M.; Ugozzoli, M.; Chesko, J.; Soenawan, E.; O’Hagan, D. T. *J. Control. Release* **2006**, *110*, 566–573.
- (7) Smirnov, D.; Schmidt, J. J.; Capecchi, J. T.; Wightman, P. D. *Vaccine* **2011**, *29*, 5434–5442.
- (8) Krummen, M.; Balkow, S.; Shen, L.; Heinz, S.; Loquai, C.; Probst, H.-C.; Grabbe, S. *J. Leukoc. Biol.* **2010**, *88*, 189–199.
- (9) Zhu, Q.; Egelston, C.; Vivekanandhan, A.; Uematsu, S.; Akira, S.; Klinman, D. M.; Belyakov, I. M.; Berzofsky, J. A. **2008**, *105*, 16260–16265.
- (10) Napolitani, G.; Rinaldi, A.; Bertoni, F.; Sallusto, F.; Lanzavecchia, A. *Nat. Immunol.* **2005**, *6*, 769–776.
- (11) Matthews, K.; Chung, N. P. Y.; Klasse, P. J.; Moore, J. P.; Sanders, R. W. *J. Immunol.* **2012**, *189*, 5729–5744.
- (12) Vasilakos, J. P.; Smith, R. M.; Gibson, S. J.; Lindh, J. M.; Pederson, L. K.; Reiter, M. J.; Smith, M. H.; Tomai, M. A. *Cell. Immunol.* **2000**, *204*, 64–74.
- (13) Weeratna, R. D.; Makinen, S. R.; McCluskie, M. J.; Davis, H. L. *Vaccine* **2005**, *23*, 5263–5270.
- (14) Xiao, Y.; Zeng, Y.; Alexander, E.; Mehta, S.; Joshi, S. B.; Buchman, G. W.; Volkin, D. B.; Middaugh, C. R.; Isaacs, S. N. *Vaccine* **2013**, *31*, 319–326.

- (15) Brandenberger, C.; Rowley, N. L.; Jackson-Humbles, D. N.; Zhang, Q.; Bramble, L. A.; Lewandowski, R. P.; Wagner, J. G.; Chen, W.; Kaplan, B. L.; Kaminski, N. E.; Baker, G. L.; Worden, R. M.; Harkema, J. R. *Part. Fibre Toxicol.* **2013**, *10*, 26.
- (16) Neuhaus, V.; Chichester, J. A.; Ebensen, T.; Schwarz, K.; Hartman, C. E.; Shoji, Y.; Guzmán, C. A.; Yusibov, V.; Sewald, K.; Braun, A. *Vaccine* **2014**, *32*, 3216–3222.
- (17) Salvador, A.; Igartua, M.; Hernández, R. M.; Pedraz, J. L. *Vaccine* **2012**, *30*, 589–596.
- (18) Orr, M. T.; Beebe, E. A.; Hudson, T. E.; Moon, J. J.; Fox, C. B.; Reed, S. G.; Coler, R. N. *PLoS One* **2014**, *9*, e83884.
- (19) Marrack, P.; McKee, A. S.; Munks, M. W. *Nat. Rev. Immunol.* **2009**, *9*, 287–293.
- (20) Didierlaurent, A. M.; Morel, S.; Lockman, L.; Giannini, S. L.; Bisteau, M.; Carlsen, H.; Kielland, A.; Vosters, O.; Vanderheyde, N.; Schiavetti, F.; Larocque, D.; Van Mechelen, M.; Garçon, N. *J. Immunol.* **2009**, *183*, 6186–6197.
- (21) Giannini, S. L.; Hanon, E.; Moris, P.; Van Mechelen, M.; Morel, S.; Dessy, F.; Fourneau, M. A.; Colau, B.; Suzich, J.; Losonksy, G.; Martin, M.-T.; Dubin, G.; Wettendorff, M. A. *Vaccine* **2006**, *24*, 5937–5949.
- (22) Ilyinskii, P. O.; Roy, C. J.; O’Neil, C. P.; Browning, E. A.; Pittet, L. A.; Altreuter, D. H.; Alexis, F.; Tonti, E.; Shi, J.; Basto, P. A.; Iannacone, M.; Radovic-Moreno, A. F.; Langer, R. S.; Farokhzad, O. C.; von Andrian, U. H.; Johnston, L. P. M.; Kishimoto, T. K. *Vaccine* **2014**, *32*, 2882–2895.
- (23) Tacke, P. J.; Zeelenberg, I. S.; Cruz, L. J.; van Hout-Kuijper, M. A.; van de Glind, G.; Fokkink, R. G.; Lambeck, A. J. A.; Figdor, C. G. *Blood* **2011**, *118*, 6836–6844.

APPENDIX

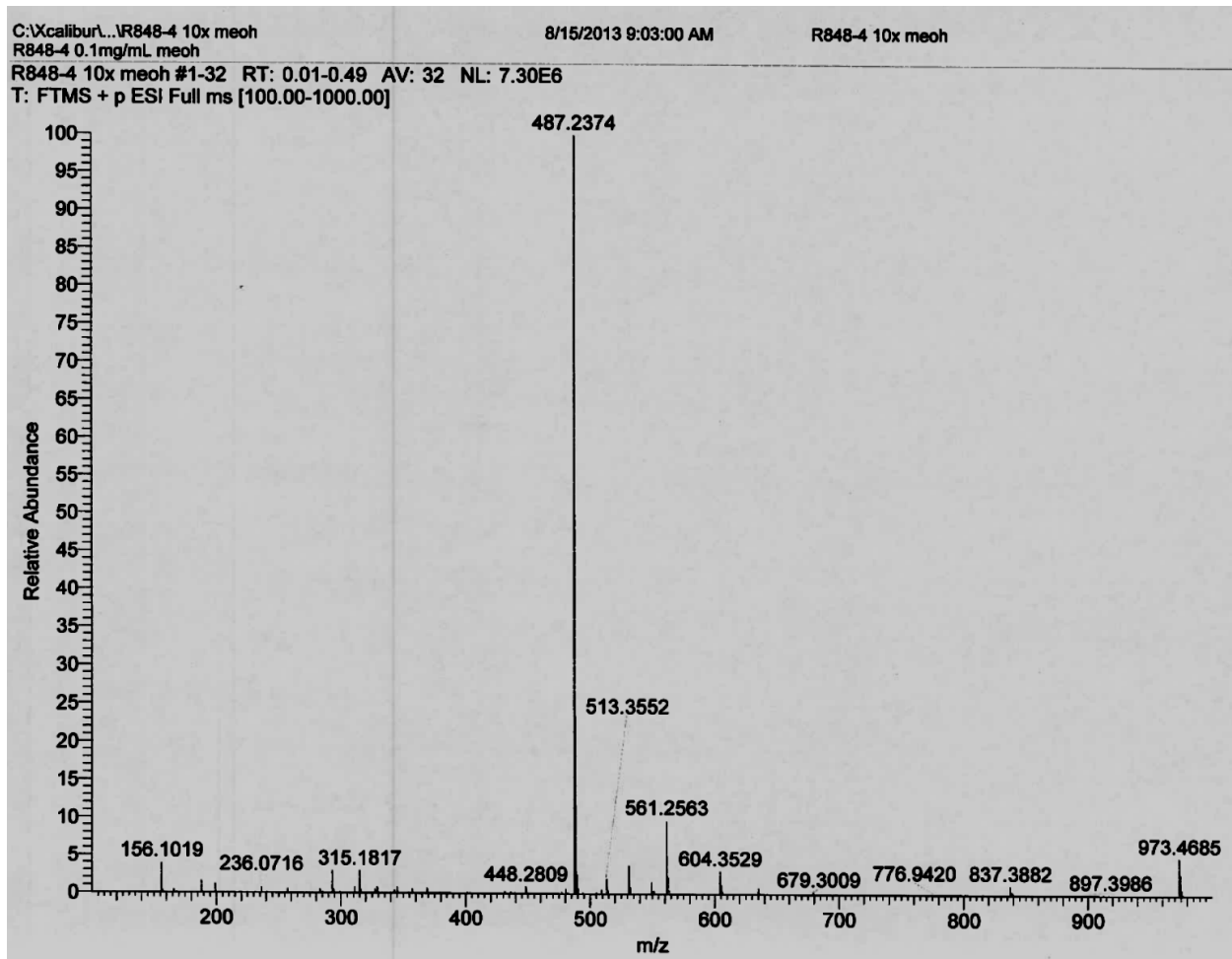


Figure A.1 MS spectrum of Me₂ProR848 dissolved in methanol. High resolution mass spectrometry (HRMS) was performed on a Thermo LTqFT (linear ion trap, Fourier transform mass spectrometry) with 7.0 Tesla magnet. HRMS (m/z) calculated for Me₂ProR848, [M]⁺ = 487.2299; found [M]⁺ m/z = 487.2347.

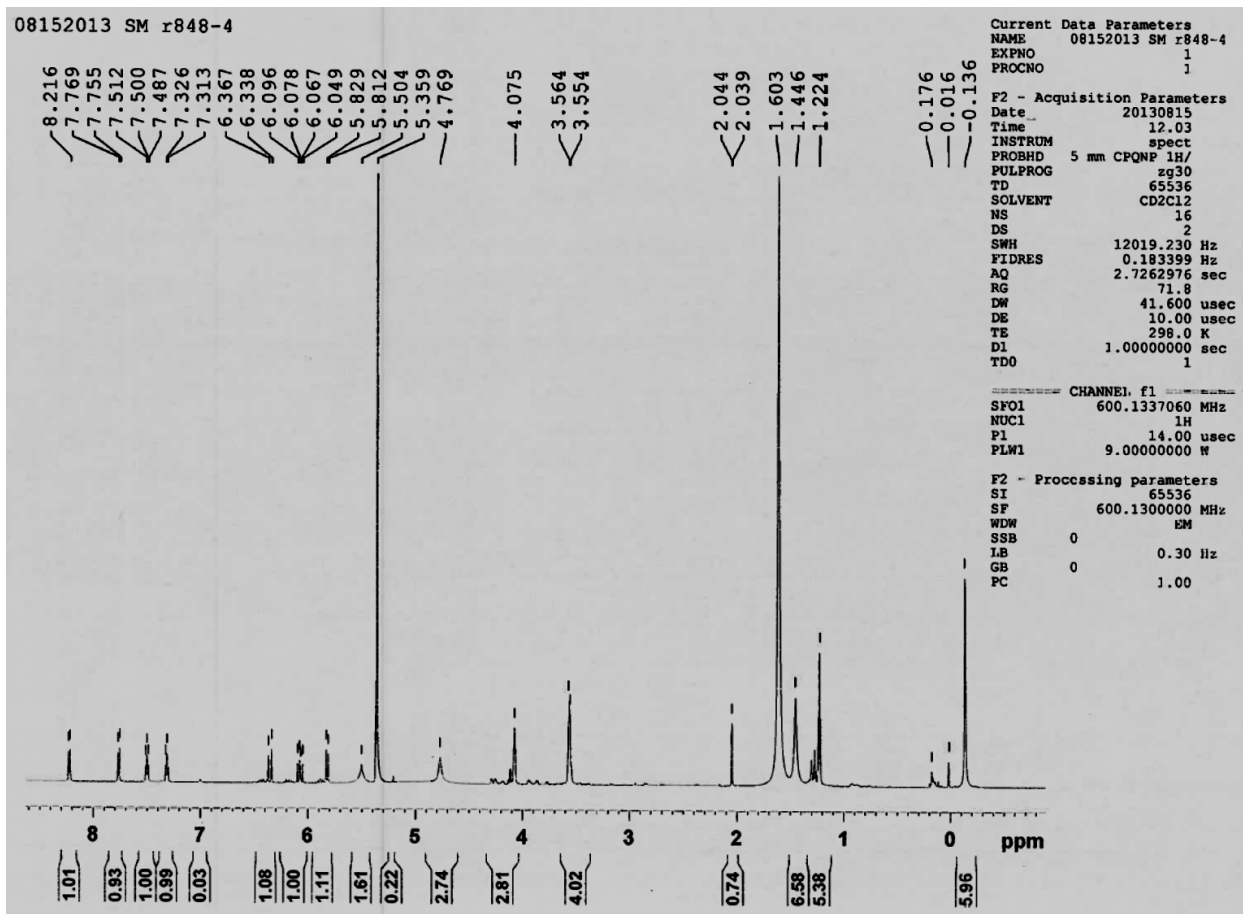


Figure A.2 ^1H NMR Spectrum of $\text{Me}_2\text{ProR848}$ dissolved in CD_2Cl_2 . NMR measurements were performed using a Bruker AVANCE III spectrometer at room temperature. ^1H NMR measurements were collected at 600 MHz

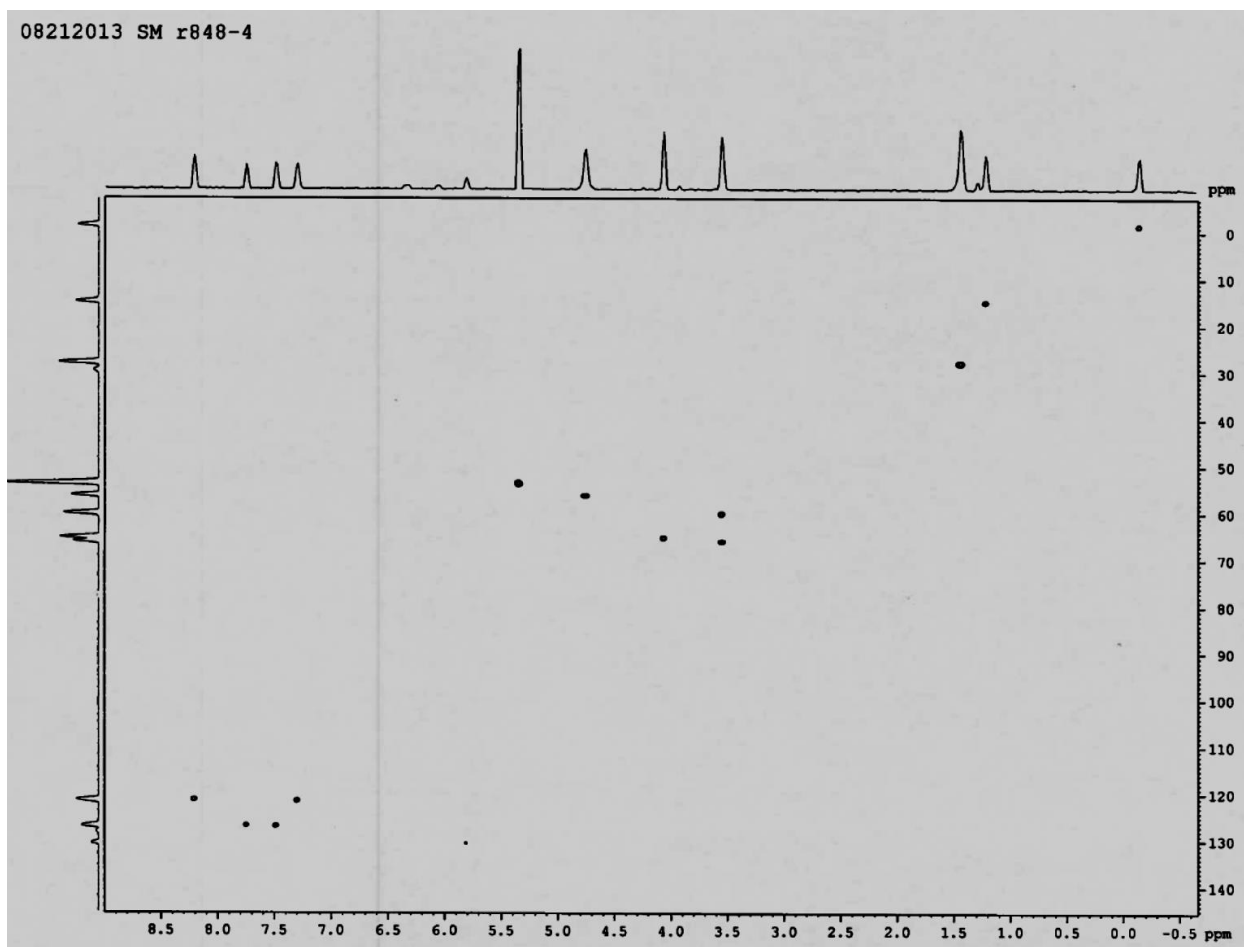


Figure A.3 Two Dimensional NMR of $\text{Me}_2\text{ProR848}$ dissolved in CD_2Cl_2 . X-axis represents ^1H NMR spectrum; y-axis represents ^{13}C NMR spectrum. NMR measurements were performed using a Bruker AVANCE III spectrometer at room temperature. ^1H NMR measurements were collected at 600 MHz and ^{13}C NMR measurements were collected at 150 MHz.

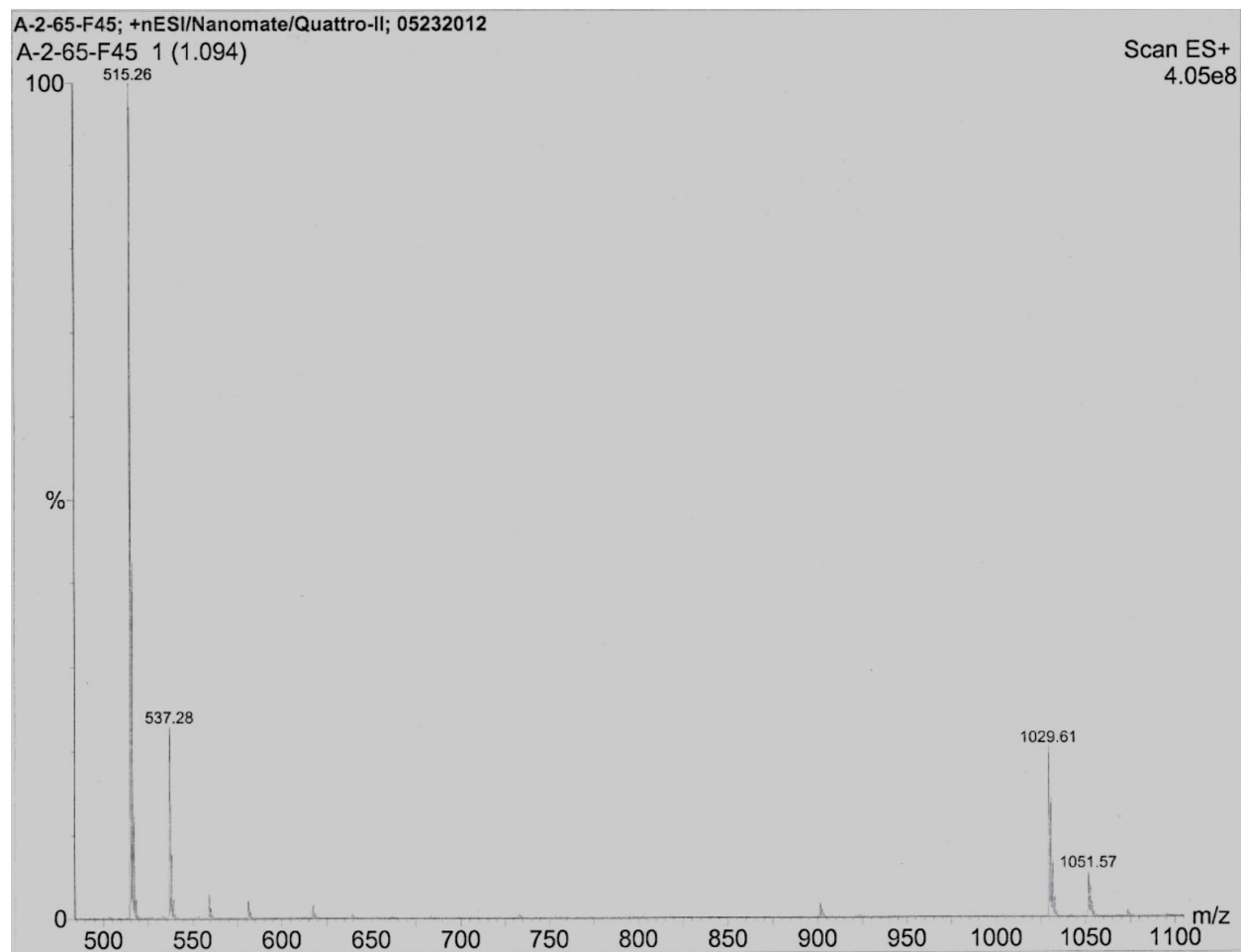


Figure A.4 MS spectrum of Et₂ProR848 dissolved in methanol. MS was performed on a TriVersa Nanomate[®] ESI Micromass Quattro II Triple Quadrupole Mass Spectrometer. HRMS (m/z) calculated for Et₂ProR848, [M]⁺ = 515.2612; found [M]⁺ m/z = 515.26.

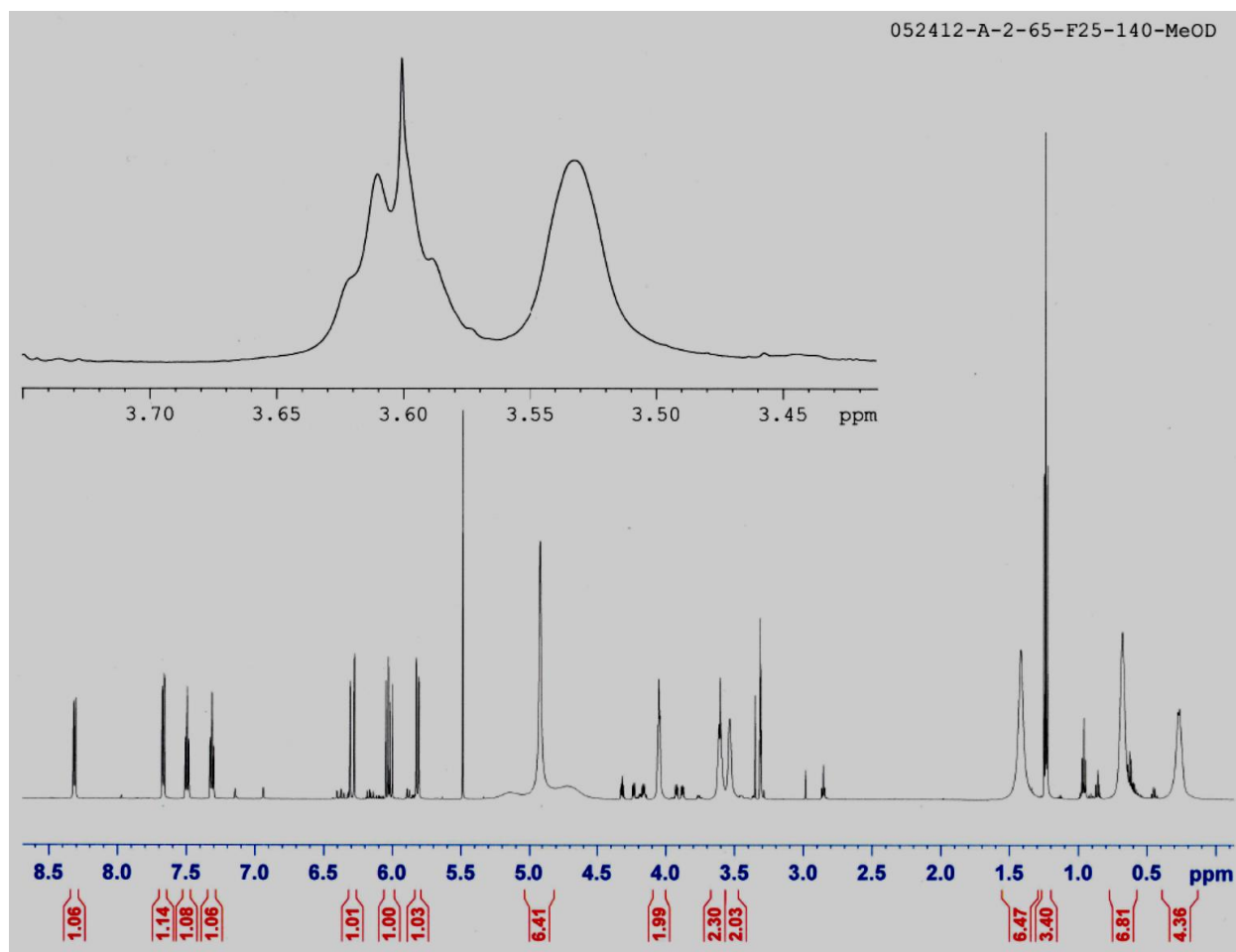


Figure A.5 ^1H NMR spectrum of $\text{Et}_2\text{ProR848}$ dissolved in deuterated methanol. NMR measurements were performed using a Bruker AVANCE III spectrometer at room temperature. ^1H NMR measurements were collected at 600 MHz.

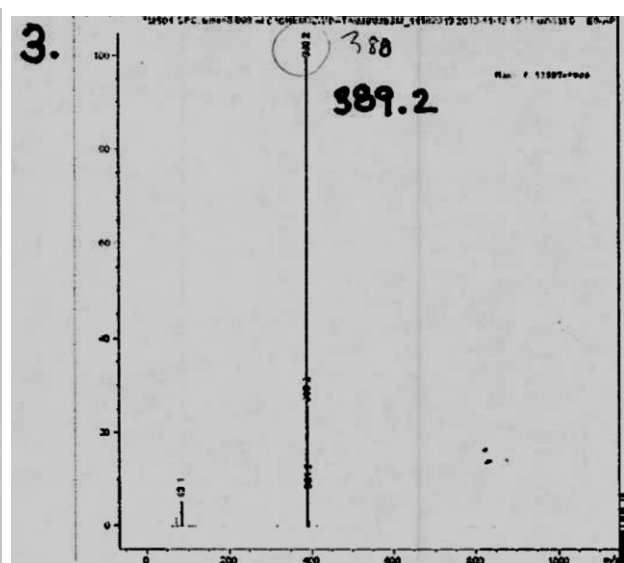
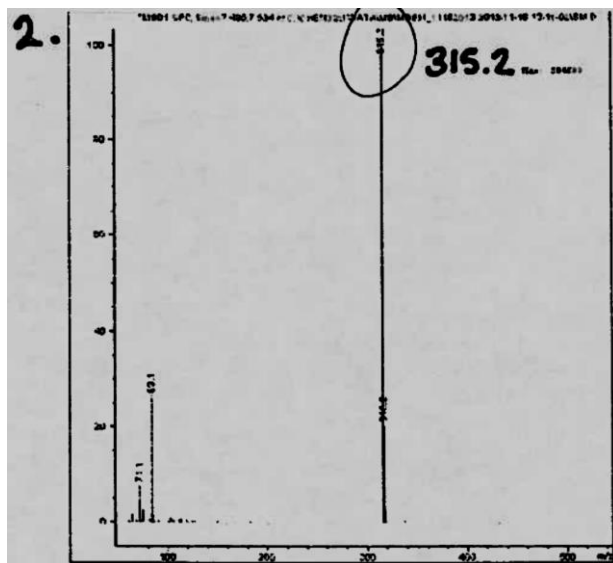
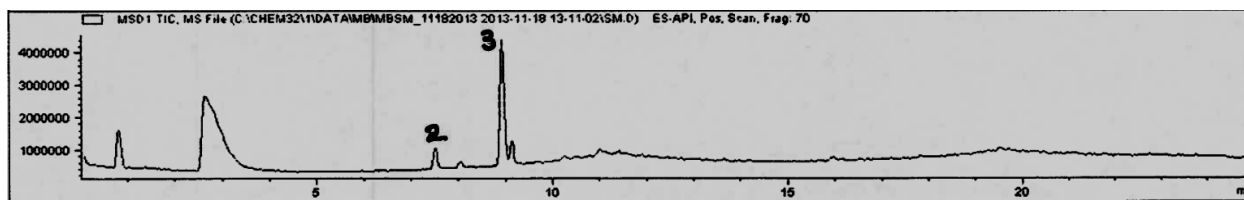


Figure A.6 LC-MS (liquid chromatograph mass spectrometry) analysis of Me₂ProR848-NP degradation products. LC-MS was performed on an Agilent 1200 Series LC-MS using a 2.7 μM HALO C₁₈ column in positive ion mode with electrospray ionization. LC-MS data were analyzed using Agilent ChemStation software. MS (m/z) calculated for R848 (Peak 2), [M]⁺ = 315.17; found [M]⁺ m/z = 315.2. MS (m/z) calculated for silanol-R848 (Peak 3), [M]⁺ = 389.19; found [M]⁺ m/z = 389.2.

Table A.1 Dengue conjugation reaction conditions.

	<i>Reaction 1</i>	<i>Reaction 2</i>	<i>Reaction 3</i>	<i>Reaction 4*</i>
Date	4/14	4/14	4/15	4/21
DV2 Prep	-1	-1	-1	0
Linker	EDC	EDC	EDC	NHS-PEG(500)-maleimide
Surface of NP	Carboxylic acid	Carboxylic acid	Carboxylic acid	Carboxylic acid
Amount of NPs	1 mg	1 mg	1 mg	1.5 mg
Amount of Protein	200 ng	Residual from rxn1	200 ng	100 ng
Final Volume	1 mL	1 mL	1 mL	0.8 mL
Buffer used	Sodium phosphate	Sodium phosphate	Sodium phosphate	Fisher pH 10
pH	~8	~8	~8	9-10
Reaction temperature	RT	RT	RT	RT
Reaction time	2 h	2 h	2 h	Over night
Protein conjugation	3.4 µg/mg	7.1 µg/mg	1.1 µg/mg	13 µg/mg
	<i>Reaction 5</i>	<i>Reaction 6*</i>	<i>Reaction 7</i>	<i>Reaction 8</i>
Date	4/24	5/15	5/19	5/19
DV2 Prep	0	1	1	1
Linker	NHS-PEG(500)-maleimide	NHS-PEG(500)-maleimide	NHS-PEG(5k)-maleimide	NHS-PEG(500)-maleimide
Surface of NP	Carboxylic acid	Acetyl group	Carboxylic acid	Carboxylic acid
Amount of NPs	3.5 mg	2 mg	1 mg	3 mg
Amount of Protein	100 ng	100 ng	30 ng	100 ng
Final Volume	0.7 mL	0.7 mL	0.3 mL	0.5 mL
Buffer used	Sodium borate + 5µL NaOH	Fisher pH 10	Fisher pH 10	Fisher pH 10
pH	10-11	9	9	9
Reaction temperature	37°C for 3 hours, then RT	RT	RT	RT
Reaction time	24 hours	Over night	Over night	Over night
Protein conjugation	3.1 µg/mg	11.4 µg/mg	0.1 µg/mg	2.6 µg/mg

* Annotates batches that were dosed *in vivo*

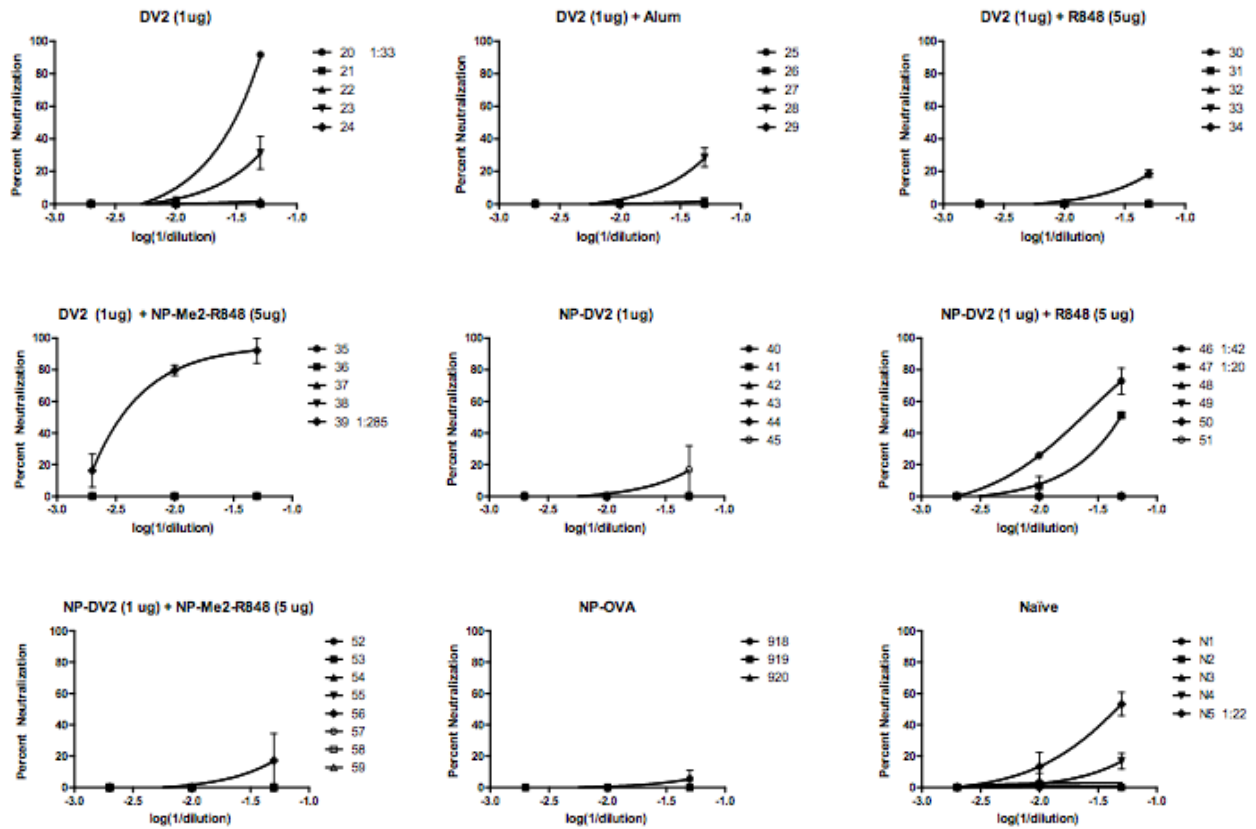


Figure A.7 Neutralizing antibody assay of DV2 study. After testing sera from mice for total anti-DV2 IgG, live DV2 virus was exposed to varying levels of IgG. Titers represent concentration of sera dosed to DV2 virus at percent neutralization against infection of wild type cell line.